Intelligent Systems, Control and Automation:
Science and Engineering

Ignacio Santín
Carles Pedret
Ramón Vilanova

Control and Decision Strategies in Wastewater Treatment Plants for Operation Improvement

Springer

Intelligent Systems, Control and Automation: Science and Engineering

Volume 86

More information about this series at http://www.springer.com/series/6259

Ignacio Santín · Carles Pedret
Ramón Vilanova

Control and Decision Strategies in Wastewater Treatment Plants for Operation Improvement

Springer

Ignacio Santín
Department of Telecommunications
and Systems Engineering
Universitat Autònoma de Barcelona
Bellaterra
Spain

Ramón Vilanova
Department of Telecommunications
and Systems Engineering
Universitat Autònoma de Barcelona
Bellaterra
Spain

Carles Pedret
Department of Telecommunications
and Systems Engineering
Universitat Autònoma de Barcelona
Bellaterra
Spain

ISSN 2213-8986 ISSN 2213-8994 (electronic)
Intelligent Systems, Control and Automation: Science and Engineering
ISBN 978-3-319-46366-7 ISBN 978-3-319-46367-4 (eBook)
DOI 10.1007/978-3-319-46367-4

Library of Congress Control Number: 2016951676

Printed on acid-free paper

This Springer imprint is published by Springer Nature
The registered company is Springer International Publishing AG
The registered company address is: Gewerbestrasse 11, 6330 Cham, Switzerland

Preface

The concern about the effects of urban life on the ecological cycle has activated several research areas that attempt to tackle part of this problem in one way or another. Nowadays, much of the efforts concentrate on new sources of clean energy, transportation and, of course, wastewater treatment. Since the quality standards for wastewater treatment plants (WWTPs) are getting tighter, efficient control methods need to be implemented for economic and environmental reasons. As an example, there are effluent requirements defined by the European Union (European Directive 91/271 Urban wastewater) with economic penalties.

From the operation and control point of view, several control methodologies have been tested for WWTPs. Ranging from simple proportional-integrative (PI) and PI-like single-loop controllers to multivariable model predictive controllers, from model-driven to model-free, data-driven controllers. However, it is well known that biological WWTPs are complex nonlinear systems with very different time constants. The intricate behavior of the microorganisms and the large disturbances in concentrations and flow rates of the influent makes the control of the WWTP a complex task. In fact, during the last decade, the community has emphasized the importance of integrated and plant-wide control and the wastewater industry is now starting to realize the benefits of such an approach.

The purpose of the control methodologies presented in this book is to operate WWTPs with the aim of improving the effluent quality and reduce operational costs. However, it is important to emphasize the distinguished viewpoint of the approach presented here with respect to existing works that can be found in the research literature. Most of the approaches concentrate their efforts in providing a trade-off between operational costs and effluent quality, being this quality measured in an aggregated way by means of an appropriately defined index. In addition, as environmental regulations establish maximum concentrations of pollutants for the discharged effluent to receiving waters, it is therefore important to concentrate on being under those limits if the plant is to be operated according to the regulations. However, usual approaches found in the research literature for WWTP control and operation do not tackle the effluent violations in an explicit way. The control and decision operation system proposed here is aimed at proving that, in addition to

achieving an improvement in the effluent quality, it is also possible to reduce the percentage of time of pollution violations. It should be emphasized that none of works in the literature are focused on reducing peaks of pollutant concentrations until the complete elimination of effluent violations. It is of significant importance because high concentrations of pollutants in the effluent can damage the environment and the health of the population.

The purpose of this book is therefore to present a proposal for WWTP operation based on an incremental construction of the intelligent decision system that prevents effluent pollutant concentrations to overpass the established environmental limits. As it is conceived, these limits can be adapted to other design values on the basis of eventually different local regulations. Even the presentation and design are based on the well-known and established Benchmark Simulation Models, the proposal idea can be conveniently extended to other WWTPs frameworks and scenarios.

This book is based on the research work that the authors have carried out over recent years. It is not intended to be a research report but a unified presentation of the works carried out. It can be found in the references chapter a complete list of journal papers in which there are a deeper discussion of some control topics. Also the comparison of the proposed design approach with some other previously existing in the literature has been minimized in the book content. These comparisons can be found in the journal referenced works whereas the main goal of the book is to serve as a methodological presentation of a design approach that, in the authors' opinion, deserves some extensions and particular applications that would be difficult to forecast just by looking at the set of disconnected results that journal papers usually constitute.

The book is intended to be used for by M.Sc. and Ph.D. students, consulting engineers and process engineers at wastewater treatment plants. Even the discourse is based on benchmark simulation scenarios, it is intended to provide a methodological, and scientifically based, steep way to deal with effluent WWTP requirements without forgetting about costs of operation.

The authors would like to acknowledge all the people who have contributed to this book in one way or another, in particular, M. Meneses, M. Barbu just to name a few. Special thanks go to the series Editor S.G. Tzafestas and the Editorial Assistants Nathalie Jacobs and Cynthia Feenstra for their help during the preparation of the manuscript. Partial support of the research that originated the results presented in this book has been provided by the Spanish Ministry of Economy and Competitivity through grant DPI2013-47825-C3-1-R.

Bellaterra, Spain

Ignacio Santín
Carles Pedret
Ramón Vilanova

Contents

Abbreviations

AE	Aeration Energy (kWh/d)
ANN	Artificial Neural Network (–)
ASM1	Activated Sludge Model No. 1 (–)
BOD_5	5-day Biological Oxygen Demand (mg/l)
BSM1	Benchmark Simulation Model No. 1 (–)
BSM2	Benchmark Simulation Model No. 2 (–)
CL1	First control strategy of the finalization of BSM2 plant layout in [46] (–)
CL2	Second control strategy of the finalization of BSM2 plant layout in [46] (–)
COD	Chemical Oxygen Demand (mg/l)
defCL	Default control strategy of the original BSM2 definition in [33] (–)
EC	Consumption of External Carbon source (kg/d)
EQI	Effluent Quality Index (kg/d)
FC	Fuzzy Controller (–)
HE_{net}	Net Heating Energy (kWh/d)
IAE	Integral of the Absolute Error (–)
ISE	Integral of the Squared Error (–)
K_La	Oxygen transfer coefficient (d^{-1})
m	Control horizon (–)
MaxIn	Maximum value of the input variable of the fuzzifier (–)
MaxOut	Maximum value of the output variable of the defuzzifier (–)
ME	Mixing Energy (kWh/d)
mean($\|e\|$)	Average of the absolute error
MET_{prod}	Methane production in the anaerobic digester (kg/d)
MinIn	Minimum value of the input variable of the fuzzifier (–)
MinOut	Maximum value of the output variable of the defuzzifier (–)
MPC	Model Predictive Control (–)
MPC+FF	Model Predictive Control with feedforward compensation (–)
OCI	Overall Cost Index (–)

p	Prediction horizon (–)
PE	Pumping Energy (kWh/d)
PI	Proportional-Integral (–)
Q	Flow rate (m^3/d)
Q_a	Internal recycle flow rate (m^3/d)
Q_{bypass}	Bypass flow rate (m^3/d)
Q_{po}	Overflow rate of the primary clarifier (m^3/d)
q_{EC}	External carbon flow rate (m^3/d)
r_{NH}	Conversion rate of ammonium and ammonia nitrogen (–)
r_{NO}	Conversion rate of nitrate nitrogen (–)
$S_{N_{tot}}$	Total nitrogen concentration (mg/l)
$S_{N_{tot,e}}$	Total nitrogen concentration in the effluent (mg/l)
$S_{N_{tot,ep}}$	Prediction of the effluent total nitrogen concentration (mg/l)
S_{NH}	Ammonium and ammonia nitrogen concentration (mg/l)
$S_{NH,bypass}$	Ammonium and ammonia nitrogen concentration in the bypass (mg/l)
$S_{NH,e}$	Ammonium and ammonia nitrogen concentration in the effluent (mg/l)
$S_{NH,ep}$	Prediction of the effluent ammonium and ammonia nitrogen concentration (mg/l)
$S_{NH,po}$	Ammonium and ammonia nitrogen concentration from the primary clarifier overflow (mg/l)
S_{NO}	Nitrate nitrogen concentration (mg/l)
S_O	Dissolved oxygen (mg/l)
S_S	Readily biodegradable substrate (mg/l)
SP	Sludge Production (kg/d)
T_{as}	Temperature (°C)
TSS	Total Suspended Solids (mg/l)
WWTP	Wastewater Treatment Plants (–)
$X_{B,A}$	Active autotrophic biomass (mg/l)
$X_{B,H}$	Active heterotrophic biomass (mg/l)

Chapter 1
Introduction

1.1 Motivation

During the last decade the importance of integrated and plant-wide control has been emphasized by the research community and the wastewater industry is now starting to realize the benefits of such an approach. Biological wastewater treatment plants (WWTPs) are considered complex nonlinear systems and its control is very challenging, due to the complexity of the biological and biochemical processes that take place in the plant and the strong fluctuations of the influent flow rate. In addition, there are effluent requirements for instance the one defined by the European Union (European Directive 91/271 Urban wastewater) with economic penalties, to upgrade existing wastewater treatment plants in order to comply with the effluent standards.

In this work, the evaluation and comparison of the different control strategies is based on Benchmark Simulation Model No.1 (BSM1) and Benchmark Simulation Model No. 2 (BSM2), developed by the International Association on Water Pollution Research and Control. These benchmarks define a plant layout, influent loads, test procedures and evaluation criteria. They provide also a default control strategy. BSM1 corresponds to the secondary treatment of a WWTP, where the biological wastewater treatment is performed using activated sludge reactors. The evaluation is based on a week of plant operation. BSM2 is extended to a complete simulation of a WWTP, including also a primary clarifier, anaerobic digesters, thickeners, dewatering systems, and other subprocesses. In BSM2, the evaluation is based on one year of operation data.

The application of different control strategies is focused on obtaining plant performance improvement. In the literature there are many works that present different methods for controlling WWTPs. Most of the works use BSM1 as working scenario. In some cases they put their focus on avoiding violations of the effluent limits by applying a direct control of the effluent variables. Nevertheless, they need to fix the set-points of the controllers at lower levels to guarantee their objective, which may imply a great increase of costs. Other works consider a trade-off between opera-

I. Santín et al., *Control and Decision Strategies in Wastewater Treatment Plants for Operation Improvement*, Intelligent Systems, Control and Automation: Science and Engineering 86, DOI 10.1007/978-3-319-46367-4_1

tional costs and effluent quality, but they do not tackle with effluent violations. They usually deal with the basic control strategy (control of dissolved oxygen (S_O) of the aerated tanks and nitrate nitrogen concentration (S_{NO}) of the second tank ($S_{NO,2}$)), or propose hierarchical control structures that regulate the S_O set-points according to some states of the plant, usually ammonium and ammonia nitrogen concentration (S_{NH}) and S_{NO} values in any tank or in the influent or S_O in other tanks.

Other existing works in the literature use BSM2 as testing plant. Some of them are focused on the implementation of control strategies in the biological treatment, as we consider here. Specifically, they propose control strategies based on S_O control by manipulating oxygen transfer coefficient (K_La) of the aerated tanks, S_{NH} hierarchical control by manipulating the S_O set-points, $S_{NO,2}$ control by manipulating the internal recycle flow rate (Q_a) or total suspended solids (TSS) control by manipulating the wastage flow rate (Q_w).

1.2 Water Quality and Plant Operation

The purpose of the methodology presented in this book is to operate WWTPs with the aim of improving the effluent quality and reducing operational costs. Of course, water quality is a concern but can be faced from different points of view. Most of the actual approaches concentrate their efforts in providing a trade-off between operational costs and effluent quality, being this quality measured in an aggregated way by means of an appropriately defined index. In addition, as environmental regulations establish maximum concentrations of pollutants for the discharged effluent to receiving waters, it is therefore important to concentrate on being under those limits if the plant is to be operated according to the regulations. However usual approaches found in the research literature for WWTP control and operation do not tackle the effluent violations in an explicit way. The control and decision operation system proposed here is aimed at proving that, in addition to achieving an improvement in the effluent quality, it is also possible to reduce the percentage of time of pollution violations. It should be emphasized that none of works in the literature are focused on reducing peaks of pollutant concentrations until the complete elimination of effluent violations. It is of significant importance because high concentrations of pollutants in the effluent can damage the environment and the health of the population.

Operational costs have not to be forgotten. Even this is true for every industrial plant, it is of special concern for WWTPs. They can be seen as a special case of industries where there is no income related to the final product. Instead, the ultimate goal of a WWTP is the environmental protection. Because of this, it is necessary to keep operational costs under some reasonable limits. This is one of motivations of the approach presented in this book that incorporates in every controller tuning selection the constraints for the operational costs. In this way, we can continuously search for water quality improvement but with the constraint of no worsening operational costs.

This book uses first BSM1, and second BSM2 as working scenarios to evaluate the applied control strategies. The main purpose of this text is to show how the use of

high level control and decision strategies allows to avoid S_{NH} in the effluent ($S_{NH,e}$) and total nitrogen ($S_{N_{tot}}$) in the effluent ($S_{N_{tot,e}}$) limits violations and, at the same time, to improve effluent quality and to reduce operational costs. The innovative proposed control strategies are based on Model Predictive Control (MPC), Fuzzy Controller (FC), functions that relate the input and manipulated variables, and Artificial Neural Networks (ANN). The MPC controllers are implemented with the aim of improving the control tracking. The control strategies applied with FCs and the functions that relate the inputs with the manipulated variables are based on the processes that take place in the biological reactors, whereas the ANNs are applied to predict effluent concentrations by evaluating the influent at each sample time, in order to select the appropriate control strategy to be applied.

1.3 Book Outline

The book is divided in nine chapters. The first two chapters introduce the working scenarios used in order to simulate wastewater treatment plants, as well as a theoretical explanation of the control techniques applied. In Chap. 2, BSM1 and BSM2 benchmarks and their default control strategies are described. In Chap. 3 the advanced control techniques of MPC, FC, and ANN are depicted.

The next two chapters are focused on to improve the control performance of the basic control loop and on the objective of effluent quality improvement and costs reduction by the application of a hierarchical structure. Chapter 4 explains the implementation and design of the MPC with feedforward compensation (MPC+FF) controllers that compose the lower level of the hierarchical control structure. Here it is also shown the control tracking improvement in comparison with the default control strategy and with other lower level control approaches. Chapter 5 focuses on the higher level of the hierarchical control, choosing first, the controller alternatives for manipulating S_O in the fifth tank ($S_{O,5}$) and second, extending the higher level control by manipulating S_O of the three aerobic reactors.

The following three chapters are related with the goal of effluent limits violations removal. In Chap. 6, the proposed control strategies for removing effluent pollutants are presented. First, $S_{N_{tot,e}}$ violations are taken into account. This follows by the consideration of $S_{NH,e}$ violations. Also it is shown how to combine both approaches for a simultaneous effluent violations removal. Chapter 7 explains the implementation of the ANNs for the required effluent predictions using BSM2 as working scenario, in order to choose the suitable control strategy to be applied. Chapter 8 presents the control strategies applied jointly with the advanced decision control system, with the consideration when a risk of violation is detected and switching to a normal operation the rest of the time in order to manage operational costs.

Finally, in Chap. 9, the concluding remarks are drawn.

Chapter 2
Process Modelling and Simulation Scenarios

The wastewater research community has extensively applied benchmark models to develop and evaluate control strategies for WWTPs. The large number of journal papers and conferences related to the use of benchmarks in WWTPs, issued up to the present, prove the utility of these tools. This book also makes use of benchmark models to test and compare the proposed control strategies. These benchmarks are briefly described in the first section of this chapter.

The WWTP benchmarks include basic control strategies, which are commonly applied in WWTPs. They are usually used in the literature in order to compare the results achieved with new control strategies or techniques, in terms of control performance and/or plant performance. These default control strategies are described in the second section of this chapter.

2.1 Working Scenarios

In order to simulate the behavior of a wastewater treatment plant and to evaluate different control strategies, two benchmarks have been used in this book, which are called BSM1 [1] and BSM2 [24]. They have been widely applied to test control strategies and to optimize the plant design.

BSM1 and BSM2 are composed by different models developed by the International Association on Water Pollution Research and Control (IAWPRC)

- The Activated Sludge Model No. 1 (ASM1) [30] describes the biological phenomena that takes place in the biological reactors.
- The model developed in [59] describes the physical separation processes that take place inside the secondary settler.
- The Anaerobic Digestion Model No. 1 (ADM1) [5] describes the dynamics of the anaerobic digester.

I. Santín et al., *Control and Decision Strategies in Wastewater Treatment Plants for Operation Improvement*, Intelligent Systems, Control and Automation: Science and Engineering 86, DOI 10.1007/978-3-319-46367-4_2

BSM1 represents an activated sludge system that operates according to ASM1 with a secondary clarifier.

BSM2 integrates BSM1 with wastewater pre-treatment and sludge treatment including ADM1.

2.1.1 Benchmark Simulation Model No. 1

This section provides a description of the BSM1 working scenario. This is a simulation environment defining a plant layout, a simulation model, the procedures for carrying out the tests, the criteria for evaluating the results and a default control strategy.

Plant Layout

The schematic representation of the WWTP layout considered in BSM1 is presented in Fig. 2.1. The plant consists of five biological reactor tanks connected in series, followed by a secondary settler. The first two tanks have a volume of 1000 m^3 each and are anoxic and perfectly mixed. The rest three tanks have a volume of 1333 m^3 each and are aerated. The settler has a total volume of 6000 m^3 and is modeled in ten layers, being the 6th layer, counting from bottom to top, the feed layer. Two recycle flows, the first from the last tank and the second from the underflow of the settler, complete the system. The sludge from the settler that is not recycled is led to be disposed and is called wastage.

The plant is designed for an average influent dry weather flow rate of 18,446 m^3/d and an average biodegradable chemical oxygen demand (COD) in the influent of 300 g/m^3. Its hydraulic retention time, based on the average dry weather flow rate and the total tank and settler volume (12,000 m^3), is 14.4 h. Q_w is fixed to 385 m^3/d that determines, based on the total amount of biomass present in the system, a biomass sludge age of about 9 days.

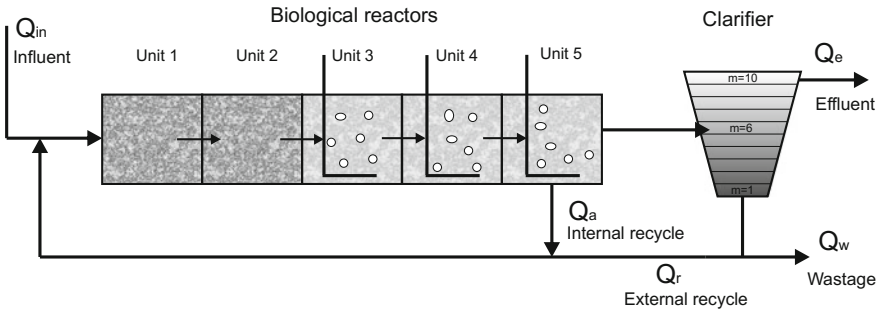

Fig. 2.1 Benchmark simulation model 1

The nitrogen removal is achieved using a denitrification step performed in the anoxic tanks and a nitrification step carried out in the aerated tanks. The internal recycle is used to supply the denitrification step with S_{NO}.

Models

The biological phenomena of the reactors are simulated by using the ASM1 that considers eight different biological processes. The vertical transfers between layers in the settler are simulated by the double-exponential settling velocity model [59]. None biological reaction is considered in the settler. The two models are internationally accepted and include 13 state variables.

The general equations for mass balancing are as follows:

- For reactor 1:

$$\frac{dZ_1}{dt} = \frac{1}{V_1}(Q_a \cdot Z_a + Q_r \cdot Z_r + Q_{in} \cdot Z_{in} + r_{z,1} \cdot V_1 - Q_1 \cdot Z_1) \tag{2.1}$$

- For reactors 2–5:

$$\frac{dZ_k}{dt} = \frac{1}{V_k}(Q_{k-1} \cdot Z_{k-1} + r_{z,k} \cdot V_k - Q_k \cdot Z_k) \tag{2.2}$$

where Z is any concentration of the process, Z_1 is Z in the first reactor, Z_a is Z in the internal recirculation, Z_r is Z in the external recirculation, Z_{in} is Z from the influent, V is the volume, V_1 is V in the first reactor, Q_r is the external recirculation flow rate, Q_{in} is the flow rate of the influent, Q_1 is the flow rate in the first tank and it is equal to the sum of Q_a, Q_r and Q_{in}, k is the number of reactor and Q_k is equal to Q_{k-1}.

The proposed control strategies in this work are based on the conversion rates of S_{NH} (r_{NH}) and S_{NO} (r_{NO}). They are expressed as:

$$r_{NH} = -0.08\rho_1 - 0.08\rho_2 - \left(0.08 + \frac{1}{0.24}\right)\rho_3 + \rho_6 \tag{2.3}$$

$$r_{NO} = -0.1722\rho_2 + 4.1667\rho_3 \tag{2.4}$$

where ρ_1, ρ_2, ρ_3, ρ_6 are four of the eight biological processes defined in ASM1. Specifically, ρ_1 is the aerobic growth of heterotrophs, ρ_2 is the anoxic growth of heterotrophs, ρ_3 is the aerobic growth of autotrophs and ρ_6 is the ammonification of soluble organic nitrogen (S_{ND}). They are defined as

$$\rho_1 = 4\left(\frac{S_S}{10 + S_S}\right)\left(\frac{S_O}{0.2 + S_O}\right)X_{B,H} \tag{2.5}$$

$$\rho_2 = 4\left(\frac{S_S}{10 + S_S}\right)\left(\frac{0.2}{0.2 + S_O}\right)\left(\frac{S_{NO}}{0.5 + S_{NO}}\right)0.8 \cdot X_{B,H} \tag{2.6}$$

$$\rho_3 = 0.5 \left(\frac{NH}{1 + NH} \right) \left(\frac{S_O}{0.4 + S_O} \right) X_{B,A} \tag{2.7}$$

$$\rho_6 = 0.05 \cdot S_{ND} \cdot X_{B,H} \tag{2.8}$$

where S_S is the readily biodegradable substrate, $X_{B,H}$ the active heterotrophic biomass and $X_{B,A}$ the active autotrophic biomass. The biological parameter values used in the BSM1 correspond approximately to a temperature of 15 °C.

Test Procedure

BSM1 [13] defines four different influent data: constant, dry weather, rain weather, and storm weather. Each scenario contains 14 days of influent data with sampling intervals of 15 min. A simulation protocol is established to assure that results are got under the same conditions and can be compared. Thus, first a 150 days period of stabilization in closed-loop using constant influent data has to be completed to drive the system to a steady-state, next a simulation with dry weather is run and finally the desired influent data (dry, rain or storm) is tested. Only the results of the last 7 days are considered for the plant operation evaluation.

Evaluation Criteria

In order to compare the different control strategies, different criteria are defined. The performance assessment is made at two levels. The first level concerns the control. Basically, this serves as a proof that the proposed control strategy has been applied properly. It is assessed by Integral of the Squared Error (ISE), Integral of the Absolute Error (IAE), and average of the absolute error (mean ($|e|$)) criteria.

$$ISE = \int_{t=7days}^{t=14days} e_i^2 \cdot dt \tag{2.9}$$

$$IAE = \int_{t=7days}^{t=14days} |e_i| \cdot dt \tag{2.10}$$

$$mean\ (\,|\,e\,|\,) = \frac{1}{T_s} \sum_{i=1}^{i=T_s} |e_i| \tag{2.11}$$

where e_i is the error in each sample between the set-point and the measured value and T_s is the total number of samples.

The second level of evaluation provides measures for the effect of the control strategy on plant performance. It includes effluent violations, Effluent Quality Index (EQI), and Overall Cost Index (OCI).

The evaluation must include the percentage of time that the effluent limits are not met. The effluent concentrations of $S_{N_{tot}}$, Total COD (COD_t), NH, TSS, and Biological Oxygen Demand (BOD_5) should obey the limits given in Table 2.1.

Table 2.1 Effluent quality limits

Variable	Value
$S_{N_{tot}}$	<18 g N $\cdot$ m^{-3}
COD_t	<100 g COD $\cdot$ m^{-3}
NH	<4 g N $\cdot$ m^{-3}
TSS	<30 g SS $\cdot$ m^{-3}
BOD_5	<10 g BOD $\cdot$ m^{-3}

Table 2.2 B_i values

Factor	B_{TSS}	B_{COD}	B_{NKj}	$B_{S_{NO}}$	B_{BOD_5}
Value (g pollution unit g^{-1})	2	1	30	10	2

$S_{N_{tot}}$ is calculated as the sum of S_{NO} and Kjeldahl nitrogen (NKj), being this the sum of organic nitrogen and S_{NH}.

EQI is defined to evaluate the quality of the effluent. It is related with the fines to be paid due to the discharge of pollution. EQI is averaged over a 7 days observation period and it is calculated weighting the different compounds of the effluent loads.

$$EQI = \frac{1}{1000 \cdot T} \int_{t=7days}^{t=14days} (B_{TSS} \cdot TSS(t) + B_{COD} \cdot COD(t) + B_{NKj} \cdot NK_j(t) +$$

$$+ B_{S_{NO}} \cdot S_{NO}(t) + B_{BOD_5} \cdot BOD_5(t)) Q(t) \cdot dt \tag{2.12}$$

where B_i are weighting factors (Table 2.2) and T is the total time.

OCI is defined as

$$OCI = AE + PE + 5 \cdot SP + 3 \cdot EC + ME \tag{2.13}$$

where AE is the aeration energy, PE is the pumping energy, SP is the sludge production to be disposed, EC is the consumption of carbon from external source and ME is the mixing energy.

AE is calculated according to the following relation:

$$AE = \frac{S_o^{sat}}{T \cdot 1.8 \cdot 1000} \int_{t=7days}^{t=14days} \sum_{i=1}^{5} V_i \cdot K_L a_i(t) \cdot dt \tag{2.14}$$

where i is the reactor number and S_o^{sat} is the saturation concentration for oxygen that is equal to 8 mg/l.

PE is calculated as:

$$PE = \frac{1}{T}\int_{7days}^{14days}(0.004 \cdot Q_{in}(t) + 0.008 \cdot Q_a(t) + 0.05 \cdot Q_w(t))dt \tag{2.15}$$

SP is calculated from the TSS in the flow wastage (TSS_w) and the solids accumulated in the system:

$$SP = \frac{1}{T}(TSS_a(14days) - TSS_a(7days) + TSS_s(14days) - TSS_s(7days) + \\ + \int_{t=7days}^{t=14days} TSS_w \cdot Q_w \cdot dt) \tag{2.16}$$

where TSS_a is TSS in the reactors and TSS_s is TSS in the settler.

EC refers to the carbon that could be added to improve denitrification.

$$EC = \frac{COD_{EC}}{T \cdot 1000}\int_{t=7days}^{t=14days}\left(\sum_{i=1}^{i=n} q_{EC,i}\right)dt \tag{2.17}$$

where $q_{EC,i}$ is external carbon flow rate (q_{EC}) added to compartment i, $COD_{EC} = 400\ gCOD.m^{-3}$ is the concentration of readily biodegradable substrate in the external carbon source.

ME is a function of the compartment volume

$$ME = \frac{24}{T}\int_{t=7days}^{t=14days}\sum_{i=1}^{5}\left[0.005 \cdot V_i \textbf{ if } K_L a_i(t) < 20d^{-1} \textbf{ otherwise } 0\right]dt \tag{2.18}$$

2.1.2 Benchmark Simulation Model No. 2

In order to include plant-wide operation considerations, BSM1 was extended in a new version, BSM2, in [33] which was updated in [46]. BSM2 also defines a plant layout, a simulation model, a test procedure, evaluation criteria and default control strategies.

Plant Layout

The finalized BSM2 layout (Fig. 2.2) includes BSM1 for the biological treatment of the wastewater and the sludge treatment. A primary clarifier, a thickener for the sludge wasted from the clarifier of biological treatment, a digester for treatment of the solids wasted from the primary clarifier and the thickened secondary sludge, as well as a dewatering unit have been added. The liquids collected in the thickening and dewatering steps are recycled ahead of the primary settler.

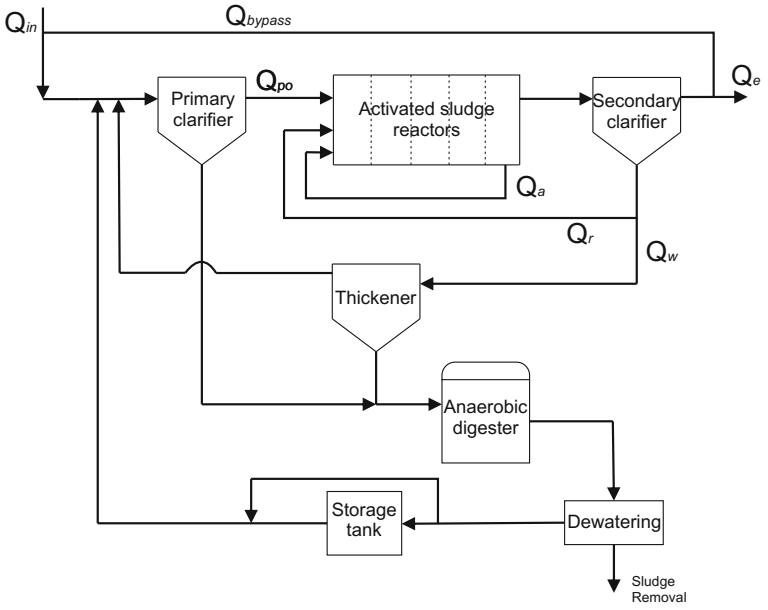

Fig. 2.2 BSM2 plant with notation used for flow rates

Models

This book is based on the implementation of control strategies in the zone of biological treatment of BSM2. For this reason, the explanation of the simulation model is focused on the activated sludge reactors. As in BSM1, the activated sludge reactors consist in five biological reactor tanks connected in series. Q_a from the last tank complete the system. The design of the BSM2 plant is modified with respect to BSM1. It has an average influent dry weather flow rate of 20,648.36 m^3/d and an average COD in the influent of 592.53 mg/l. The total volume of the bioreactor is 12,000, 1500 m^3 each anoxic tank and 3000 m^3 each aerobic tank. Its hydraulic retention time, based on the average dry weather flow rate and the total tank volume, is 14 h. The internal recycle is used to supply the denitrification step with S_{NO}.

ASM1 also describes the biological phenomena that take place in the biological reactors of BSM2. However, unlike BSM1, the temperature is considered in the BSM2.

The general equations for mass balancing are the same as in BSM1, but in this case Q_{in} and Z_{in} are replaced by Q from the primary clarifier (Q_{po}) and Z from the primary clarifier (Z_{po}), respectively

- For reactor 1:

$$\frac{dZ_1}{dt} = \frac{1}{V_1}(Q_a \cdot Z_a + Q_r \cdot Z_r + Q_{po} \cdot Z_{po} + r_{z,1} \cdot V_1 - Q_1 \cdot Z_1) \tag{2.19}$$

- For reactors 2–5:

$$\frac{dZ_k}{dt} = \frac{1}{V_k}(Q_{k-1} \cdot Z_{k-1} + r_{z,k} \cdot V_k - Q_k \cdot Z_k) \tag{2.20}$$

The proposed control strategies in this work are based on r_{NH} and r_{NO}. They are shown in the following equations:

$$r_{NH} = -0.08\rho_1 - 0.08\rho_2 - \left(0.08 + \frac{1}{0.24}\right)\rho_3 + \rho_6 \tag{2.21}$$

$$r_{NO} = -0.1722\rho_2 + 4.1667\rho_3 \tag{2.22}$$

where ρ_1, ρ_2, ρ_3, ρ_6 are four of the eight biological processes defined in ASM1. Specifically, ρ_1 is the aerobic growth of heterotrophs, ρ_2 is the anoxic growth of heterotrophs, ρ_3 is the aerobic growth of autotrophs and ρ_6 is the ammonification of S_{ND}. They are defined as

$$\rho_1 = \mu_{HT}\left(\frac{S_S}{10 + S_S}\right)\left(\frac{S_O}{0.2 + S_O}\right)X_{B,H} \tag{2.23}$$

where μ_{HT} is

$$\mu_{HT} = 4 \cdot exp\left(\left(\frac{Ln\left(\frac{4}{3}\right)}{5}\right)(T_{as} - 15)\right) \tag{2.24}$$

where T_{as} is the temperature

$$\rho_2 = \mu_{HT}\left(\frac{S_S}{10 + S_S}\right)\left(\frac{0.2}{0.2 + S_O}\right)\left(\frac{S_{NO}}{0.5 + S_{NO}}\right)0.8 \cdot X_{B,H} \tag{2.25}$$

$$\rho_3 = \mu_{AT}\left(\frac{S_{NH}}{1 + S_{NH}}\right)\left(\frac{S_O}{0.4 + S_O}\right)X_{B,A} \tag{2.26}$$

where μ_{AT} is:

$$\mu_{AT} = 0.5 \cdot exp\left(\left(\frac{Ln\left(\frac{0.5}{0.3}\right)}{5}\right)(T_{as} - 15)\right) \tag{2.27}$$

$$\rho_6 = k_{aT} \cdot S_{ND} \cdot X_{B,H} \tag{2.28}$$

where k_{aT} is defined as:

$$k_{aT} = 0.05 \cdot exp\left(\left(\frac{Ln\left(\frac{0.05}{0.04}\right)}{5}\right)(T_{as} - 15)\right) \tag{2.29}$$

Test Procedure

The influent dynamics are defined for 609 days by means of a single file, which takes into account rainfall effect and temperature. Following the simulation protocol, a 200-day period of stabilization in closed-loop using constant inputs with no noise on the measurements has to be completed before using the influent file (609 days). Nevertheless, only the data generated during the final 364 days of the dynamic simulation are used for plant performance evaluation.

Evaluation Criteria

In the same way, as in BSM1, the assessment is made at two levels. The control performance is assessed by the ISE and IAE criteria, whereas the plant performance is evaluated by EQI, OCI, and the percentage that the pollutants concentration is over the limits given in Table 2.1. However, in this case OCI is modified adding the methane production (MET_{prod}) generated in the anaerobic digester and the net heating energy (HE_{net}), which is calculated as:

$$HE^{net} = max(0,\ HE - 7 \cdot MET_{prod}) \tag{2.30}$$

where HE is the necessary energy to heat the anaerobic digester to the operating temperature, and it is calculated as:

$$HE = \frac{1000 \cdot 4.186}{86400 \cdot T} \int_{t=245days}^{t=609days} (T_{ad} - T_{ad,i}) Q_{ad}(t) \cdot dt \tag{2.31}$$

where T_{ad} is the temperature of the anaerobic digester, $T_{ad,i}$ is the temperature in the entrance of the anaerobic digester and Q_{ad} is the flow rate of the anaerobic digester.

Finally, the OCI in BSM2 is calculated as

$$OCI = AE + PE + 3 \cdot SP + 3 \cdot EC + ME - 6 \cdot MET_{prod} + HE_{net} \tag{2.32}$$

2.2 Basic Plant Operation

The definition of the BSM1 and BSM2 scenarios include default control strategies, which are commonly used as a reference for comparison.

The default control strategy of BSM1 [1] uses two Proportional-Integral (PI) control loops as shown in Fig. 2.3. The first one involves the control of $S_{O,5}$ by manipulating K_La in the fifth tank (K_La_5). The set-point for $S_{O,5}$ is 2 mg/l. The second control loop has to maintain $S_{NO,2}$ at a set-point of 1 mg/l by manipulating Q_a.

In the case of BSM2, [33] proposes a default control strategy (defCL). Its closed-loop control configuration consists of a PI that controls S_O in the fourth tank ($S_{O,4}$) at

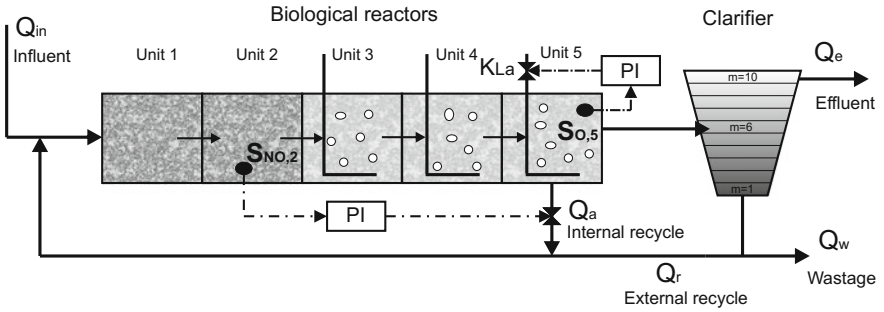

Fig. 2.3 Default control strategy of BSM1

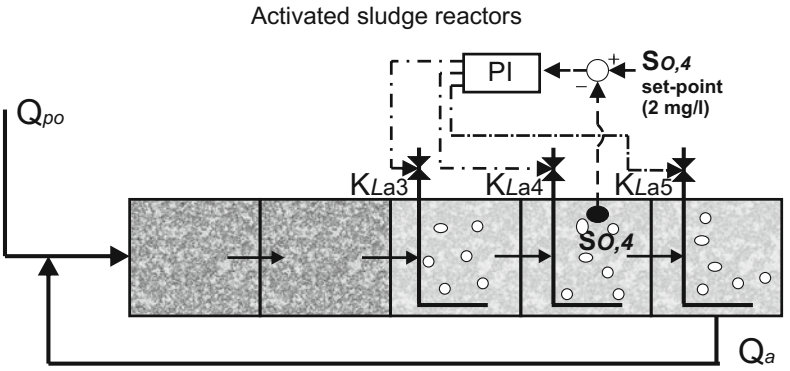

(a) defCL control strategy

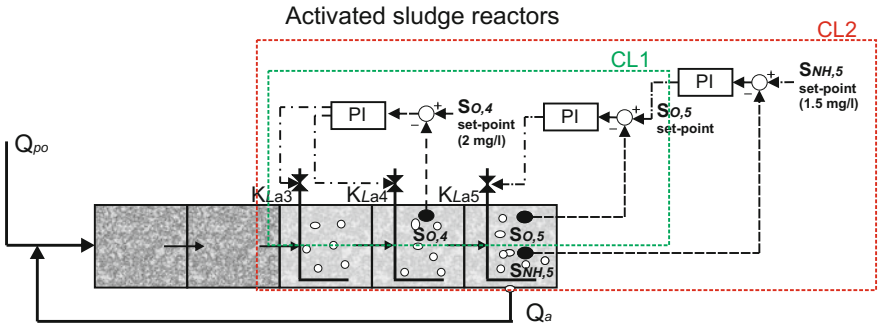

(b) CL1 and CL2 control strategies

Fig. 2.4 Default control strategies of BSM2

a set-point of 2 mg/l by manipulating K_La in the third tank (K_La_3), K_La in the fourth tank (K_La_4) and K_La_5, with K_La_5 set to the half value of K_La_3 and K_La_4. In addition, q_{EC} in the first reactor ($q_{EC,1}$) is added at a constant flow rate of 2 m^3/d. Two different Q_w values are imposed dependent on time of the year: from 0 to 180 days and from 364 to 454 days Q_w is set to 300 m^3/d; and for the remaining time periods Q_w is set to 450 m^3/d.

The finalisation of BSM2 plant layout is reported in [46], in which two new control strategies are proposed. The first control strategy (CL1) is based on modifying the defCL, controlling the $S_{O,4}$ set-point at 2 mg/l, by manipulating K_La_3 and K_La_4, and adding another loop to control $S_{O,5}$ by manipulating K_La_5. PI controllers are applied for both control loops. The second control strategy (CL2) adds a hierarchical control to CL1. Therefore, a PI controller is applied to control S_{NH} in the fifth tank ($S_{NH,5}$) at a set-point of 1.5 mg/l by manipulating $S_{O,5}$ set-point. In the case of CL2, $q_{EC,1}$ is added at a constant value of 1 m^3/d.

Figure 2.4 shows the three explained control strategies.

2.3 Summary

This chapter has introduced the scenarios where the evaluation of the control and operation approaches will be tested. These scenarios are based upon the well known benchmarks commonly used within the wastewater research community. A short description of the BSM1 and BSM2 as well as their basic control strategies have been provided. They are used in the literature in order to compare the results achieved with new control strategies or techniques, in terms of control performance and/or plant performance.

Chapter 3
Control Approaches

In WWTPs, the large number of variables, their intricate interrelation and the strong fluctuations of the influent make the control very complex. Therefore, advanced control techniques are proposed in this book for a successful control in WWTPs: MPC, FC, and ANN. These controllers are briefly described in this chapter.

3.1 Model Predictive Control

3.1.1 Introduction

Model Predictive Control (MPC) refers to a large class of computer control methods which make an explicit use of the process model to predict the future response of the plant. An MPC algorithm attempts to optimize future plant behavior at each control interval by computing a sequence of future manipulated variables. Only the first element of the computed optimal sequence is sent into the plant and the entire calculation is repeated at subsequent control intervals.

Early achievements and industrial implementations in MPC include IDCOM presented in [53] and Dynamic Matrix Control presented in [16]. These first algorithms were based on step or impulse response models. More general linear input–output models structures were presented as Generalized Predictive Control in [12]. Nevertheless, an interest in MPC implementations based on state-space models were created by the proposal presented in [44].

MPC is very popular nowadays in the industry: in process industries, concretely, it is widely used and accepted. Probably the reason is due to its ability to deal with multivariable processes and to handle state and input constraints explicitly. In the field of waste water treatment processes, MPC has demonstrated to be effective and has been vastly used [31, 56, 58, 63] or [54], among others).

I. Santín et al., *Control and Decision Strategies in Wastewater Treatment Plants for Operation Improvement*, Intelligent Systems, Control and Automation: Science and Engineering 86, DOI 10.1007/978-3-319-46367-4_3

The basic concepts of MPC provided in this section are fairly standard and only a brief description with main features is presented here. Nevertheless, the theoretical and practical issues associated with MPC technology are well known in the literature [9, 39].

3.1.2 MPC Principle

The principle of all the controllers belonging to the MPC class is characterized by the following methodology, as represented in Fig. 3.1:

1. At each sampling time k, the future outputs for a horizon p, called the *prediction horizon*, are calculated using the process model. The predicted outputs

$$y(k+i|k), \quad i = 1, 2, \ldots, p \tag{3.1}$$

depend on the known values up to the instant k, i.e., past inputs and outputs, and on the future control signals, for a horizon m, called the *control horizon*, $(m < p)$,

$$u(k+i|k), \quad i = 0, 1, \ldots, m-1 \tag{3.2}$$

Commonly, the control signal (3.2) is implemented as the rate of change,

$$\Delta u(k+i|k) = u(k+i|k) - u(k+i-1|k), \quad i = 0, 1, \ldots, m-1 \tag{3.3}$$

Here, $y(k+i|k)$ is the output, at time $k+i$, predicted based on the measurements at time k; $y(k|k)$ refers to the output measured at time k. Similarly, $\Delta u(k+i|k)$ is the control move at time $k+i$, computed at time k;
2. The sequence of future control signals (3.3) is calculated by minimizing an objective function $J_p(k)$ defined over the prediction horizon p as follows:

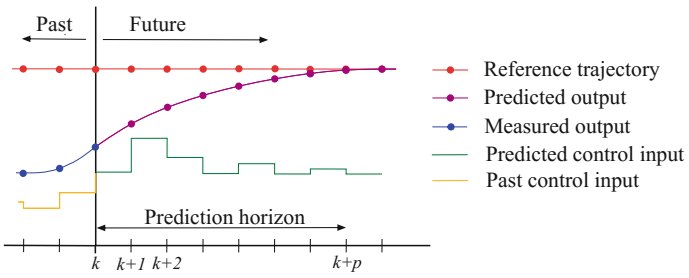

Fig. 3.1 Model predictive control performance

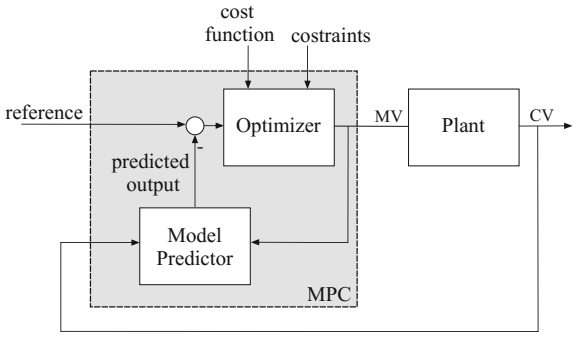

Fig. 3.2 Model predictive control structure

$$\min_{\Delta u(k+i|k),\, i=0,1,\ldots,m-1} J_p(k), \tag{3.4}$$

In essence, the purpose is to keep the process outputs close to the reference signals $r(k+i)$, $i = 0, 1, \ldots$. It should be noted that the objective function (3.4) can be constrained. Nevertheless, with a quadratic criterion, a linear model and without constraints, an explicit solution can be obtained. Otherwise, an iterative optimization method has to be used.

3. Although a sequence of optimal control inputs (3.3) is computed, only the first computed control move $\Delta u(k|k)$ is used. At the next sampling time $k+1$, new measurements are obtained from the plant and the optimization problem (3.4) is solved again. Both the control horizon m and the prediction horizon p move ahead by one step as time moves ahead by one step. The new measurements taken at each time step serve to compensate for unmeasured disturbances and model inaccuracy both of which cause the system output to be different from the one predicted by the model.

The basic structure of an MPC configuration is illustrated in Fig. 3.2 in which MV and CV represent the manipulated and the controlled variables respectively.

The objective function $J_p(k)$ in the optimization problem (3.4) can take many forms to reflect the desired behavior of the predicted output (3.1). The most common among them is the following quadratic form:

$$J_p(k) = \sum_{i=1}^{p} ||\Gamma_y[y(k+i|k) - r(k+i)]||^2 + \sum_{i=1}^{m} ||\Gamma_{\Delta u}[\Delta u(k+i-1)]||^2, \tag{3.5}$$

where $\Gamma_y, \Gamma_{\Delta u} \geq 0$ are weighting matrices.

The following constrains on the manipulated input and output variables can be enforced in the framework of MPC:

Component-wise constrains on the state and output:

$$y_{j,\min} \leq y_j(k+i|k) \leq y_{j,\max}, \quad k \geq 0, \quad i = 1, 2, \ldots, p, \quad j = 1, 2, \ldots, n_y$$

Component-wise constraint on the rate of change of u:

$$|\Delta u_j(k+i|k)| \leq \Delta u_{j,\max}, \quad k \geq 0, \quad i = 0, 1, \ldots, m-1, \quad j = 1, 2, \ldots, n_u$$

It can be shown that the optimization problem (3.4), with $J_p(k)$ given by (3.5), in the presence of any or all of the above mentioned constraints can be reduced to a quadratic program [23] of moderate size.

3.1.3 Predictive Model Identification

The MPC algorithm requires a model to foresee how the plant outputs, $y(k)$, react to the possible variations of the control variables, $\Delta u(k)$, and to compute the control moves at each sampling time k. For the reason that MPC calculates the control signals based on an optimization problem over a prediction horizon, closed-loop performance will depend strongly on the predictive capabilities of the system model. Most industrial MPC algorithms are currently based on linear model representations of the process dynamics [51] and, typically, model parameters are regressed based on prediction error methods.

WWTPs are nonlinear systems, but their operation can be approximated in the vicinity of a working point by a discrete-time state-space liner model,

$$\begin{aligned} x(k+1) &= Ax(k) + Bu(k) \\ y(k) &= Cx(k) + Du(k) + \xi(k), \end{aligned} \tag{3.6}$$

where $u(k)$ is a vector of measured variables (MV), $y(k)$ is a vector of controlled variables (CV), $x(k)$ is a vector of state variables, $\xi(k)$ is a vector of measurement noise and A, B, C, and D are the state-space matrices. A discrete-time transfer function model equivalent to the state-space representation (3.6) can be written in the form of a matrix fraction description [35]:

$$y(k) = [I - \Phi_y(q^{-1})]^{-1}[\Phi_u(q^{-1})u(k)] + \xi(k), \tag{3.7}$$

where q^{-1} denotes the backward shift operator, so $q^{-1}y(k+1) = y(k)$. Multiplying $[I - \Phi_y(q^{-1})]$ on both sides of (3.7) we obtain an Auto Regressive model with eXogenous inputs (ARX) representation,

$$y(k) = \Phi_y(q^{-1})y(k) + \Phi_u(q^{-1})u(k) + \epsilon(k), \tag{3.8}$$

where $\epsilon(k) = [I - \Phi_y(q^{-1})]\xi(k)$.

Models in MPC are usually developed using identification techniques based on process response data [38], in which ARX representation are widely used since the parameter estimation in this model structure is a convex problem. In this context, the multivariable ARX model (3.8) can be written in a vector form as an identification model:

$$y(k) = \phi^T(k)\theta + \epsilon(k), \tag{3.9}$$

where θ is the vector that contains the estimated parameters and $\phi(k)$ is the information matrix, i.e., the set of collected data containing previous outputs and inputs on which the current output depends. Assuming $\epsilon(k) = 0$, the output prediction is denoted by $\hat{y}(k|\theta) = \phi^T(k)\theta$ to empathize that the estimate of $y(k)$ depends from past data and on the parameter vector.

The model parameter estimation approaches in most MPC implementations are mainly based on minimizing a least squares criterion of the form,

$$J = \sum_{k=1}^{L} ||(y(k) - \phi^T(k)\theta||^2 \tag{3.10}$$

The problem is to estimate the vector θ^* that best makes $\hat{y}(k|\theta)$ fit $y(k)$.

3.1.4 Tuning Parameters

The control horizon m, the prediction horizon p, input rate weight $\Gamma_{\triangle u}$, the output weight Γ_y, the sampling time Δt, i.e., the time difference between two consecutive samples, and the overall estimator gain can be used as tuning parameters for the process to perform as required.

The value of the sampling time Δt has a significant effect on the effectiveness of the controller. High values of Δt can give poorer control performance, mainly when there are important input disturbances, and low values of Δt can produce changes too quickly in the actuators and also high energy consumption. Therefore, it is recommended to choose k as the lowest value that allows achieving a successful tracking of the controlled variables, without abrupt changes in the actuators and without a significant aeration cost increase.

To decrease $\Gamma_{\triangle u}$ or to increase Γ_y gives better performance of the controlled variable, otherwise they could produce strong oscillations in the actuators, which must be avoided.

The meaning of prediction horizon p is rater intuitive. It determines the limit of the instants in which it is desirable for the output to follow the reference. If a high value of p is taken it will originate a smooth response of the process and an increase of the computational time. On the other hand, small values reduce the computational effort at expenses of a possible oscillatory process response.

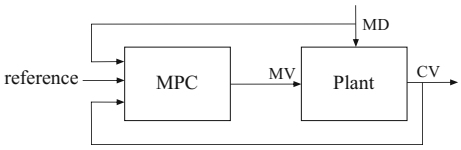

Fig. 3.3 MPC with feedforward control scheme

The control horizon is also another basic tuning parameter for these controllers. Performance of the process output improves as m increases, at the expense of additional computation. Values that are too high can increase the computational time in excess, and on the other hand, values that are too small may result in oscillatory responses.

At each sampling time k, the controller compares the measured values of the outputs with the expected values. The difference can be due to noise, to measurement errors and to unmeasured disturbances. With the overall estimator gain parameter, the percentage of this difference that is attributed to unmeasured disturbances is determined and the calculation matrix is consequently adjusted. Higher overall estimator gains improve the results, but too high values can make the controller unfeasible.

3.1.5 Feedforward Compensation

Due to the presence of strong measurable disturbances (MD) on WWTPs, MPC has difficulties in keeping the controlled variables at their reference level. To compensate the disturbances, a feedforward control action is added, as in [14, 15, 56, 57]. This is illustrated in Fig. 3.3.

MPC provides feedforward compensation for the measured disturbances as they occur to minimize their impact on the output. The combination of feedforward plus feedback control can significantly improve the performance over simple feedback control whenever there is a major disturbance that can be measured before it affects the process output. The idea of the feedforward control is to act on the process when the disturbances appear and before they cause deterioration in the effluent quality.

3.2 Fuzzy Control

3.2.1 Introduction

Fuzzy control methods and algorithms, including many specialized software and hardware available on the market today, may be classified as one type of intelligent control. This is because fuzzy systems modeling, analysis, and control incorporate a certain amount of human knowledge into its components (fuzzy sets, fuzzy logic, and

fuzzy rule base). Using human expertise in system modeling and controller design are not only advantageous but often necessary. Classical controller design has already incorporated human skills and knowledge: for instance, what type of controller to use and how to determine the controller structure and parameters largely depend on the decision and preference of the designer, especially when multiple choices are possible.

Compared with conventional approaches, fuzzy control utilizes more information from domain experts and relies less on mathematical modeling about a physical system. On the one hand, fuzzy control theory can be quite heuristic and somewhat *ad hoc*. This sometimes is preferable or even desirable, particularly when low cost and easy operations are required where mathematical rigor is not the main concern. Within this context, determining a fuzzy set or a fuzzy rule base seems to be somewhat subjective, where human knowledge about the underlying physical system comes into play. On the other hand, fuzzy control theory can be rigorous and fuzzy controllers can have precise and analytic structures with guaranteed closed-loop system stability and some performance specifications, if such characteristics are intended.

It is the purpose of this section not to perform an extensive review neither deep presentation of Fuzzy control. For that purpose there do exists quite good references such as [4, 11, 55] the reader is referred to. Instead, here we intend to present the basic concepts and formulations of a Fuzzy control system that are needed in order to present the Fuzzy controllers that will be applied in subsequent chapters.

3.2.2 Fuzzy Logic Controllers

The task of modeling complex real-world processes for the control system design is a challenging engineering problem. Even if a relatively accurate model to control the process is developed, it is often too complex to use it in controller development, as much simpler process model is required by most of the conventional control design techniques. Fuzzy logic control was first introduced by Mamdani [40] and is based on Zade's theory of fuzzy sets. Conventional controllers, for instance Proportional–Integral–Derivative (PID), employ a process modeled by differential equations. On the other hand, fuzzy control focuses on gaining intuitive understanding for better control of the process, and this information is then loaded directly into fuzzy controller.

The general structure of fuzzy logic controller consists of three basic portions, that is, fuzzification unit at the input terminal, the inference engine built on fuzzy logic control rule base in the core, and the defuzzification unit at the output terminal as shown in Fig. 3.4.

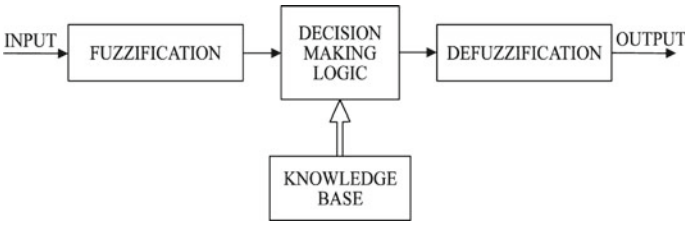

Fig. 3.4 Architecture of a fuzzy logic controller

3.2.3 Fuzzy Sets

A fuzzy set is represented by a membership function defined on the universe of discourse. The universe of discourse is the space where the fuzzy variables are defined. The membership function gives the grade, or degree, of membership within the set, of any element of the universe of discourse. The membership function maps the elements of the universe onto numerical values in the interval [0, 1]. A membership function value of zero implies that the corresponding element is definitely not an element of the fuzzy set, while a value of unity means that the element fully belongs to the set. A grade of membership in between these two values corresponds to the *fuzzy membership* to the set. In crisp set theory, if someone is taller than 1.8 m, we can state that such person belongs to the set of "tall people." However, such sharp change from 1.79 m of a "short person" to 1.81 m of a "tall person" is against the commonsense. Another example could be given as follows: Suppose a highway has a speed limit of 110 km/h. Those who drive faster than 110 km/h belongs to the set A whose elements are violators and their membership function has the value of 1. On the other hand, those who drive slower do not belong to the set A. The sharp transition between membership and nonmembership would be realistic? Should there be a traffic summons issued to drivers who are caught at 110.5 km/h? Or at 110.9 km/h? Therefore, in practical situations there is always a natural fuzzification when someone analyses statements. In such situations a smooth membership curve usually better describes the grade in which an element belongs to a set.

Fuzzification

Fuzzification is the process of decomposing a system input and/or output into one or more fuzzy sets. Many types of curves can be used, but triangular or trapezoidal shaped membership functions are the most common because they are easier to represent in embedded controllers. Figure 3.5 shows a system of fuzzy sets for an input with trapezoidal and triangular membership functions. Each fuzzy set spans a region of input (or output) value graphed with the membership. Any particular input is interpreted from this fuzzy set and a degree of membership is interpreted. The membership functions should overlap to allow smooth mapping of the system. The process of fuzzification allows the system inputs and outputs to be expressed in linguistic terms so that rules can be applied in a simple manner to express a complex system.

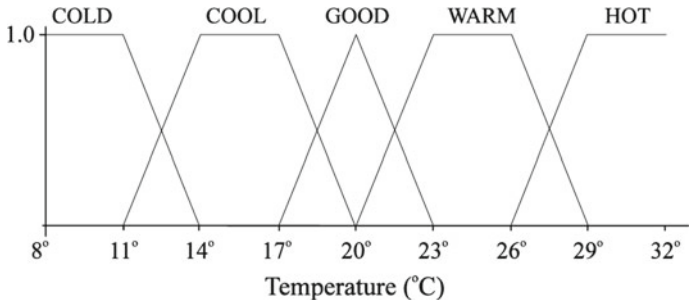

Fig. 3.5 Fuzzification by means of different membership functions

Suppose a simplified implementation for an air conditioning system with a temperature sensor. The temperature might be acquired by a microprocessor which has a fuzzy algorithm to process an output to continuously control the speed of a motor which keeps the room in a *good temperature*. It also can direct a vent upward or downward as necessary. Figure 3.5 illustrates the process of fuzzification of the air temperature. There are five fuzzy sets for temperature: COLD, COOL, GOOD, WARM, and HOT.

The membership function for fuzzy sets COOL and WARM are trapezoidal, the membership function for GOOD is triangular, and the membership functions for COLD and HOT are half triangular with shoulders indicating the physical limits for such process (staying in a place with a room temperature lower than 8 °C or above 32 °C would be quite uncomfortable). The way to design such fuzzy sets is a matter of degree and depends solely on the designer's experience and intuition. The figure shows some nonoverlapping fuzzy sets, which can indicate any nonlinearity in the modeling process. There an input temperature of 18 °C would be considered COOL with a degree of 0.75 and would be considered GOOD with a degree of 0.25.

The fuzzifier adapts the input variables into suitable linguistic values by membership functions. Range of membership functions values are also set: minimum value of the input variable ($MinIn$), maximum value of the input variable ($MaxIn$), minimum value of the output variable ($MinOut$), maximum value of the output variable ($MaxOut$). As the usual situation will be that of an input value that belongs to different membership functions, its degree of membership to each one of those fuzzy concepts should be determined. For example, Fig. 3.6 shows three triangular membership functions ($mf1, mf2$, and $mf3$) with an input value that ranges between $MinIn = 0$ and $MaxIn = 5$. Thus, an input of 1.5 can be transformed into fuzzy expressions as 0.25 of $mf1$ and simultaneously 0.5 of $mf2$.

In order to build the rules that will control the air conditioning motor, we could watch how a human expert would adjust the settings to speed up and slow down the motor in accordance to the temperature, obtaining the rules empirically. If the room temperature is good, keep the motor speed medium, if it is warm, turn the knob of the speed to fast, and blast the speed if the room is hot. On the other hand, if the temperature is cool, slow down the speed and stop the motor if it is cold. This is the

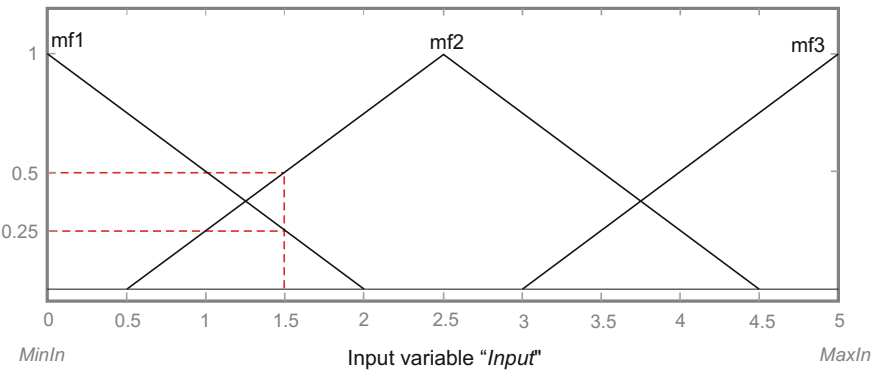

Fig. 3.6 Example of membership functions of fuzzifier

beauty of fuzzy logic: to turn commonsense, linguistic descriptions, into a computer controlled system. Therefore, it is required to understand how to use some logical operations to build the rules.

Boolean logic operations must be extended in fuzzy logic to manage the notion of partial truth - truth values between "completely true" and "completely false." A fuzziness nature of a statement like "X is LOW" might be combined to the fuzziness statement of "Y is HIGH" and a typical logical operation could be given as "X is LOW and Y is HIGH". What is the truth value of this and operation? The logic operations with fuzzy sets are performed with the membership functions. Although there various other interpretations for fuzzy logic operations, the following definitions are very convenient in embedded control applications:

truth(X and Y) = Min(**truth**(X), **truth**(Y))
truth(X or Y) = Max(**truth**(X), **truth**(Y))
truth(not X) = 1.0 - **truth**(X)

Defuzzification

After fuzzy reasoning we have a linguistic output variable which needs to be translated into a crisp value. The objective is to derive a single crisp numeric value that best represents the inferred fuzzy values of the linguistic output variable. Defuzzification is such inverse transformation which maps the output from the fuzzy domain back into the crisp domain. Some defuzzification methods tend to produce an integral output considering all the elements of the resulting fuzzy set with the corresponding weights. Other methods take into account just the elements corresponding to the maximum points of the resulting membership functions. The following defuzzification methods are of practical importance [55]:

- Center-of-Area (C-o-A) - The C-o-A method is often referred to as the Center-of-Gravity method because it computes the centroid of the composite area representing the output fuzzy term.

- Center-of-Maximum (C-o-M) - In the C-o-M method only the peaks of the membership functions are used. The defuzzified crisp compromise value is determined by finding the place where the weights are balanced. Thus the areas of the membership functions play no role and only the maxima (singleton memberships) are used. The crisp output is computed as a weighted mean of the term membership maxima, weighted by the inference results.
- Mean-of-Maximum (M-o-M) - The M-o-M is used only in some cases where the C-o-M approach does not work. This occurs whenever the maxima of the membership functions are not unique and the question is as to which one of the equal choices one should take.

3.2.4 Fuzzy Inference

A connection between cause and effect, or a condition and a consequence is made by reasoning. Reasoning can be expressed by a logical inference, or by the evaluation of inputs in order to draw a conclusion. We usually follow rules of inference which have the form:

if (cause$_1$=A and cause$_2$=B) **then** (effect=C),

where A, B, and C are linguistic variables. For example, **if** "room temperature" is Medium **then** "set fan speed to Fast." Medium is a function defining degrees of room temperature while Fast is a function defining degrees of speed. The intelligence lies in associating those two terms by means of an inference expressed in heuristic **if**-**then** terms.

In order to convert a linguistic term into a computational framework one needs to use the fundamentals of set theory. On the statement **if** "room temperature" is Medium, we have to ask the following question: "Is the room temperature Medium?" A traditional logic, also called Boolean logic, would have two answers: YES and NO. Therefore, the idea of membership of an element x in a set A is a function $\mu_A(x)$ whose value indicates if that element belongs to the set A. Boolean logic would indicate, for example, $\mu_A(x) = 1$, then the element belongs to set A, or $\mu_A(x) = 0$, the element does not belong to set A.

The fuzzy rule base is a set of **if-then** rules that store the empirical knowledge of the experts about the operation of the process. First the fuzzy logic computes the grade of membership of each condition of a rule, and then aggregates the partial results of each condition using fuzzy set operator. The inference engine combines the results of the different rules to determine the actions to be carried out, and the defuzzifier converts the control actions of the inference engine into numerical variables, determining the final control action that is applied to the plant. There are two different methods to operate these modules: Mamdani and Takagi–Sugeno. Mamdani system aggregates the area determined by each rule and the output is determined by the center of gravity of that area. In a Takagi–Sugeno system the

Table 3.1 **if-then** rule base for fuzzy logic control

u(t)		e(t)						
		NB	NM	NS	Z0	PS	PM	PB
$\Delta e(t)$	NB	NB	NB	NB	NB	NM	NS	Z0
	NM	NB	NB	NB	NM	NS	Z0	PS
	NS	NB	NB	NM	NS	Z0	PS	PM
	Z0	NB	NM	NS	Z0	PS	PM	PB
	PS	NM	NS	Z0	PS	PM	PB	PB
	PM	NS	Z0	PS	PM	PM	PB	PB
	PB	Z0	PS	PM	PB	PB	PB	PB

results of the **if-then** rules are already numbers determined by numerical functions of the input variables and therefore no defuzzifier is necessary. The output is determined weighting the results given by each rule with the values given by the **if** conditions.

To implement the fuzzy rules on a digital computer, the discrete-time version is used. Another alternate for determining the weight of control is to design fuzzy rule base in tabular form for the complex control system, that is, representation of linguistic terms in negative big (NB), negative medium (NM), negative small (NS), zero (ZO), positive small (PS), positive medium (PM), and positive big (PB). A typical rule base in tabular form to control the process is shown in Table 3.1.

Using above table, fuzzy logic rule base can be designed for the different processes to be controlled. Let us take an example of the rule.

if $\Delta e(t)$ is NS **and** $e(t)$ is NB **then** $u(t)$ is NB.

Mamdani Model

Fuzzy logic control attempts to design the informal nature of the control design process. The Mamdani architecture [40] is the way to design a fuzzy control system, that is, in the absence of an explicit plant model and/or clear statement of control design objectives, informal knowledge of the operation of the given plant can be coded in terms of **if-then** or condition action, rules and form the basis for the linguistic control strategy, for example, a fuzzy rule.

if speed is high **and** acceleration is small **then** braking is modest

where the speed and acceleration are input variables and on the other hand, braking is an output variable. High, small, and modest are fuzzy sets, and the first two sets are input fuzzy sets and the last one is the output fuzzy set.

Takagi–Sugeno Model

Takagi–Sugeno model [60] is an alternative architecture that uses a combination of linguistic rules and linear functions to form a fuzzy logic control strategy. In the Takagi–Sugeno fuzzy system, the conclusion of the fuzzy set is not a fuzzy set but a crisp function of the inputs. Fuzzy **if-then** rule can be also designed using Takagi–Sugeno modeling and can be expressed as

if (x_1 is A_1) **and** (x_2 is B_1) **then** $y = f_1(x) = c_{10} + c_{11}x_1 + c_{12}x_2$
if (x_1 is A_1) **and** (x_2 is B_2) **then** $y = f_2(x) = c_{20} + c_{21}x_1 + c_{22}x_2$

The functions $f_i(x),\ i = 1, 2, \ldots$ of the input vector $x = [x_1, x_2, \ldots]$ can be very complex but the most commonly used function is linear one that can be described by the coefficients $[c_0, c_1, c_2, \ldots]$.

3.3 Artificial Neural Networks

3.3.1 Introduction

Artificial Neural Networks (ANNs) are inspired by the structure and function of nervous systems. ANNs consist of a large number of simple processors, called neurons [67], with many interconnections computed in parallel. ANNs have proved to be effective for many complex functions, as pattern recognition, system identification, classification, speech vision, and control systems [50, 66]. ANNs are frequently used for nonlinear system identification to model complex relationships between the inputs and the outputs of a system, as it is the case of WWTPs.

Early artificial neural networks were inspired by perceptions of how the human brain operates. In the recent years, applied mathematical techniques have produced a great technological development. ANNs retain two characteristics of the brain as primary features: the ability to *learn* and generalize from limited information [28, 29].

Both biological and artificial neural networks employ massive, interconnected simple processing elements, or neurons. The knowledge stored as the strength of the interconnecting weights (a numeric parameter) in ANNs is modified through a process called learning, using a learning algorithm. This algorithmic function, in conjunction with a learning rule (i.e., backpropagation) is used to modify the weights in the network in an orderly fashion. An ANN is not *programmed*, rather it is *taught* to give an acceptable answer to a particular problem. Input and output values are sent to the ANN, initial weights to the connections in the architecture of the ANN are assigned, and the ANN repeatedly adjusts these interconnecting weights until it successfully produces output values that match the original values. This weighted matrix of interconnections allows the neural network to learn and remember.

3.3.2 The Artificial Neuron

Each neuron performs a simple computation. It receives signals from its input links and uses these values to compute the activation level (or output) for the neuron. This value is passed to other neurons via its output links. Therefore, it is a device that

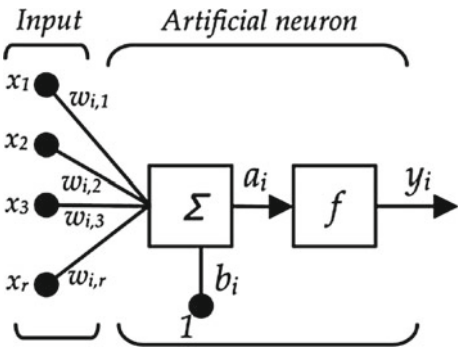

Fig. 3.7 Artificial neuron

generates a single output y from a set of inputs x_j ($j = 1, 2, \ldots, r$). This artificial neuron consists of the following elements (Fig. 3.7):

- Set of x_j inputs with r components
- Set of weights w_{ij} that represent the interaction between the neuron i and neuron j.
- Propagation rule, a weighted sum of the scalar product of the input vector and the weight vector: $a_i = \sum w_{ij} \cdot x_j$.
- Activation function provides the state of the neuron based on the previous state and the propagation rule, i.e., threshold, piecewise linear, sigmoid, or Gaussian.
- The output $y(t)$ that depends on the activation state and is computed according to the equation shown below. This is the result of applying the activation function to the weighted sum of the inputs, less the threshold.

$$a_i = f\left(\sum_{j=1}^{r} w_{ij} \cdot x_j\right) \tag{3.11}$$

Different activation functions can be applied as threshold, piecewise linear, sigmoid, or Gaussian among others. In this book, the sigmoid function is used, which is the most usual one applied. The activation function is often the same for all neurons or at least for a set of neurons. The neurons can have a threshold value that indicates when a neuron is activated. Thus, the threshold value is a parameter of the activation function. For the concrete sigmoid case, the activation function takes the form:

$$f(x) = \frac{1}{1 - e^{-\beta x}}. \tag{3.12}$$

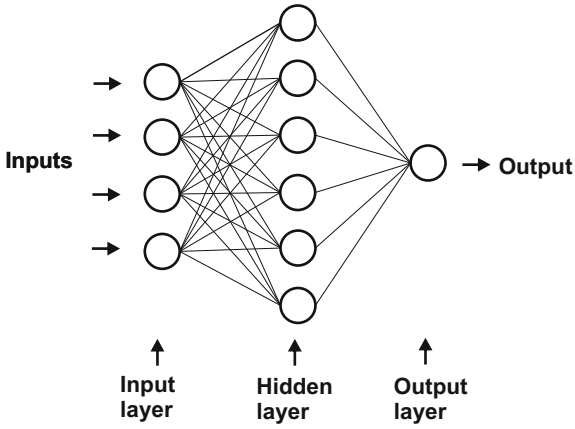

Fig. 3.8 Structure of artificial neural network layers

3.3.3 Types of Artificial Neural Networks

The inner workings and processing of an ANN are often thought of as a *black box* with inputs and outputs. The architecture of an ANN is the structure of network connections. The connections between neurons are directional and the information is transmitted only in one direction. In general, neurons are usually grouped into structural units called layers. Within a layer, the neurons are usually of the same type. The most common type of artificial neural network consists of three groups, or layers, of units: a layer of **input** units is connected to a layer of **hidden** units, which is connected to a layer of **output** units. Figure 3.8 shows the typical network architecture with three layers. The activity of the input units represents the raw information that is fed into the network. The activity of each hidden unit is determined by the activities of the input units and the weights on the connections between the input units and the hidden units. The behavior of the output units depends on the activity of the hidden units and the weights between the hidden units and output units [29].

ANNs are classified according to the structure of network connections. There are two basic structures to connect neurons as follows: feedforward and feedback.

Feedforward Structure

In a feedforward network, which has been proposed in this book, each neuron is connected to the neurons of the following layer and the information flows only from inputs to outputs. They are static in the sense that the output only depends on the inputs and not in the previous states of the network. There are no limitations on number of layers, type of transfer function used in individual artificial neuron or number of connections between individual artificial neurons. The simplest feedforward artificial neural network is a single perceptron that is only capable of learning linear separable problems.

Feedback Structure

In a feedback network the information flows not only in one direction from input to output but also in opposite direction. In addition, they are dynamic, due to the feedback connections, and the output also depends on the previous state. Sometimes, feedback loops involve the use of unit delay elements, which results in nonlinear dynamic behavior, assuming that neural network contains non linear units.

3.3.4 Training of the ANN

Once a network has been structured for a particular application, it is ready to be trained. To start this process, the initial weights are chosen at random. Then, the training, or learning, begins.

Data Collection

Typically, a large data set of inputs / outputs data is needed to design an ANN. If the number of samples is small, the ANN will find a specific solution for the training samples but will not give the general solution. Samples must be representative of the general population.

The choice of input variables of the ANN is a fundamental consideration and it depends largely on the finding of relationships between data available to identify suitable predictors of the output of ANN. The difficulty of selecting input variables occurs due to the number of available variables, which can be very large; correlations between potential input variables, which creates redundancy; and variables that have little or no predictive power.

Learning Methods

ANNs are subjected to a learning process also called training. Typically, a large data set of inputs and outputs is needed to design an ANN, and the input and output data are divided into a set used for training the ANN and the rest for testing the results of the ANN.

In a training process the following actions could be theoretically carried out: Addition and/or removal of connections, addition and/or removal of neurons, modification of weights of the propagation function, modification of thresholds and/or activation functions of neurons. Mostly, the procedure applied in the learning process is the change of weights.

Performance is improved by updating iteratively the weights in the network. Each training section including weights adjustment is called epoch. Usually many epochs, are required to train an ANN. Different algorithms are available for training. When the training is over, the ANN performance is validated, and depending on the results, the ANN has to be trained again or can be implemented. The number of input nodes, output nodes and the nodes in the hidden layer depend upon the problem being studied. If the number of nodes in the hidden layer is small, the network may not

have sufficient degrees of freedom to learn the process correctly, and if the number is too high, the training will take a long time and the network may sometimes overfit the data [36].

There are two main types of training: Supervised training and unsupervised training. In the supervised training, inputs and output samples are supplied. The response of the network to the inputs is measured and the ANN modifies its weights to reduce the error between actual outputs and sample outputs. The backpropagation algorithm is the most usual method in supervised training and it has been chosen for the proposal of the present book. This algorithm is based on the calculation of the derivatives of the output errors and their propagation backwards through the network. In the unsupervised training, only inputs samples are supplied and the ANN adjusts its weights to achieve that similar inputs cause similar outputs.

3.4 Summary

The basis of the control techniques applied in the subsequent chapters of this book have been briefly described here. First, the fundamentals of Model Predictive Control have been provided. Then, the basic concepts and formulations of Fuzzy Control systems have been presented. Finally, the essentials of Artificial Neural Networks have been summarized. It should be empathized that it is not the objective of this chapter to perform a deep presentation nor an extensive review of the control approaches. For this purpose there exists good bibliography the reader is referred to.

Chapter 4
Tracking Improvement of the Basic Lower Level Loops

This chapter presents the lower level control of a hierarchical structure using BSM1 as working scenario. This lower level is based on the default control strategy, i.e., $S_{O,5}$ and $S_{NO,2}$ control by manipulating K_La_5 and Q_a, respectively. Next, the S_O control is extended to the third and fourth tanks by manipulating K_La_3 and K_La_4. In this chapter, MPC+FF has been employed with the objective of improving the S_O and $S_{NO,2}$ tracking in comparison with the default control strategy and with the literature.

4.1 Applying Model Predictive Control Plus Feedforward Compensation

The two PI controllers of the default BSM1 control strategy are replaced here by an MPC+FF with two inputs ($S_{O,5}$ and $S_{NO,2}$) and two outputs (K_La_5 and Q_a), in order to improve the tracking of $S_{O,5}$ and $S_{NO,2}$ set-points, whose results are evaluated by the ISE criterion. Some studies deal with this basic control strategy (S_O of the aerated tanks and S_{NO} of the last anoxic tank), but testing with different controllers such as MPC and FC [6, 15, 27, 31, 62, 65].

In addition, two MPC+FF controllers are added to control S_O in the third tank ($S_{O,3}$) and in the fourth tank ($S_{O,4}$) by manipulating K_La_3 and K_La_4, respectively, see Fig. 4.1.

Different variables have been considered for the feedforward action in the literature, but in our case Q_{in} has been selected for its better results and easiness of measurement. Any change in Q_{in} affects directly the flow rates of all the tanks, modifying their hydraulic retention time. Therefore, it is necessary to adjust the manipulated variables immediately to compensate the Q_{in} disturbances.

I. Santín et al., *Control and Decision Strategies in Wastewater Treatment Plants for Operation Improvement*, Intelligent Systems, Control and Automation: Science and Engineering 86, DOI 10.1007/978-3-319-46367-4_4

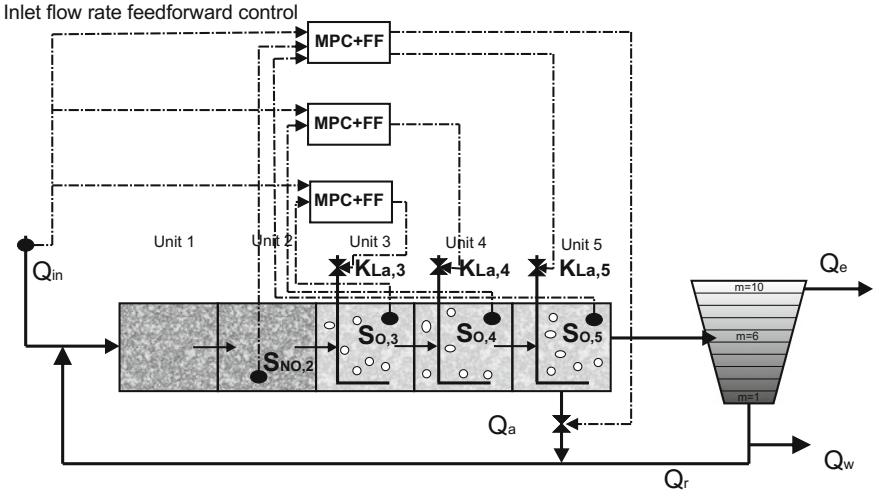

Fig. 4.1 BSM1 with MPC+FF for the control of $S_{NO,2}$ and S_O in the three aerobic tanks

The variables of the state-space model (3.6) for the three MPC controllers are described following: in the controller of $S_{O,5}$ and $S_{NO,2}$ the variable $u_1(k)$ is Q_a, $u_2(k)$ is K_La_5, $u_3(k)$ is Q_{in} and $y_1(k)$ is $S_{NO,2}$ and $y_2(k)$ is $S_{O,5}$; in the controller of $S_{O,4}$ the variable $u_1(k)$ is K_La_4, $u_2(k)$ is Q_{in} and $y_1(k)$ is $S_{O,4}$; finally, in the controller of $S_{O,3}$ the variable $u_1(k)$ is K_La_3, $u_2(k)$ is Q_{in} and $y_1(k)$ is $S_{O,3}$.

The identification of the linear predictive models for the MPC controllers was performed using MATLAB® System Identification Tool. The data of the output variables ($S_{O,3}$, $S_{O,4}$, $S_{O,5}$, and $S_{NO,2}$) are obtained by making changes to the manipulated variables (K_La_3, K_La_4, K_La_5, and Q_a) with a maximum variation of 10 % regarding its operating point, which is the value of K_La necessary to obtain 2 mg/l of S_O and the value of Q_a necessary to obtain 1 mg/l of $S_{NO,2}$. Specifically, the working points are 264.09 day $^{-1}$, 209.23 day $^{-1}$, 131.65 day $^{-1}$ and 16,486 m^3/day for K_La_3, K_La_4, K_La_5 and Q_a, respectively. Different sources were tested to modify the input variables as random, sinusoidal, or step and finally the best fit was obtained with random source. These input variations are performed every 2.4 h, in order to be realistic and to allow sufficient time to ensure the effect of these variations on the output signals. Furthermore, for the feedforward compensation, a step to Q_{in} of +10 % is added over 18,446 m^3/day, which is the average value during the stabilization period.

Two methods were tested for determining the model with the obtained data, prediction error method (PEM) [38] and subspace state-space system identification (N4SID) [49]. Finally, PEM was selected because it fits better with the real data of the plant. The order of the models was chosen from a trade-off between the best fit and the lowest order. Therefore the following third order state-space models are obtained:

$S_{O,5}$ and $S_{NO,2}$ control

$$
\begin{aligned}
A &= \begin{bmatrix} 0.8748 & 0.04463 & 0.1314 \\ 0.04091 & 0.7331 & 0.1796 \\ 0.2617 & -0.1318 & 0.3007 \end{bmatrix} \\
B &= \begin{bmatrix} 7.641 \cdot 10^{-6} & 0.004551 & -2.749 \cdot 10^{-5} \\ -2.631 \cdot 10^{-5} & 0.006562 & -4.551 \cdot 10^{-6} \\ -9.63 \cdot 10^{-6} & -0.02161 & 2.447 \cdot 10^{-5} \end{bmatrix} \\
C &= \begin{bmatrix} 0.8812 & -0.5948 & 0.02114 \\ 1.187 & 0.9893 & -0.3754 \end{bmatrix} \\
D &= \begin{bmatrix} 0 & 0 & 0 \\ 0 & 0 & 0 \end{bmatrix}
\end{aligned}
\tag{4.1}
$$

$S_{O,3}$ control

$$
\begin{aligned}
A &= \begin{bmatrix} 0.7859 & 0.4576 & -0.131 \\ 0.3334 & 0.2599 & 0.2718 \\ -0.003132 & 0.03235 & -1.003 \end{bmatrix} \\
B &= \begin{bmatrix} 0.009308 & -2.285 \cdot 10^{-5} \\ -0.01546 & 3.503 \cdot 10^{-6} \\ 0.003654 & -1.987 \cdot 10^{-5} \end{bmatrix} \\
C &= \begin{bmatrix} 0.6376 & -0.4621 & 0.03698 \end{bmatrix} \\
D &= \begin{bmatrix} 0 & 0 \end{bmatrix}
\end{aligned}
\tag{4.2}
$$

$S_{O,4}$ control

$$
\begin{aligned}
A &= \begin{bmatrix} 0.8201 & 0.371 & -0.1016 \\ 0.3054 & 0.307 & 0.2544 \\ -0.003381 & 0.03144 & -0.9993 \end{bmatrix} \\
B &= \begin{bmatrix} 0.007712 & -4.65 \cdot 10^{-5} \\ -0.0148 & 8.164 \cdot 10^{-6} \\ 0.004523 & -2.526 \cdot 10^{-5} \end{bmatrix} \\
C &= \begin{bmatrix} 0.947 & -0.496 & 0.02472 \end{bmatrix} \\
D &= \begin{bmatrix} 0 & 0 \end{bmatrix}
\end{aligned}
\tag{4.3}
$$

In order to predict the possible application in a real plant, data acquisition for the identification is performed while the plant is kept at a certain desired operating point, whose values are considered suitable for the biological wastewater treatment of this plant. Therefore, what the identification needs is only the possibility of adding some incremental changes to those operating conditions. As mentioned before, the inputs used for identification purposes represent a maximum variation of 10 %. Therefore, they will not disturb the actual plant operation. The generated outputs will reflect the effect of such input variables manipulation. Data for identification has been generated

simulating one week. However, in the case of the real plant, the identification could be carried out in different periods and not necessarily in consecutive days. Plant operator knowledge can in addition be used to know the more appropriate days to perform the experiment.

The selected tuning values for the MPC controllers are $m = 5$, $p = 20$, $\triangle t = 0.00025$ d (21.6 s), $\Gamma_y = 1$ and $\Gamma_{\triangle u} = 0.01$ for $S_{O,3}$, $S_{O,4}$ and $S_{O,5}$ control and $\Gamma_y = 1$ and $\Gamma_{\triangle u} = 0.0001$ for $S_{NO,2}$ control and overall estimator gain = 0.8. It should be noted that the values of m and p are not critical and they can be slightly changed with similar results.

4.2 Simulation Results

4.2.1 $S_{O,5}$ and $S_{NO,2}$ Control

Figure 4.2 shows $S_{O,5}$ and $S_{NO,2}$ for the dry weather case compared with the default PI control. Table 4.1 shows that MPC+FF reduces ISE of $S_{NO,2}$ control more than 99 % and ISE of $S_{O,5}$ control more than 97 % in comparison with the default PI controllers. This control performance improvement results in a 1.1 % of EQI reduction, keeping a similar OCI (residual increment of 0.0063 %).

This comparison is also done for the rain (see Fig. 4.3 and Table 4.1) and storm influents (see Fig. 4.4 and Table 4.1), obtaining similar percentages of improvement: ISE 99.6 % (rain) and 99.5 % (storm) for $S_{NO,2}$ control and 92.02 % (rain) and 90.8 % (storm) for $S_{O,5}$ control, and reducing EQI with MPC+FF 1.03 % for rain and 1.09 %

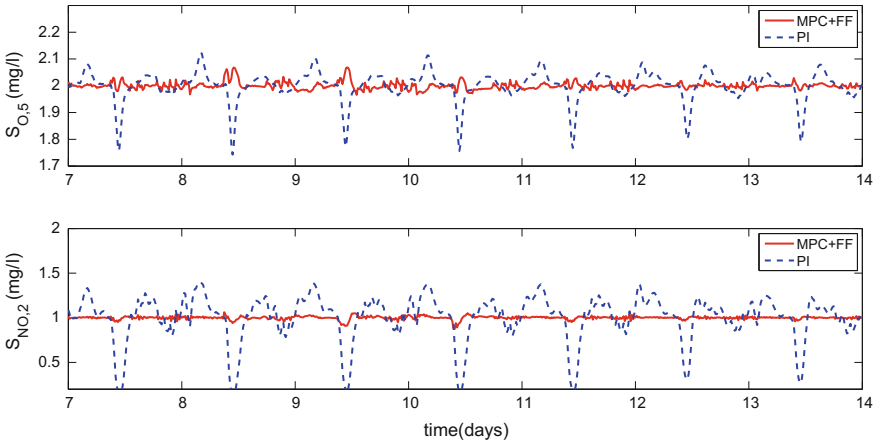

Fig. 4.2 Dry influent: Control performance of $S_{O,5}$ and $S_{NO,2}$ with default PI controllers and with MPC+FF

Table 4.1 ISE, EQI, and OCI results using default PI controllers and MPC+FF for dry, rain, and storm influents

	PI	MPC+FF	%
Dry weather			
ISE ($S_{NO,2}$ control)	0.47	0.0013	−99.7
ISE ($S_{O,5}$ control)	0.022	0.00067	−96.9
EQI (kg pollutants/d)	6115.63	6048.25	−1.1
OCI	16381.93	16382.97	+0.0063
Rain weather			
ISE ($S_{NO,2}$ control)	0.69	0.0028	−99.6
ISE ($S_{O,5}$ control)	0.016	0.0013	−92.02
EQI (kg pollutants/d)	8174.98	8090.29	−1.03
OCI	15984.85	15990.85	+0.037
Storm weather			
ISE ($S_{NO,2}$ control)	0.69	0.0032	−99.5
ISE ($S_{O,5}$ control)	0.020	0.0018	−90.8
EQI (kg pollutants/d)	7211.48	7132.60	−1.09
OCI	17253.75	17261.39	+0.044

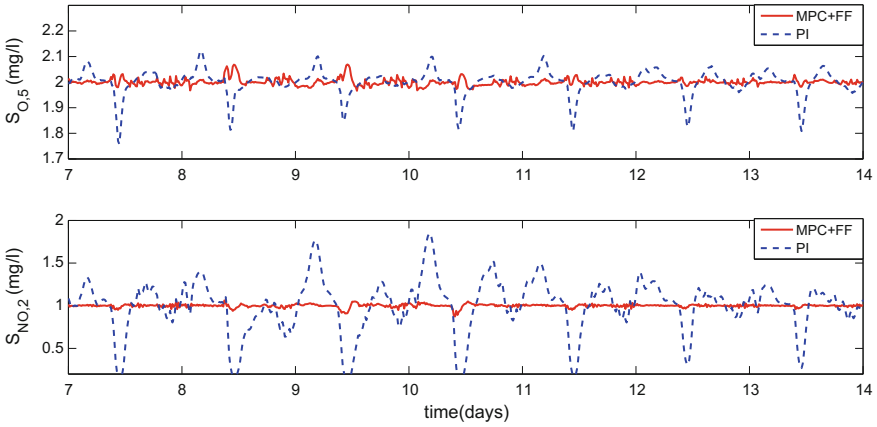

Fig. 4.3 Rain influent: Control performance of $S_{O,5}$ and $S_{NO,2}$ with default PI controllers and with MPC+FF

for storm. OCI is similar, increasing a 0.037 % for rain and 0.044 % for storm; nevertheless this increment cannot be considered significant.

For a more complete comparison, results of works that are present in the literature that provide indicators of the control performance have been added and compared with the proposed MPC+FF for dry influent in Table 4.2. To ensure a fair comparison, it is done with the referenced works, which control $S_{O,5}$ at the set-point of 2 mg/l

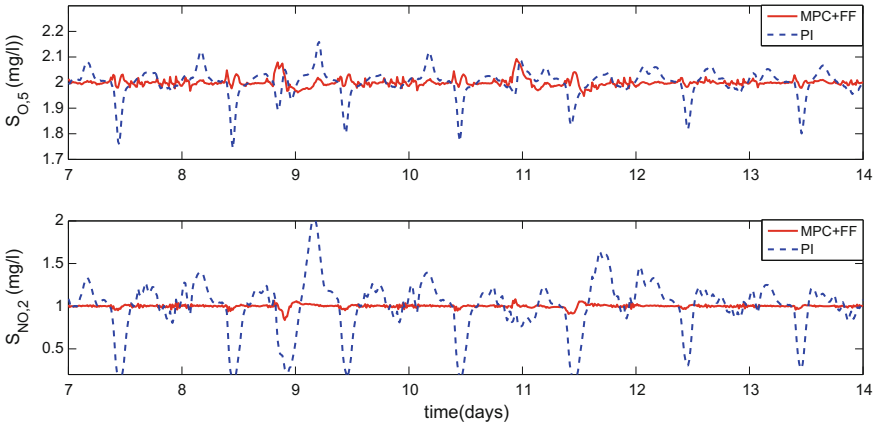

Fig. 4.4 Storm influent: Control performance of $S_{O,5}$ and $S_{NO,2}$ with default PI controllers and with MPC+FF

Table 4.2 Comparison of the performance of $S_{O,5}$ and $S_{NO,2}$ control between MPC+FF and the referenced works

Proposed MPC+FF	$S_{O,5}$ control			$S_{NO,2}$ control			$S_{O,5}$ and $S_{NO,2}$ control
	ISE	IAE	mean($\|e\|$)	ISE	IAE	mean($\|e\|$)	mean($\|e\|$)
	0.00067	0.047	0.0068	0.0013	0.067	0.0096	0.0082
Reference [27]	–	–	–	–	–	–	0.024
Reference [65]	–	–	0.9	–	–	–	–
Reference [31]	0.0026	0.0892	–	–	–	–	–
Reference [6]	0.0012	0.0792	–	–	–	–	–
Reference [62]	0.00092	0.049	–	0.408	1.21	–	–

and/or $S_{NO,2}$ at the set-point of 1 mg/l and use the original version of BSM1. To allow the comparison with the greatest possible number of works, two control performance criteria have been added to the usual ISE: IAE and mean($|e|$).

The improvement of $S_{NO,2}$ and $S_{O,5}$ tracking as a result of applying MPC+FF compared with other control techniques present in the existing literature is shown.

4.2.2 $S_{O,3}$ and $S_{O,4}$ Control

It is also important to obtain a good $S_{O,3}$ and $S_{O,4}$ tracking, because the variation of the S_O set-point is applied to the three aerobic reactors, as shown in the next chapter. Figures 4.5, 4.6, and 4.7 show $S_{O,3}$ and $S_{O,4}$ evolution applying MPC+FF

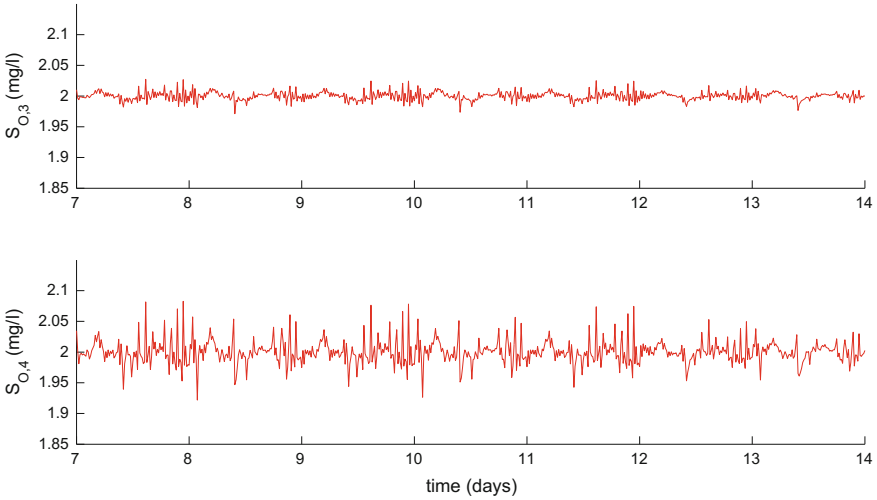

Fig. 4.5 Dry influent: Control performance of $S_{O,3}$ and $S_{O,4}$ with MPC+FF

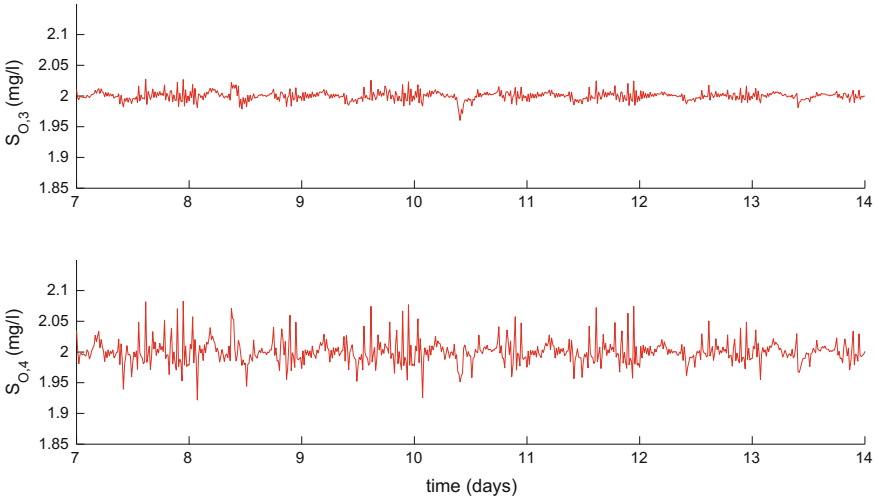

Fig. 4.6 Rain influent: Control performance of $S_{O,3}$ and $S_{O,4}$ with MPC+FF

controllers for the dry, rain and storm influents. Table 4.3 shows satisfactory results of $S_{O,3}$ and $S_{O,4}$ control with the MPC+FF controllers. Comparison of the results has been accomplished only with [65] for dry weather, due to it is the only referred work that provides results of $S_{O,3}$ and $S_{O,4}$ control. However, it can be seen that the control performance results are similar to those obtained with $S_{O,5}$, and even better in the case of $S_{O,3}$, as it is shown in Tables 4.1 and 4.2 of previous section.

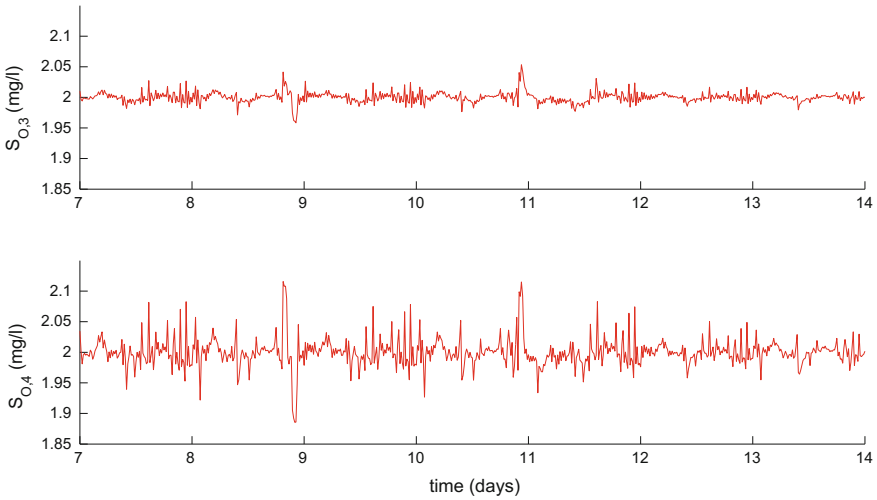

Fig. 4.7 Storm influent: Control performance of $S_{O,3}$ and $S_{O,4}$ with MPC+FF

Table 4.3 Results of $S_{O,3}$ and $S_{O,4}$ control with MPC+FF controllers for dry, rain and storm weather conditions

	$S_{O,3}$ control			$S_{O,4}$ control		
	ISE	IAE	mean($\|e\|$)	ISE	IAE	mean($\|e\|$)
Dry weather						
MPC+FF	0.00037	0.038	0.0054	0.0027	0.096	0.014
Reference [65]	–	–	1.5	–	–	2.7
Rain weather						
MPC+FF	0.0004	0.039	0.0055	0.0027	0.094	0.013
Storm weather						
MPC+FF	0.00056	0.043	0.0062	0.004	0.11	0.015

4.3 Summary

In this chapter, the lower level of a hierarchical control structure has been implemented using BSM1 as working scenario. This is based on $S_{O,3}$, $S_{O,4}$, $S_{O,5}$ and $S_{NO,2}$ control by manipulating K_La_3, K_La_4, K_La_5, and Q_a, respectively.

First, the default control strategy has been evaluated. Next, an MPC+FF controller has tracked $S_{O,5}$ and $S_{NO,2}$, improving the control performance with an ISE reduction of more than 90 % compared to the default PI controllers for the three influents. The control performance of the MPC+FF configuration has been also compared with other approaches existing in the literature, showing the improvement of the proposed method and thus the successful tracking. Next, the S_O control has been extended to

the third and fourth tanks. Thus, two MPC+FF controllers have been added to control $S_{O,3}$ and $S_{O,4}$ by manipulating $K_L a_3$ and $K_L a_4$, respectively, obtaining similar control performance results as in $S_{O,5}$ control.

The tracking improvement of $S_{O,5}$ and $S_{NO,2}$ using MPC+FF controllers result in an EQI reduction of around 1 % with a similar OCI, in comparison with the default PI controllers. In addition, the importance of the satisfactory S_O tracking achieved in the three aerobic tanks is remarkable. This fact is especially important for the implementation of the hierarchical control structure that will be introduced in the next chapter, in order to ensure that the value of S_O is as close as possible to the set-point provided by the higher level.

Chapter 5
Variable Dissolved Oxygen Set-Points Operation

In this chapter the higher level control of a two-level hierarchical structure is proposed using BSM1 as testing plant. The lower level is composed of the MPC + FF controllers described in the previous chapter. The higher level controller has to manipulate S_O set-points of the lower level controllers according to $S_{NH,5}$. The biological treatment of S_{NH} and S_{NO} is the result of various processes given by ASM1. When S_{NH} increases, more S_O is needed for nitrification. On the contrary, when S_{NH} decreases, less S_O is required, producing less S_{NO} (Fig. 5.1).

In this chapter, three alternatives are tested for the higher level: An MPC, an affine function and a FC. For each of these alternatives a range of tuning parameters is proposed. The control alternatives have been tested only by controlling the fifth reactor.

5.1 Higher Level Control Alternatives

Some investigations propose a hierarchical control that regulates the DO set-points, depending on some states of the plant, usually S_{NH} and S_{NO} concentration values in any tank or in the influent [47, 48, 58, 62, 63] or DO in other tanks [17]. Nevertheless, these investigations use PI controllers or MPC as higher level control, trying to keep the controlled variable at a fixed set-point, but with a large resulting error.

5.1.1 Proposed Alternatives

First, a MPC is proposed for the higher level control, with the aim of keeping $S_{NH,5}$ at a fixed set-point by manipulating the $S_{O,5}$ set-point.

Next, an affine function is applied based on the biological processes. The nitrification process is performed by the autotrophic bacteria whose growth is obtained by

I. Santín et al., *Control and Decision Strategies in Wastewater Treatment Plants for Operation Improvement*, Intelligent Systems, Control and Automation: Science and Engineering 86, DOI 10.1007/978-3-319-46367-4_5

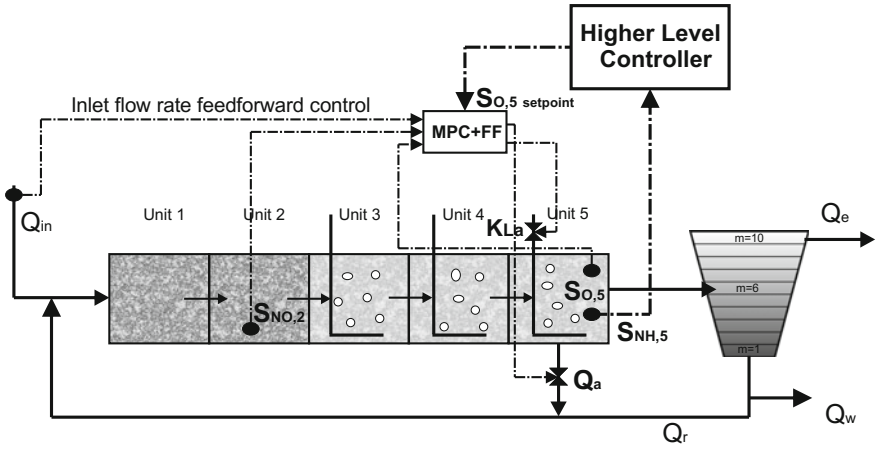

Fig. 5.1 BSM1 with MPC + FF and Hierarchical control

ρ_3 (2.7). As it can be observed, higher S_{NH} and S_O produce a greater S_{NH} removal. However, increasing the S_O value also increases S_{NO} and operational costs, as it can be observed in equations. For this reason it is important to increase S_O when S_{NH} increases to reduce S_{NH} peaks, and decrease S_O when S_{NH} decreases, producing less S_{NO} and reducing costs. Unlike MPC, the affine function regulates $S_{O,5}$ set-point based on $S_{NH,5}$, to obtain the $S_{O,5}$ value, but without having the aim of keeping $S_{NH,5}$ at a reference level. Thus the following affine function is proposed:

$$S_{O,5}\, set - point(t) = S_{NH,5}(t) - k \tag{5.1}$$

where k is a constant. $S_{O,5}$ value obtained is directly proportional to $S_{NH,5}$, subtracting the k value. Also, a constraint of a maximum value of $S_{O,5}$ has been added to improve the EQI and OCI trade-off. Values of k and $S_{O,5}$ maximum are considered as tuning parameters.

Finally, a higher level FC is also implemented, with the same idea of the higher level affine function. Thus, the higher level FC modifies $S_{O,5}$ based on $S_{NH,5}$, but does not try to keep $S_{NH,5}$ at a given set-point. However, the methodology to obtain the $S_{O,5}$ set-point is modified, using fuzzy logic in this case.

5.1.2 Controllers Tuning

Higher Level MPC

As it has been done with lower level MPC in the previous chapter, a linear model (3.6) of the plant is needed to compute predictions of the output variables of the

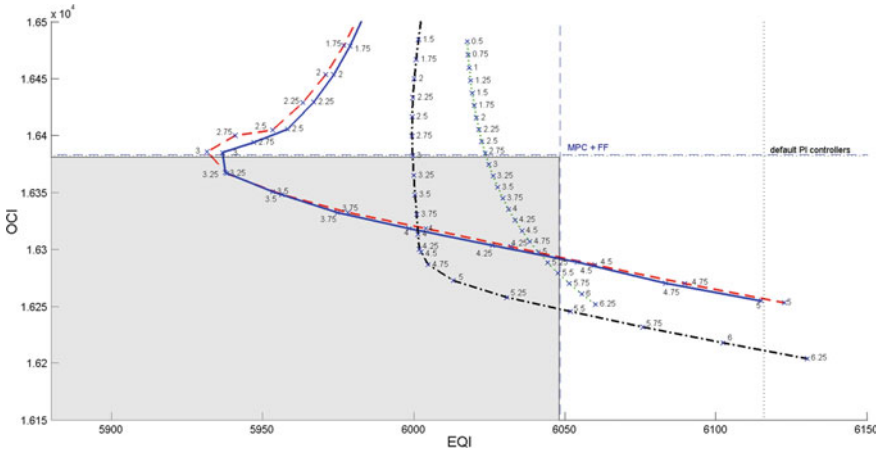

Fig. 5.2 Dry influent: OCI and EQI trade-off with higher level MPC for a range of $S_{NH,5}$ values (points marked with *crosses*) and $\Gamma_{\triangle u} = 0.001$ (*dashed line*), 0.01 (*solid line*), 0.05 (*dash-dotted line*) and 0.1 (*dotted line*)

MPC. In this case, the plant model has one input and one output. Concretely, $u(t)$ is the set-point value of $S_{O,5}$, the manipulated variable, and $y(t)$ is $S_{NH,5}$, the controlled variable.

In order to identify the linear model, $S_{NH,5}$ has been determined by varying the $S_{O,5}$ set-point around 2 mg/l, with maximum values of $\pm 10\,\%$.

By using a prediction error method, a second order state-space model (3.6) is obtained, as

$$A = \begin{bmatrix} 0.2531 & 0.3691 \\ 0.2781 & -0.2695 \end{bmatrix} \qquad B = \begin{bmatrix} -0.4507 \\ -0.1712 \end{bmatrix}$$
$$C = \begin{bmatrix} 0.08655 & -0.01681 \end{bmatrix} \qquad D = 0 \tag{5.2}$$

The following tuning parameters have been selected: $\triangle t = 0.035$ days (50.4 min), $m = 2$, $p = 10$. To determine $\Gamma_{\triangle u}$ and $S_{NH,5}$ set-point values, a trade-off representation for OCI and EQI is provided and showed in Fig. 5.2. Every line corresponds to the results obtained for different $\Gamma_{\triangle u}$ (0.1, 0.05, 0.01 and 0.001), and the points marked with crosses are the results for a range of $S_{NH,5}$ set-point values, from 0.5 to 6.5 with increments of 0.25.

The results with MPC + FF alone and with default PI controllers alone are also represented. Figure 5.2 shows an area in which results obtained with higher level MPC controller improve simultaneously OCI and EQI in comparison with MPC + FF and with default PI controllers alone. This is the proposed tuning region, which determines the ranges for $\Gamma_{\triangle u}$ and $S_{NH,5}$ set-point that outperform both MPC + FF alone as well as PI controllers. In fact the curves within the shaded area provide a Pareto front whose corresponding tunings dominates the previous options.

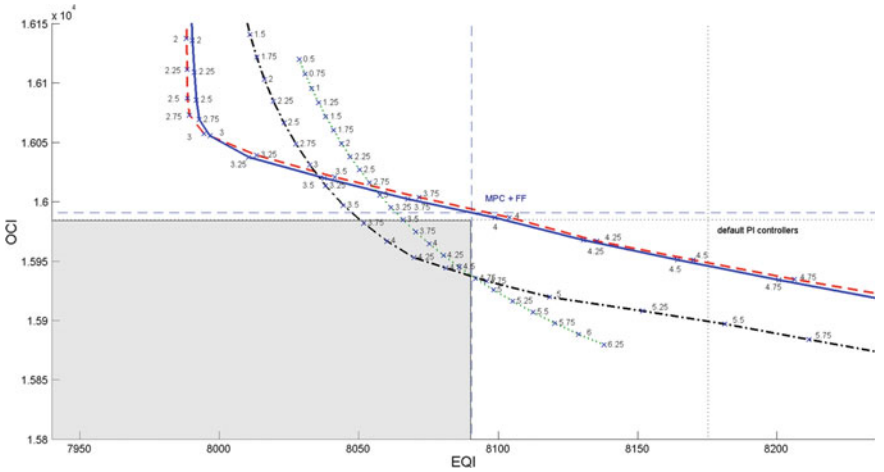

Fig. 5.3 Rain influent: OCI and EQI trade-off with higher level MPC for a range of $S_{NH,5}$ values (points marked with *crosses*) and $\Gamma_{\triangle u} = 0.001$ (*dashed line*), 0.01 (*solid line*), 0.05 (*dash-dotted line*) and 0.1 (*dotted line*)

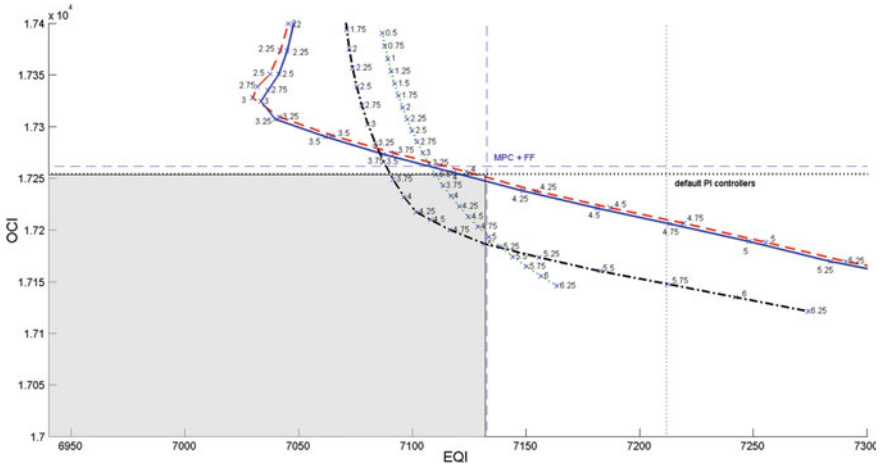

Fig. 5.4 Storm influent: OCI and EQI trade-off with higher level MPC for a range of $S_{NH,5}$ values (points marked with *crosses*) and $\Gamma_{\triangle u} = 0.001$ (*dashed line*), 0.01 (*solid line*), 0.05 (*dash-dotted line*) and 0.1 (*dotted line*)

The OCI and EQI trade-off representation has also been done for rain and storm influents (Figs. 5.3 and 5.4 respectively), obtaining also the corresponding tuning regions. However, they are smaller than the one obtained for the dry influent.

Taking into account, the OCI and EQI trade-off representations for dry, rain, and storm influents (Figs. 5.2, 5.3 and 5.4 respectively), $\Gamma_{\triangle u}$ and $S_{NH,5}$ set-points have been selected for the cases of lowest EQI without increasing OCI and the lowest

Table 5.1 Higher level MPC tuning: $\Gamma_{\triangle u}$ and $S_{NH,5}$ set-point

	Dry		Rain		Storm	
	Lowest EQI	Lowest OCI	Lowest EQI	Lowest OCI	Lowest EQI	Lowest OCI
$\Gamma_{\triangle u}$	0.001	0.05	0.05	0.05	0.05	0.05
$S_{NH,5}$ set-point	3.1	5.4	3.75	4.6	3.7	5

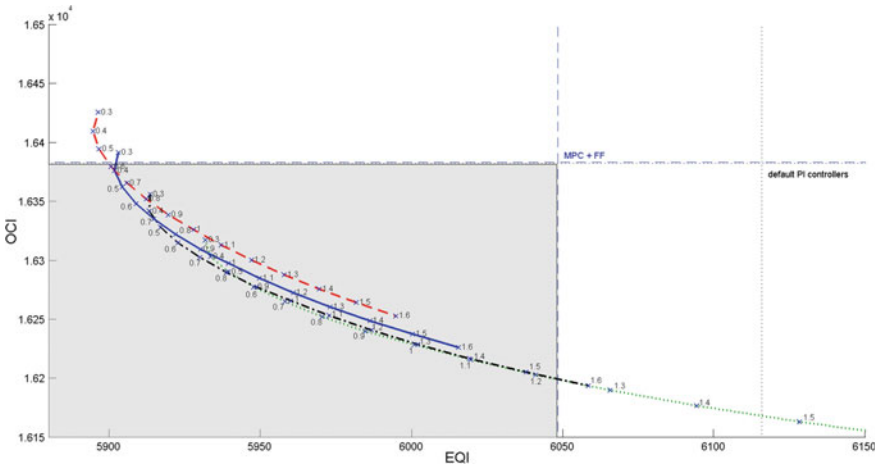

Fig. 5.5 Dry influent: OCI and EQI trade-off with higher level affine function for a range of k values (points marked with *crosses*) and $S_{O,5}$ maximum = 4 (*dashed line*), 3.5 (*solid line*), 3 (*dash-dotted line*), 2.5 (*dotted line*)

OCI without worsening EQI for every influent in comparison with MPC + FF alone (Table 5.1). The selected values correspond with the crossing of the tuning Pareto front with the horizontal and vertical lines passing to the MPC + FF tuning point.

Higher Level Affine Function

For the affine function, k values and maximum values of $S_{O,5}$ have been selected for the OCI and EQI trade-off representation showed in Fig. 5.5. In this case, each line corresponds to the results obtained with different $S_{O,5}$ maximum values (2.5-k; 3-k; 3.5-k; 4-k and 4.5-k), while each one of the points marked with crosses are the results obtained for different values of k (from 0.3 to 1.6 with increments of 0.1). In the same way, the results obtained with MPC + FF alone and with PI default controllers alone are also shown.

The same range of k and $S_{O,5}$ maximum values have been tested for rain and storms influents, obtaining also the trade-off representations (Figs. 5.6 and 5.7 respectively).

As for the MPC + FF controller, a Pareto front is obtained, which provides the tuning region that results in a simultaneous improvement of OCI and EQI in com-

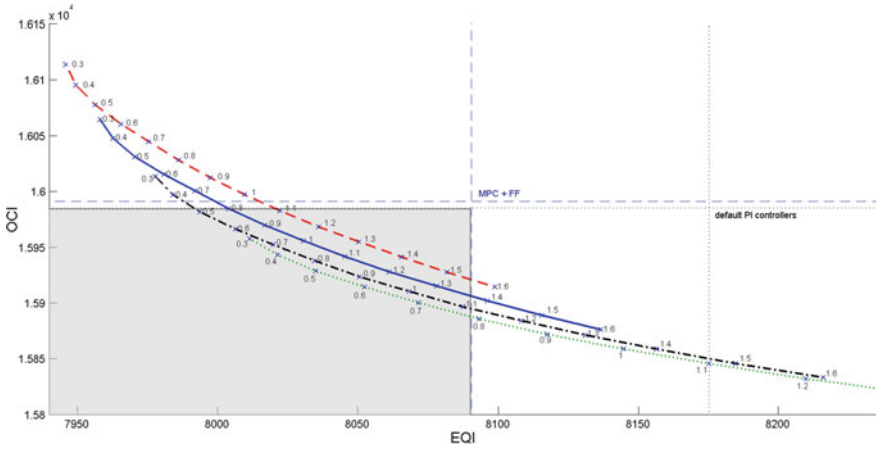

Fig. 5.6 Rain influent: OCI and EQI trade-off with higher level affine function for a range of k values (points marked with *crosses*) and $S_{O,5}$ maximum = 4 (*dashed line*), 3.5 (*solid line*), 3 (*dash-dotted line*), 2.5 (*dotted line*)

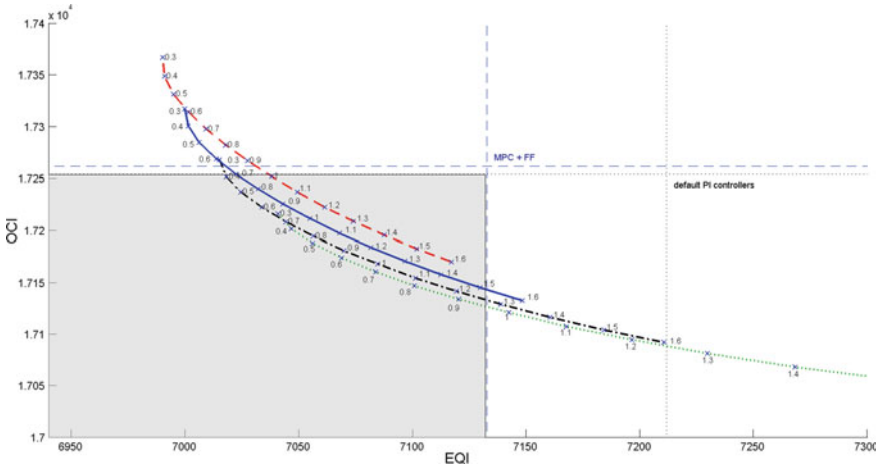

Fig. 5.7 Storm influent: OCI and EQI trade-off with higher level affine function for a range of k values (points marked with *crosses*) and $S_{O,5}$ maximum = 4 (*dashed line*), 3.5 (*solid line*), 3 (*dash-dotted line*), 2.5 (*dotted line*)

parison with MPC + FF alone and with default PI controllers alone, are larger than those obtained with higher level MPC.

Taking into account the trade-off representations (see Figs. 5.5, 5.6, and 5.7), Table 5.2 shows $S_{O,5}$ maximum and k values for the extreme cases of lowest EQI without increasing OCI and the lowest OCI without worsening EQI in comparison with MPC + FF alone and default PI controllers alone.

Table 5.2 Higher level affine function tuning: k and $S_{O,5}$ maximum values

	Dry		Rain		Storm	
	Lowest EQI	Lowest OCI	Lowest EQI	Lowest OCI	Lowest EQI	Lowest OCI
k	0.59	1.23	0.48	0.79	0.39	0.96
$S_{O,5}$ maximum	3.41	1.27	2.52	1.71	2.61	1.54

Higher Level Fuzzy Controller

The design of a FC is based on the knowledge of the process behavior. Here, the implementation of the proposed FC was based on the observation of the simulations results obtained by operating the plant with the default control of BSM1.

The input of the FC is $S_{NH,5}$, the controlled variable. Three triangular membership functions are applied to this input to fuzzify. The following fuzzy sets have been used: *low*, *medium*, and *high*.

The output of the controller is the $S_{O,5}$ set-point for the lower level control. Also three triangular membership functions have been applied to the output with the same fuzzy sets: *low*, *medium*, and *high*.

The if-then fuzzy rules, in fact the controllers decision logic, that relate the input and output are:

if ($S_{NH,5}$ is *low*) **then** ($S_{O,5}$ is *low*)
if ($S_{NH,5}$ is *medium*) **then** ($S_{O,5}$ is *medium*)
if ($S_{NH,5}$ is *high*) **then** ($S_{O,5}$ is *high*)

The Mamdani method has been chosen to defuzzify the results of the above if-then fuzzy rules and thereby to obtain a single value of the $S_{O,5}$ set-point based on the value of $S_{NH,5}$.

Values of *MinIn* and *MinOut* are both fixed to 0.1. Several OCI and EQI results have been obtained for different values of *MaxIn* (3, 4, 5 and 7) and *MaxOut* (2, 2.5, 3, 3.5, 4, 4.5, 5 and 5.5). With these results, trade-off representations of EQI and OCI for the three influents (dry, rain and storm) are made (Figs. 5.8, 5.9, and 5.10), obtaining a tuning area where both OCI and EQI are improved in comparison with MPC + FF alone and with the default PI controllers.

The areas of the tuning regions, which result in a simultaneous improvement of OCI and EQI in comparison with MPC + FF alone and with default PI controllers alone, are similar to the ones corresponding to the higher level with affine function. Therefore, both higher level controllers provide similar advantages.

Table 5.3 shows the *MaxIn* and *MaxOut* values for the extreme cases of lowest EQI without increasing OCI and lowest OCI without worsening EQI in comparison with MPC + FF alone and default PI controllers alone for the three influents.

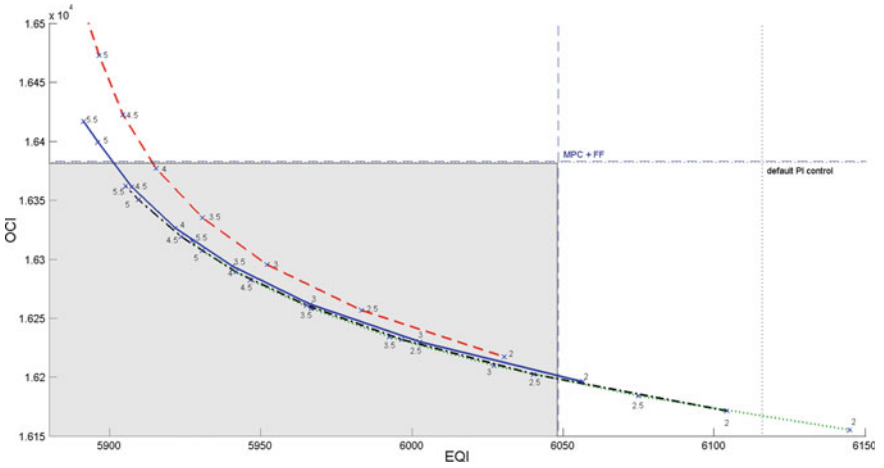

Fig. 5.8 Dry influent: OCI and EQI trade-off with higher level FC for a range of *MaxOut* values (points marked with *crosses*) and *MaxIn* = 3 (*dashed line*), 5 (*solid line*), 7 (*dash-dotted line*), and 9 (*dotted line*)

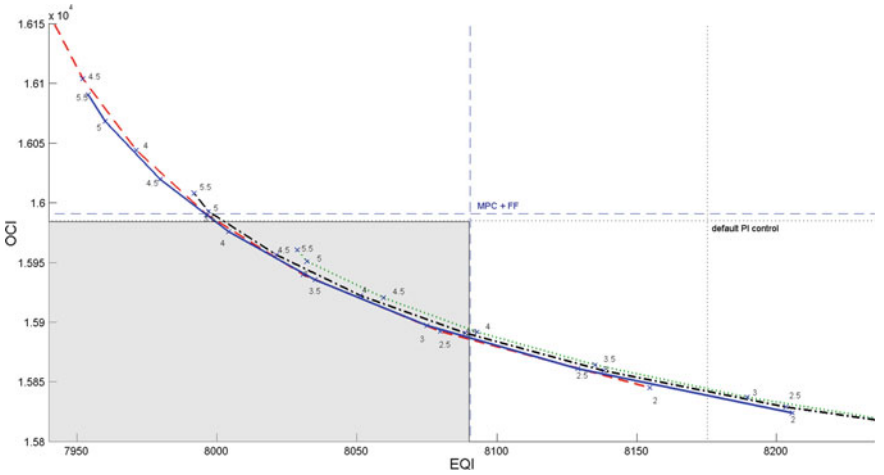

Fig. 5.9 Rain influent: OCI and EQI trade-off with higher level FC for a range of *MaxOut* values (points marked with *crosses*) and *MaxIn* = 3 (*dashed line*), 5 (*solid line*), 7 (*dash-dotted line*), and 9 (*dotted line*)

5.1.3 Simulations Results

In this section the selected controllers tunings will be applied in order to analyze its results. For each one of the three controllers, the two extreme tunings will be tested and compared. Results of the two-level control architecture will also be faced against the use of the lower level MPC + FF alone.

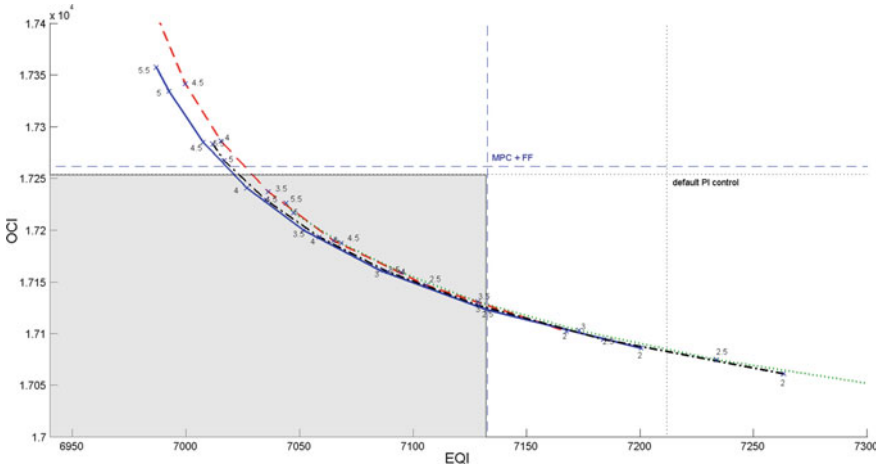

Fig. 5.10 Storm influent: OCI and EQI trade-off with higher level FC for a range of *MaxOut* values (points marked with *crosses*) and *MaxIn* = 3 (*dashed line*), 5 (*solid line*), 7 (*dash-dotted line*) and 9 (*dotted line*)

Table 5.3 Higher level FC tuning: *MaxIn* and *MaxOut* values

	Dry		Rain		Storm	
	Lowest EQI	Lowest OCI	Lowest EQI	Lowest OCI	Lowest EQI	Lowest OCI
MaxIn	5	9	5	3	5	5
MaxOut	4.78	2.76	4.1	2.41	4.14	2.5

Higher Level MPC

In order to improve EQI, the values of S_{NH} and S_{NO} have to be reduced because they are the pollutants with largest influence on the effluent quality. Figure 5.11 shows $S_{NH,5}$, S_{NO} in the fifth tank ($S_{NO,5}$) and $S_{O,5}$ for dry influent with the tuning parameters where the best EQI without increasing OCI is obtained. As it is shown in Fig. 5.11, by varying the $S_{O,5}$ set-point with two-level hierarchical control, $S_{NH,5}$ peaks and $S_{NO,5}$ are reduced. In the case of higher level MPC, when $S_{NH,5}$ is over the fixed set-point, $S_{O,5}$ reference of the lower level control is increased, which produces more oxidation of $S_{NH,5}$ and consequently softens its peaks, while $S_{NO,5}$ and the aeration costs grow. In opposition, when the $S_{NH,5}$ is under the fixed set-point, $S_{O,5}$ reference is decreased, $S_{NH,5}$ goes up and $S_{NO,5}$ and aeration costs go down. The final balance from day 7 to day 14 is a reduction of 1.8 % of EQI in comparison with MPC + FF alone (see Table 5.4).

The same concentrations ($S_{NH,5}$, $S_{NO,5}$, and $S_{O,5}$) for rain and storm influents are shown in Figs. 5.12 and 5.13 respectively. Within 7 days of simulation (day 7 to 14), two days are shown coinciding with a rainfall (Fig. 5.12) and a storm (Fig. 5.13) events. As it is observed, during the rain and storm events, the differences of $S_{NH,5}$

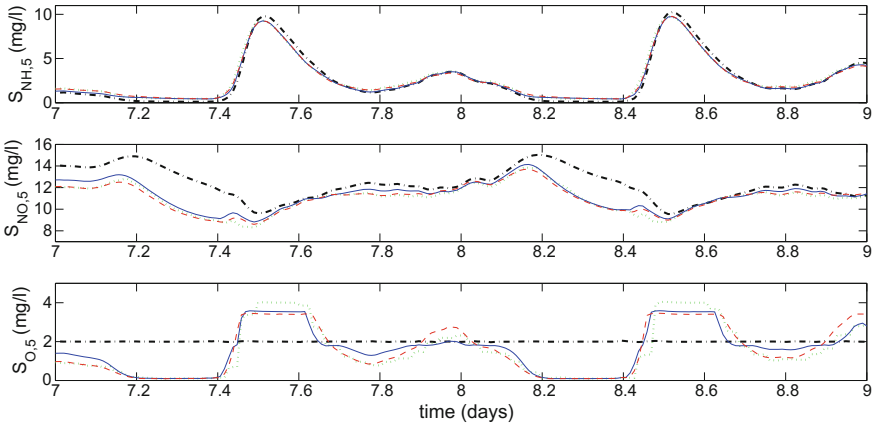

Fig. 5.11 Dry influent: Comparison of $S_{NH,5}$, $S_{NO,5}$, and $S_{O,5}$. MPC + FF (*dash-dotted line*), higher level MPC (*dotted line*), higher level affine function (*dashed line*), and higher level FC (*solid line*)

peaks and $S_{NO,5}$ for higher level MPC and MPC + FF are lower compared with dry weather. This has a direct consequence on the EQI results shown in Table 5.4. As it can be seen, there is also an improvement by working with higher level MPC in comparison with MPC + FF alone, but with a lower percentage compared with dry weather. For the rain influent case, EQI is decreased by 0.4 % and for the storm influent case, EQI is decreased by 0.5 %.

In the opposite point of the trade-off representations (Figs. 5.2, 5.3, 5.4) (best OCI without worsening effluent quality), OCI results are compared for the different control structures with the three weather conditions. Figure 5.14 shows K_La_5 for the higher level MPC. The aeration costs depend directly on the K_La_5 values. Figure 5.14 shows that the values of K_La_5 with higher level MPC are lower most of the time than those obtained with MPC + FF alone, proving that costs can be reduced without increasing EQI with a better optimization of K_La_5. This reduction of K_La_5 results in a reduction of 0.8 % of OCI (Table 5.4).

The K_La_5 evolution is also shown for rain and storm influents (Figs. 5.15 and 5.16 respectively), obtaining also an OCI reduction when working with the higher level MPC in comparison with MPC + FF alone. In this case, with less percentage in comparison with dry influent results (see Table 5.4): for rain influent, higher level MPC reduces OCI by 0.3 %, and for storm influent the reduction is 0.4 %.

The optimization of the $S_{O,5}$ set-point value results in an AE reduction of 202.2, 96.42 and 137.92 KWh/d for dry, rain and storm influents respectively, compared with default BSM1 control, which corresponds, in terms of percentage, to an AE reduction of 5.4, 2.6, and 3.7 %, respectively.

Higher Level Affine Function

With the tuning parameters where the best EQI without increasing OCI is obtained (see Table 5.2), comparing $S_{NH,5}$ peaks and $S_{NO,5}$ for higher level affine function and higher level MPC for the three influents (see Figs. 5.11, 5.12, and 5.13), a remarkable

Table 5.4 EQI and OCI results with MPC + FF, higher level MPC, higher level affine function and higher level FC for dry, rain, and storm influents

	MPC + FF	Higher level MPC			Higher level affine function			Higher level FC		
		Lowest EQI	Lowest OCI	%	Lowest EQI	Lowest OCI	%	Lowest EQI	Lowest OCI	%
Dry weather										
EQI (kg pollutants/d)	6048.31	5936.16	6045.44	−1.8	5900.98	6047.52	−2.4	5900.73	6047.95	−2.4
OCI	16382.97	16382.64	16248.79	−0.8	16381.54	16196.68	−1.1	16382.67	16197.86	−1.1
Rain weather										
EQI (kg pollutants/d)	8090.29	8056.07	8089.98	−0.4	7994.58	8090.38	−1.1	7998.78	8090.27	−1.1
OCI	15990.85	15982.47	15939.32	−0.3	15984.16	15887.47	−0.6	15984.23	15884.21	−0.6
Storm weather										
EQI (kg pollutants/d)	7132.60	7094.90	7131.57	−0.5	7019.08	7132.21	−1.5	7020.83	7132.25	−1.5
OCI	17261.39	17252.84	17186.58	−0.4	17252.51	17126.55	−0.8	17252.6	17123.01	−0.8

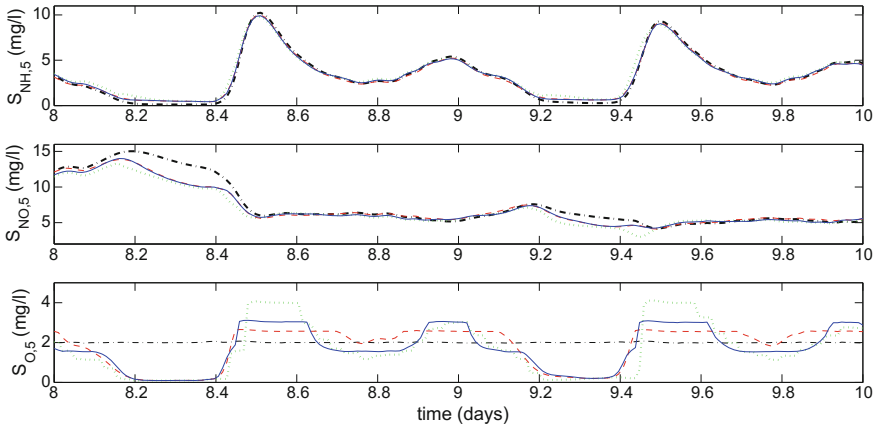

Fig. 5.12 Rain influent: Comparison of $S_{NH,5}$, $S_{NO,5}$, and $S_{O,5}$. MPC + FF (*dash-dotted line*), higher level MPC (*dotted line*), higher level affine function (*dashed line*) and higher level FC (*solid line*)

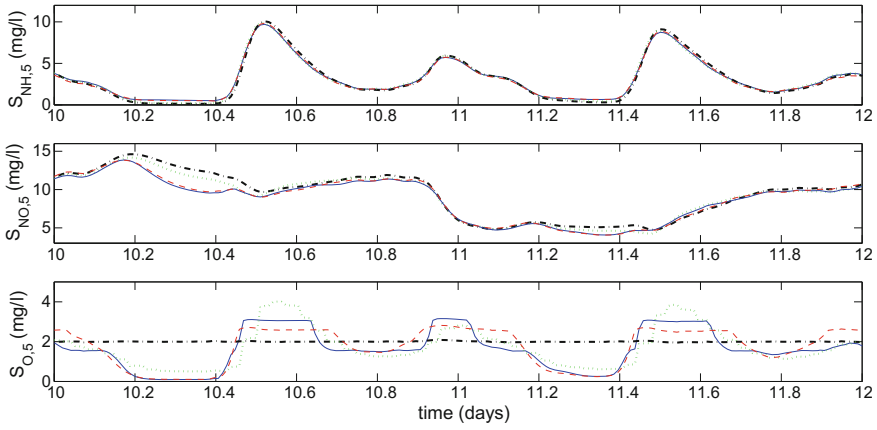

Fig. 5.13 Storm influent: Comparison of $S_{NH,5}$, $S_{NO,5}$, and $S_{O,5}$. MPC + FF (*dash-dotted line*), higher level MPC (*dotted line*), higher level affine function (*dashed line*) and higher level FC (*solid line*)

difference is not observed. However Table 5.4 shows that affine function is able to reduce EQI in comparison with higher level MPC by 0.6 % for dry influent, 0.7 % for rain influent and 1 % for storm influent. In comparison with MPC + FF alone the reduction is 2.4 % for dry influent, 1.1 % for rain influent and 1.5 % for storm influent.

Applying the tuning parameters to obtain the best OCI without worsening effluent quality, $K_L a_5$ is compared with the other control structures for the three weather conditions (see Figs. 5.14, 5.15, and 5.16), obtaining better $K_L a_5$ optimization compared with MPC + FF alone and higher level MPC for the three influents, which result in

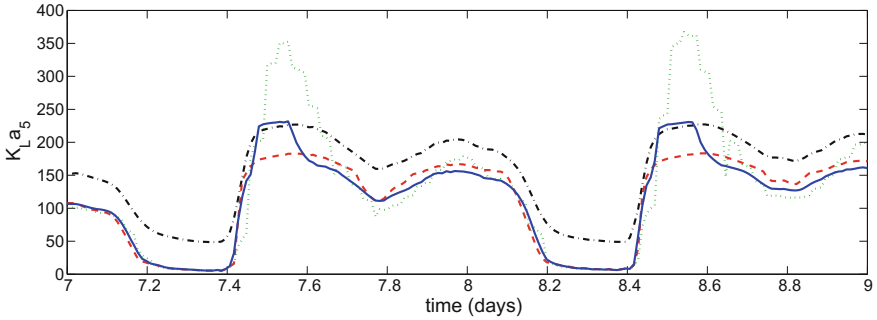

Fig. 5.14 Dry influent: Comparison of $K_L a_5$ in the fifth tank. MPC + FF (*dash-dotted line*), higher level MPC (*dotted line*), higher level affine function (*dashed line*), and higher level FC (*solid line*)

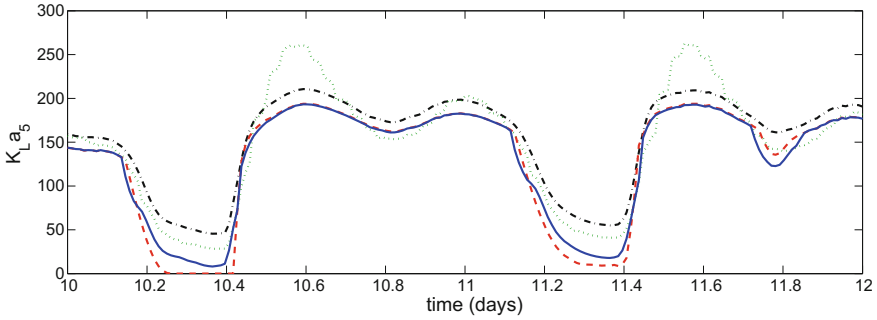

Fig. 5.15 Rain influent: Comparison of $K_L a_5$ in the fifth tank. MPC + FF (*dash-dotted line*), higher level MPC (*dotted line*), higher level affine function (*dashed line*), and higher level FC (*solid line*)

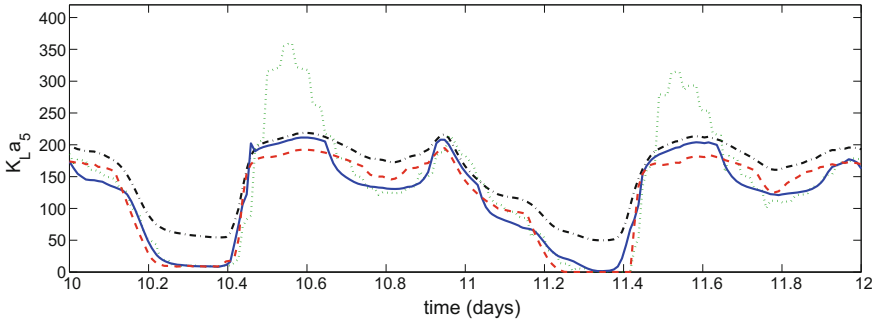

Fig. 5.16 Storm influent: Comparison of $K_L a_5$ in the fifth tank. MPC + FF (*dash-dotted line*), higher level MPC (*dotted line*), higher level affine function (*dashed line*), and higher level FC (*solid line*)

an OCI reduction in comparison with higher level MPC of 0.3 % for dry influent, 0.3 % for rain influent and 0.4 % for storm influent. In comparison with MPC + FF the reduction is 1.1 % for dry influent, 0.6 % for rain influent and 0.8 % for storm influent (see Table 5.4).

This cost reduction is due primarily to an AE reduction of 259.45, 170.87 and 209.85 KWh/d for dry, rain and storm influents respectively, compared with default BSM1 control, which corresponds, in terms of percentage, to an AE reduction of 7, 4.7, 5.6 %, respectively.

Higher Level Fuzzy Controller

For the case of the best EQI obtained, Figs. 5.11, 5.12, and 5.13 show that $S_{NH,5}$ and $S_{NO,5}$ for the three influents are similar compared to higher level affine function. The EQI results are shown in Table 5.4 and they are very similar to the ones obtained with the higher level affine function.

Applying the tuning parameters for obtaining the lowest OCI, Figs. 5.14, 5.15, and 5.16 show K_La_5 for the three sweather conditions. Looking at the OCI results in Table 5.4, there is no significant difference compared with higher level affine function, getting also the same percentages of improvement over MPC + FF alone and higher level MPC.

The reduction of AE is also similar to the results obtained using an affine function as higher level controller: 255.67, 199.99, and 199.72 KWh/d for dry, rain, and storm influents respectively, compared with default BSM1 control, which corresponds, in terms of percentage, to an AE reduction of 6.9, 5.4, 5.3 %, respectively. As a result, for the higher level control, with affine function and FC, the following improvements are obtained in comparison with higher level MPC: For dry influent, AE reduction of 57.25 and 53.47 KWh/d respectively. For rain influent, 74.45 and 103.57 KWh/d respectively. And for storm influent, 71.93 and 61.8 KWh/d respectively.

The reason of the improvement of the results of EQI and OCI by using the higher level FC or the higher level affine function compared to the higher level MPC is that the higher level MPC tries to maintain the value of $S_{NH,5}$ at a fixed reference, but the error is too high. Specifically, the ISE is 36.21 to achieve the best EQI and the ISE is 22.69 to achieve the best OCI. Conversely, higher level affine function and higher level FC regulate $S_{O,5}$ set-point based on the biological process dynamics that take place in the reactors (2.3, 2.4, 2.5, 2.6, 2.7, 2.8). On the one hand improving the nitrification process (2.7) when $S_{NH,5}$ increases, and therefore reducing its peaks. On the other hand, reducing the $S_{O,5}$ set-point level when $S_{NH,5}$ decreases in order to reduce the S_{NO} generation (2.4) and the operational costs (2.13).

5.2 Application of Variable Dissolved Oxygen in the Three Aerobic Reactors

The hierarchical control presented in the previous section is based on manipulating the $S_{O,5}$ set-point. In this section the lower level control is expanded with an independent manipulation of the $S_{O,3}$, $S_{O,4}$, and $S_{O,5}$ set-points.

As it has been shown in Sect. 5.1, the results of OCI and EQI with higher level affine function and higher level FC were similar and better than those obtained with higher level MPC. Thus, the manipulation of the three aerobic reactors (see Fig. 5.17)

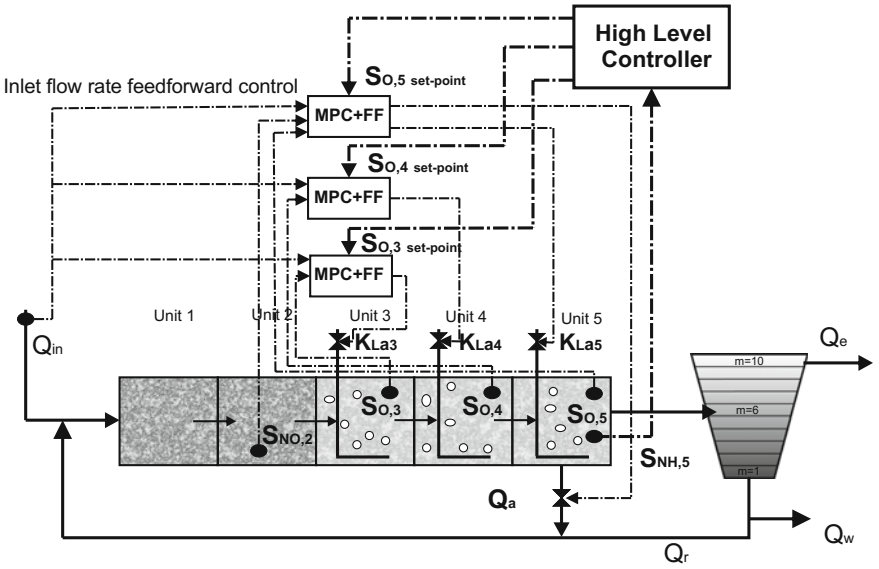

Fig. 5.17 BSM1 with MPC + FF and Hierarchical control for the three aerobic reactors

has been tested with an affine function and a FC in the higher level of the hierarchical structure, but not with an MPC.

5.2.1 Controllers Tuning

Higher Level Affine Function

The same affine function (5.1) is proposed to manipulate the three aerobic reactors. Thus, the set-point value determined for $S_{O,5}$ is also applied to $S_{O,3}$ and $S_{O,4}$ set-points. Also a constraint for the maximum $S_{O,3}$, $S_{O,4}$, and $S_{O,5}$ values has been considered. The OCI and EQI trade-off representations of the higher level affine function are made based on k and S_O maximum values, which is the same for the three aerobic tanks. These trade-off analysis for the three weather conditions are shown in Figs. 5.18, 5.19, and 5.20. Each line corresponds to one of the S_O maximum values considered: 2, 3, 4, and 4.5. And each point of one line, marked with crosses, is obtained with a different value of k.

A tuning area is obtained where OCI and EQI are reduced compared to the default PI controllers. S_O maximum and k values have been selected for the extreme cases of lowest EQI without increasing OCI and the lowest OCI without worsening EQI are achieved. Table 5.5 shows these tuning parameters selection for the three influents.

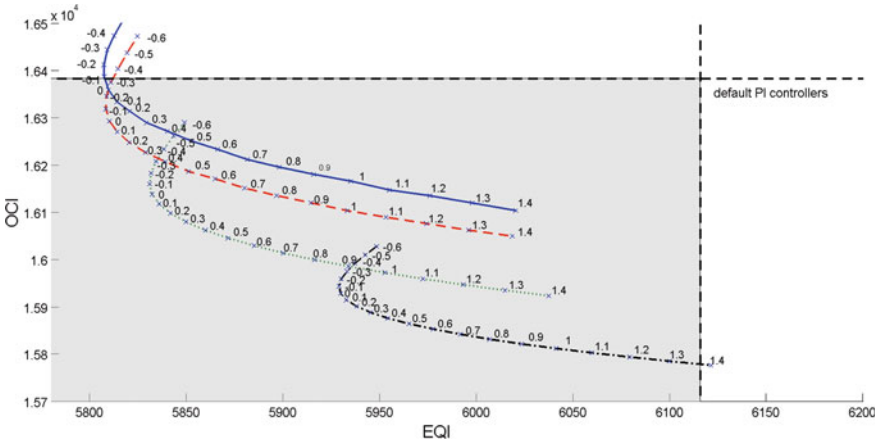

Fig. 5.18 Dry weather: OCI and EQI trade-off representation with higher level affine function for a range of k values from -0.6 to 1.4 with increments of 0.1 (points marked with *crosses*) and S_O maximum = 4.5 (*solid line*), 4 (*dashed line*), 3 (*dotted line*), 2 (*dash-dotted line*)

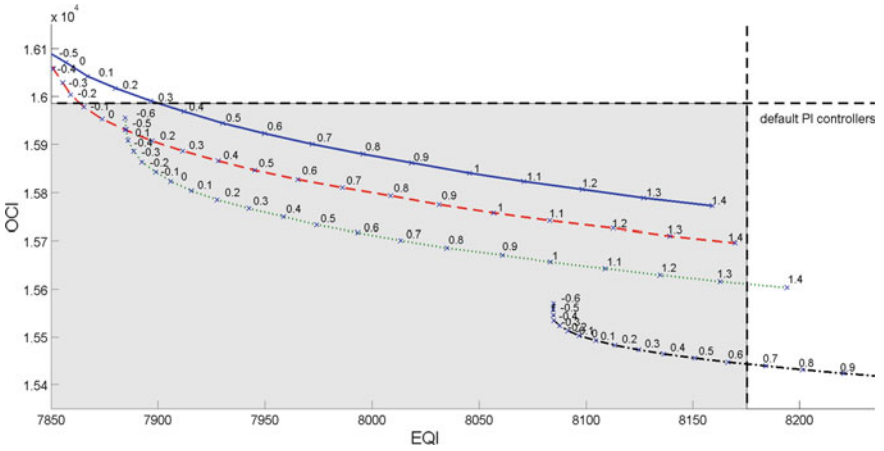

Fig. 5.19 Rain weather: OCI and EQI trade-off representation with higher level affine function for a range of k values from -0.6 to 1.4 with increments of 0.1 (points marked with *crosses*) and S_O maximum = 4.5 (*solid line*), 4 (*dashed line*), 3 (*dotted line*), 2 (*dash-dotted line*)

Higher Level Fuzzy Controller

For the higher level FC, three triangular membership functions for input and for output are used (*low*, *medium*, and *high*). The rules implemented are:

if ($S_{NH,5}$ is *low*) **then** (S_O is *low*)
if ($S_{NH,5}$ is *medium*) **then** (S_O is *medium*)
if ($S_{NH,5}$ is *high*) **then** (S_O is *high*)

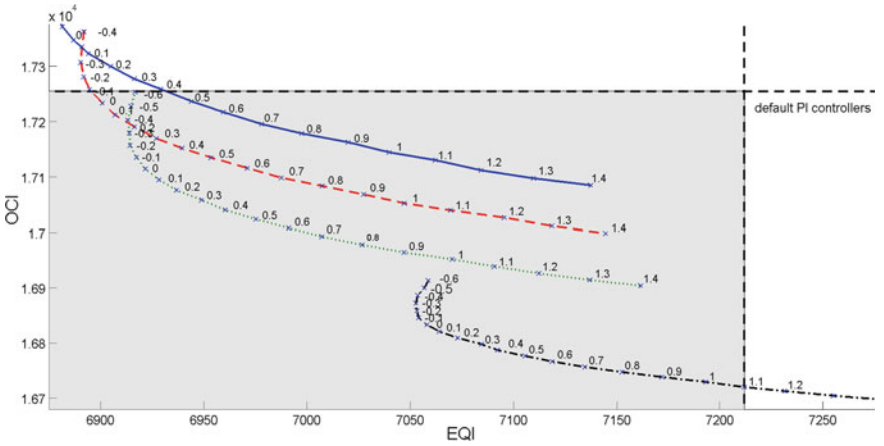

Fig. 5.20 Storm weather: OCI and EQI trade-off representation with higher level affine function for a range of k values from -0.6 to 1.4 with increments of 0.1 (points marked with *crosses*) and S_O maximum = 4.5 (*solid line*), 4 (*dashed line*), 3 (*dotted line*), 2 (*dash-dotted line*)

Table 5.5 Higher level affine function tuning of the three aerobic tanks: k and S_O maximum values

	Dry		Rain		Storm	
	Lowest EQI	Lowest OCI	Lowest EQI	Lowest OCI	Lowest EQI	Lowest OCI
k	−0.08	1.37	−0.1	0.62	−0.09	1.08
S_O maximum	4.5	2	3.5	2	3.5	2

Table 5.6 Higher level FC tuning of the three aerobic tanks: *MaxIn* and *MaxOut* values

	Dry		Rain		Storm	
	Lowest EQI	Lowest OCI	Lowest EQI	Lowest OCI	Lowest EQI	Lowest OCI
MaxIn	3	3	3	3	3	3
MaxOut	6.5	2.75	5.6	3.4	5.6	3.15

The same output S_O is applied for the three aerobic tanks. *MinIn* and *MinOut* are 0.1 and 0.8, respectively. *MaxIn* and *MaxOut* have been determined with OCI and EQI trade-off representations, for the three weather conditions, shown in Figs. 5.21, 5.22, and 5.23. Each one of the lines corresponds to the results obtained with different *MaxIn*, i.e., 3, 5, 7, and each one of the points marked with crosses is the result of a different *MaxOut*. The results obtained with the default PI controllers are also shown.

In the same way as for the higher level affine function, for the three weather conditions, a tuning region is obtained where OCI and EQI are improved in comparison with the default PI controllers. The *MaxIn* and *MaxOut* values of the extreme cases of lowest EQI without increasing OCI and lowest OCI without worsening EQI are shown in Table 5.6.

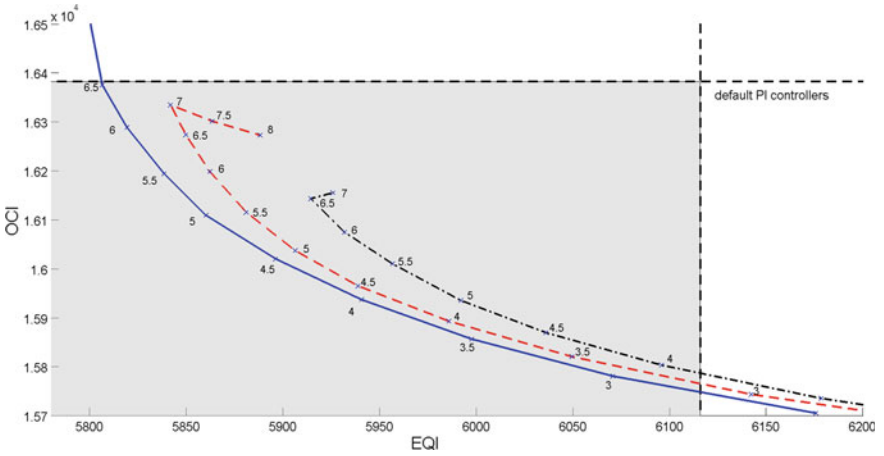

Fig. 5.21 Dry weather: OCI and EQI trade-off with higher level FC for a range of *MaxOut* from 2.5 to 8 with increments of 0.5 (points marked with *crosses*) and $MaxIn = 3$ (*solid line*), 5 (*dashed line*), 7 (*dash-dotted line*)

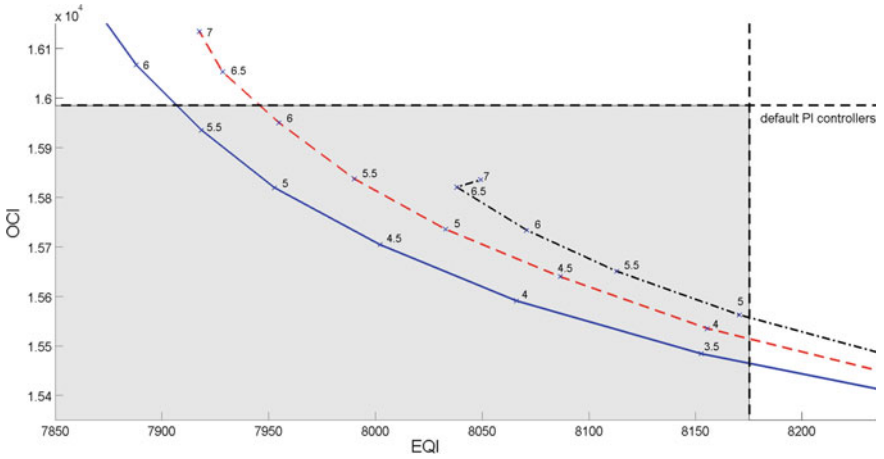

Fig. 5.22 Rain weather: OCI and EQI trade-off with higher level FC for a range of *MaxOut* from 2.5 to 7 with increments of 0.5 (points marked with *crosses*) and $MaxIn = 3$ (*solid line*), 5 (*dashed line*), 7 (*dash-dotted line*)

5.2.2 Simulations Results

Table 5.7 presents the results of best EQI without increasing OCI and best OCI without worsening EQI of the hierarchical control for the three aerobic reactors in comparison with the default control strategy. The comparison is done with the two higher level alternatives (affine function and FC), using the three influent files (dry,

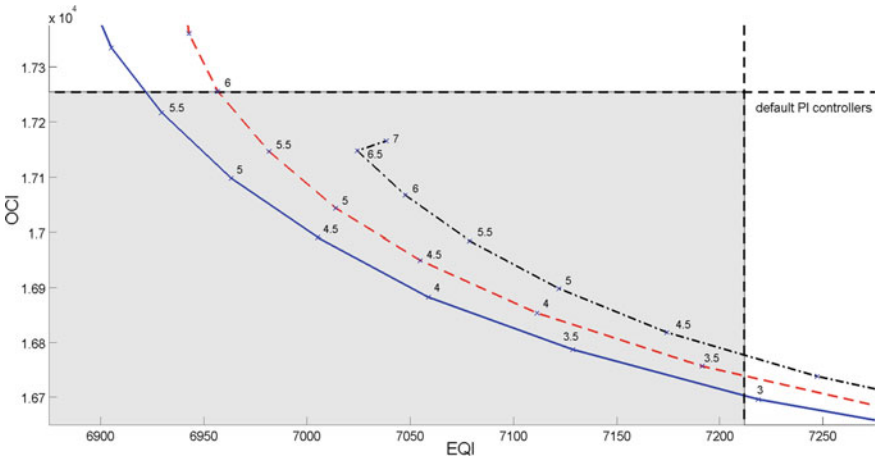

Fig. 5.23 Storm weather: OCI and EQI trade-off with higher level FC for a range of *MaxOut* from 2.5 to 7 with increments of 0.5 (points marked with *crosses*) and $MaxIn = 3$ (*solid line*), 5 (*dashed line*), 7 (*dash-dotted line*)

rain, and storm). As it is shown, a satisfactory reduction in OCI and EQI is achieved with the proposed hierarchical control. This reduction is higher in dry weather conditions, especially the EQI reduction. The results obtained with higher level affine function and higher level FC are similar, in the same way as the hierarchical control by manipulating only $S_{O,5}$, as shown in the previous section.

In order to explain the EQI improvement, Fig. 5.24 shows the behavior of S_O of the aerated tanks, $S_{NH,5}$ and $S_{NO,5}$ from day 7 to day 14. This is performed with the default control strategy and the proposed hierarchical control with the tuning parameters that give the lowest EQI for dry weather. Due to the results obtained with higher level affine function and higher level FC are very similar, only the variables of one of the two controllers (specifically affine function) are shown. As it is shown, with hierarchical control, when S_{NH} increases more S_O is added for nitrification, reducing S_{NH} peaks (2.3 and 2.7). On the contrary, when S_{NH} decreases, less S_O is required, producing less S_{NO} in comparison with the default control strategy (2.4 and 2.7).

In order to clarify the reason of the cost reduction, Table 5.8 shows the average values of the parameters that compose the OCI equation. They are the values obtained for dry influent by using the default control strategy and by applying hierarchical control with higher level FC that is the alternative that achieves the lowest OCI. As it is seen, the cost reduction is the result of an AE reduction of 683.72 KWh/d. This fact is due to the reduction of S_O (and hence a reduction of K_La) of the aerated tanks when $S_{NH,5}$ is low. Although there is a PE increase of 53.43 KWh/d, the saving energy, considering both parameters, is 630.29 KWh/d.

Table 5.7 EQI and OCI results with default PI controllers and hierarchical control of the three aerobic tanks

	Default PI controllers	Hierarchical Control (three aerobic tanks) higher level affine function			Hierarchical Control (three aerobic tanks) higher level FC		
		Lowest EQI	Lowest OCI	% of reduction	Lowest EQI	Lowest OCI	% of reduction
Dry Weather							
EQI (kg pollutants/d)	6115.63	5807.77	6046.51	5	5804.38	6037.07	5
OCI	16381.93	16381.51	15779.58	3.7	16377.51	15743.91	3.9
Rain weather							
EQI (kg pollutants/d)	8174.98	7865.31	8172.01	3.8	7910.26	8168.45	3.2
OCI	15984.85	15977.56	15445.31	3.4	15959.92	15466.01	3.2
Storm weather							
EQI (kg pollutants/d)	7211.48	6895.74	7211.48	3.3	6919.2	7200.51	3
OCI	17253.75	17251.71	16721.06	3.1	17254.25	16711.96	3.1

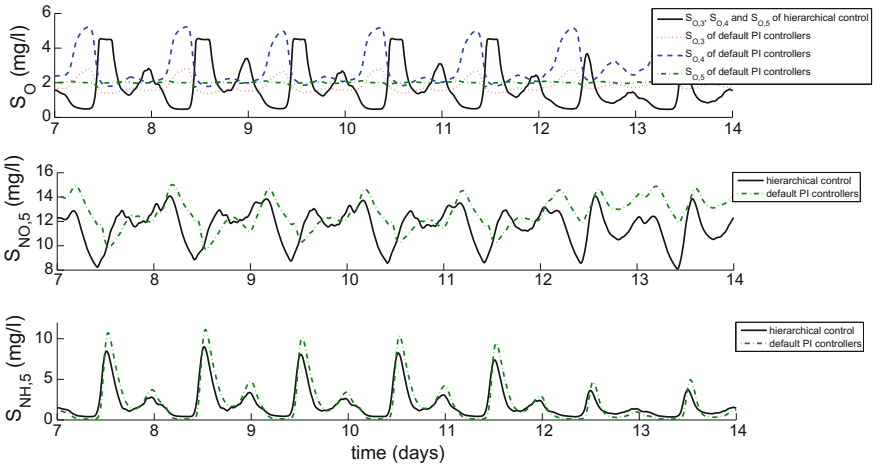

Fig. 5.24 S_O in the aerated tanks, $S_{NO,5}$ and $S_{NH,5}$ evolution from day 7 to day 14 with the default PI controllers and with the proposed hierarchical control with higher level affine function for the case of lowest EQI

Table 5.8 Average values of the parameters that compose the OCI equation for PI controllers of the default control strategy and the proposed hierarchical control of the three aerobic tanks with higher level FC for the case of lowest OCI

Average values of the OCI parameters	Default PI controllers	Hierarchical control	Reduction
AE (KWh/d)	3696.67	3012.95	683.72
PE (KWh/d)	241.72	295.15	−53.43
ME (KWh/d)	240	240	0
EC (Kg/d)	0	0	0
SP (Kg/d)	2440.71	2439.16	1.55

5.3 Summary

In this chapter, the higher level control of the hierarchical structure has been applied using BSM1 as testing plant. This level regulates the S_O set-points of the aerated tanks based on $S_{NH,5}$.

First, for the selection of the higher level controller, three different alternatives have been proposed by manipulating only $S_{O,5}$ set-point: an MPC, an affine function and a FC. They have been tested and compared in the three weather conditions: dry, rain and storm. As a result, EQI and OCI have been reduced significantly. The results of OCI and EQI with higher level affine function and higher level FC have been similar and better than those obtained with higher level MPC. This is due to the fact that the higher level MPC tries to keep the value of $S_{NH,5}$ at a reference level, but this is not possible. For that reason, the alternatives of affine function and FC for

the higher level have been tested with the idea of varying $S_{O,5}$ based on the $S_{NH,5}$ measured, taking into account the variables behavior in the biological processes, but without trying to keep $S_{NH,5}$ at a fixed reference. Thus, improving the nitrification process when $S_{NH,5}$ increases, to oxidize more S_{NH} and worsening the nitrification process when $S_{NH,5}$ decreases to generate less S_{NO} and to reduce costs. To ensure the right tuning of the controllers and therefore the correct relationship between the applied control and the results, a trade-off analysis between OCI and EQI has been performed by varying two tuning parameters for each controller.

Next, the higher level control has been extended, manipulating the three aerobic tanks. Simulation results show that manipulating the S_O set-points of the three aerobic tanks, an EQI reduction of 5 % and an OCI reduction of 3.9 % has been achieved for dry weather compared to the default control strategy. For the rain and storm influent cases, also a satisfactory reduction of EQI and OCI has been obtained, higher than 3 %.

Chapter 6
Denitrification and Nitrification Processes Improvement for Avoiding Pollutants Limits Violations in the Effluent

In this chapter, different control strategies are applied with the aim of avoiding $S_{N_{tot,e}}$ or $S_{NH,e}$ violations using BSM1 as testing plant. These control strategies are implemented simultaneously with the hierarchical control structure explained in previous chapter, in order to achieve, at the same time, an EQI and OCI reduction. The tuning of both higher level controllers is modified based on the required objective. The controllers applied for the proposed control strategies are divided into two alternatives: functions that relate the inputs and the manipulated variables, and FCs. Therefore, on one hand, an affine function is proposed to eliminate $S_{N_{tot,e}}$ violations and a combination of a linear function with an exponential function to remove $S_{NH,e}$ violations. At the same time, the higher level affine function is applied. On the other hand, two FCs are proposed to avoid $S_{N_{tot,e}}$ and $S_{NH,e}$ violations. The higher level FC is also applied. For the cases of a rain or storm event and for the simultaneous $S_{N_{tot,e}}$ and $S_{NH,e}$ violations removal, an extra control is added based on affine functions, for both alternatives.

6.1 $S_{N_{tot,e}}$ Violations Removal

The variables with the highest influence in $S_{N_{tot,e}}$ are S_{NO} and S_{NH}. Further efforts to reduce more S_{NH} by increasing nitrification also results in an increment of S_{NO} and consequently $S_{N_{tot,e}}$ is not decreased. According to the biological processes of ASM1, an increase of substrate produces a growth of $X_{B,H}$ and therefore the denitrification process and the consequently reduction of S_{NO} are improved. Therefore, $S_{N_{tot,e}}$ is reduced with the dosage of EC in the first tank (EC1). However, dosing EC1 results in an increase of operational costs (2.13), so it is important to dosage EC1 only when a violation of $S_{N_{tot,e}}$ could take place. Consequently, the control strategy is based

I. Santín et al., *Control and Decision Strategies in Wastewater Treatment Plants for Operation Improvement*, Intelligent Systems, Control and Automation: Science and Engineering 86, DOI 10.1007/978-3-319-46367-4_6

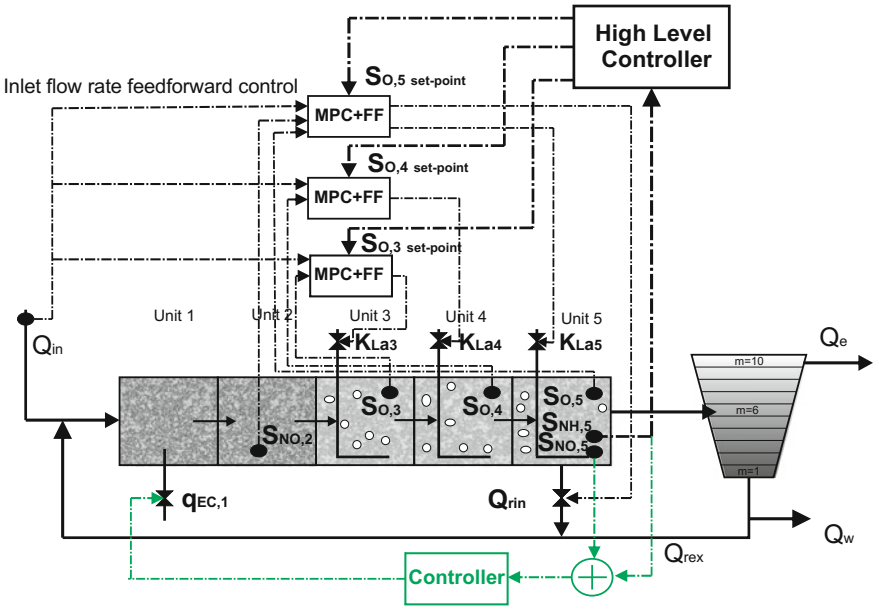

Fig. 6.1 BSM1 with a control strategy for $S_{N_{tot,e}}$ violations removal

on the manipulation of $q_{EC,1}$ according to $S_{NH,5}$ plus $S_{NO,5}$ (see Fig. 6.1). An affine function with a sliding window and an FC are proposed for this control strategy.

6.1.1 Controllers Tuning

Functions

Here, the tunings of the both affine functions, for the higher level control and for the control for $S_{N_{tot,e}}$ violations removal, are described.

First, for the higher level affine function, a trade-off analysis is made considering the percentage of operating time that $S_{NH,e}$ and $S_{N_{tot,e}}$ is over the limits. The purpose of this trade-off analysis is, besides the $S_{N_{tot,e}}$ violations removal, not to increase OCI and to reduce EQI and the percentage of time of $S_{NH,e}$ violations in comparison with the default control strategy. This is done with hierarchical control strategy and without adding EC1 (see Fig. 6.2). Tuning parameters are chosen for the point where the percentage of operating time of $S_{NH,e}$ over the limits is the same as with default control strategy (17.26 %). The tuning parameters of the higher level affine function are $k = 1.07$ and S_O maximum $= 3$, and the percentage of operating time of $S_{N_{tot,e}}$ violation with these parameters is 6.35 %.

The OCI and EQI trade-off representation shown in Fig. 5.18, in the points of the tuning parameters mentioned, a difference in OCI of 2.5 % is observed regarding the

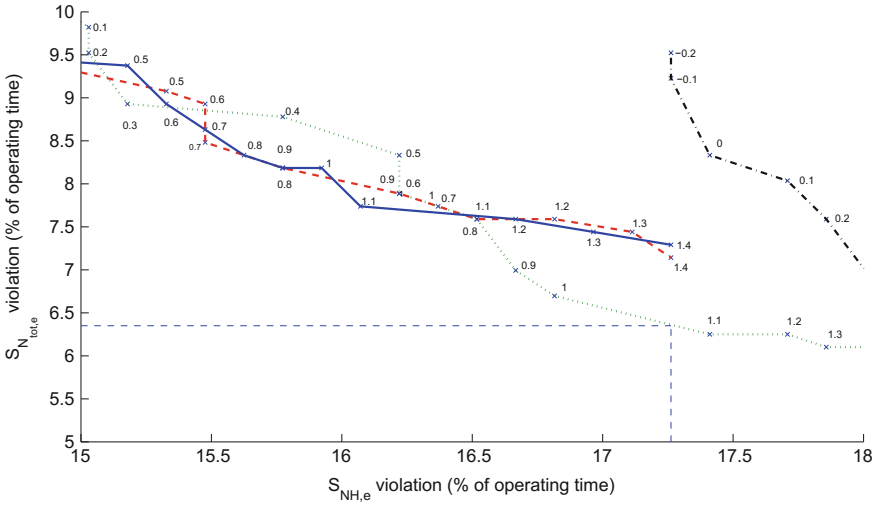

Fig. 6.2 Trade-off representation of the percentage of the operating time of $S_{NH,e}$ and $S_{N_{tot,e}}$ violations for a range of k values from -0.6 to 1.4 with increments of 0.1 (points marked with *crosses*) and $S_{O,5}$ maximum = 4.5 (*solid line*), 4 (*dashed line*), 3 (*dotted line*), 2.5 (*dash-dotted line*)

default control strategy. From this Pareto representation, this means that there is a saving in control operation costs that can be used for other purposes before exceeding the initial costs. In our case, we will use $q_{EC,1}$ dosage. However, it cannot be used in a fixed or arbitrary way. The purpose of such additional dosage will be to deal with violations removal but we cannot exceed the operational costs provided by the OCI value of the default control.

Then, the following affine function is proposed for $q_{EC,1}$ manipulation with the objective of $S_{N_{tot,e}}$ violations removal:

$$q_{EC1} = ((S_{NH,5} + S_{NO,5}) - a)b, \tag{6.1}$$

where a and b are used as tuning parameters, whose values are set depending on the maximum value of $S_{N_{tot,e}}$ given by a sliding window, which is shifted at each sample time and presents only the values measured the s, 1 week before. Specifically, the chosen equations for a and b values are

$$b = M_d \cdot 2 - 35.5 \tag{6.2}$$

$$a = 34.25 - M_d, \tag{6.3}$$

where M_d is the maximum value of the day, 1 week before. This approach tries to dosage the minimum of $q_{EC,1}$ to remove $S_{N_{tot,e}}$ violations. The maximum $q_{EC,1}$ value was limited to 5 m^3/d.

Fuzzy Controllers

The tuning of the FCs is implemented with the objectives of removing $S_{N_{tot,e}}$ violations and, at the same time, reducing EQI, OCI, and the percentage of time of $S_{NH,e}$ violations. First for the higher level FC and next for the FC that manipulates $q_{EC,1}$ for $S_{N_{tot,e}}$ violations removal.

For the tuning parameters selection of the higher level FC, a trade-off analysis of the percentage of time over the limits of $S_{NH,e}$ and $S_{N_{tot,e}}$ is made (see Fig. 6.3). For this analysis, the hierarchical control strategy is included but not the addition of EC1. The tuning parameters of the higher level FC are selected in the point whose percentage of operating time of $S_{NH,e}$ over the limits is the same as with the default control strategy (17.26 %). These tuning parameters are $MaxIn = 3$ and $MaxOut = 4.1$, and the percentage of operating time of $S_{N_{tot,e}}$ violation with these parameters is 6.39 %.

The OCI and EQI trade-off representation shown in Fig. 5.21, in the points of the tuning parameters mentioned, a difference in OCI of 2.6 % is observed regarding the default control strategy, which may be used for the EC1 dosage.

With these parameters selected for the higher level, an FC is added to manipulate $q_{EC,1}$. For this controller, three triangular membership functions for input and for output are used (*low*, *medium*, and *high*). The rules implemented are

if ($S_{NH,5}$+$S_{NO,5}$ is *low*) **then** ($q_{EC,1}$ is *low*)
if ($S_{NH,5}$+$S_{NO,5}$ is *medium*) **then** ($q_{EC,1}$ is *medium*)
if ($S_{NH,5}$+$S_{NO,5}$ is *high*) **then** ($q_{EC,1}$ is *high*)

The range of membership functions values are: $MinIn = 10, MaxIn = 17.5, MinOut = -8, MaxOut = 6.75$.

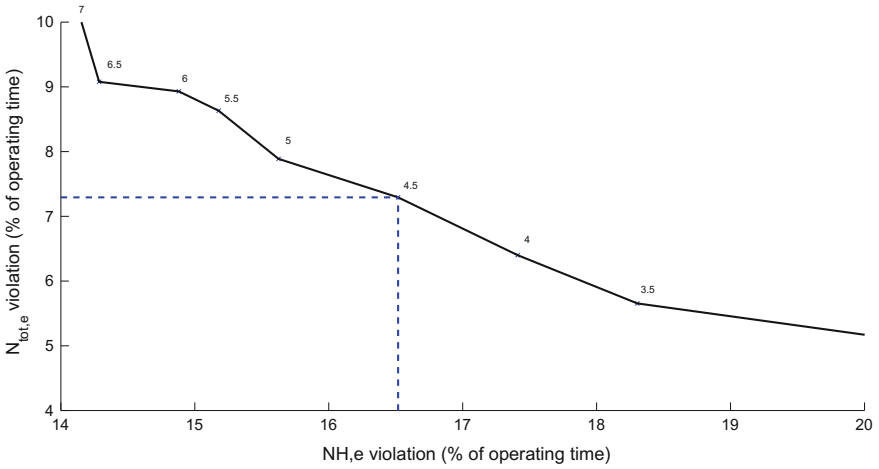

Fig. 6.3 Higher level FC: trade-off of the time percentage of $S_{NH,e}$ and $S_{N_{tot,e}}$ violations for $MaxIn = 3$ and a range of $MaxOut$ values from 3 to 7 with increments of 0.5 (points marked with *crosses*)

6.1.2 Considerations for Rain and Storm Influents

During a rain or storm event, Q_{in} increases and S_{NH} in the influent ($S_{NH,in}$) decreases. The Q_{in} increment has the effect of reducing the hydraulic retention time and the $S_{NH,in}$ reduction decreases the growth of $X_{B,A}$ and therefore the nitrification process (2.7) is worsened. Due to this reason, there is an increase of S_{NH} without incrementing the generation of S_{NO} ((2.4) and (2.7)). Therefore, the resulting $S_{N_{tot,e}}$ is lower than for dry weather. However, in the periods after the rain or storm events, the Q_{in} reduction has an immediate effect on the hydraulic retention time, but $X_{B,H}$ and $X_{B,A}$ need more time to recover their normal levels and it causes a small $S_{N_{tot,e}}$ increase. To compensate this, $q_{EC,1}$ is added based on $S_{NH,5}$ plus $S_{NO,5}$ and on the average of $S_{NH,in}$ of the 2 days before ($S_{NH,inmean_2}$) with the following affine function:

$$q_{EC,1} = (S_{NH,5} + S_{NO,5})5 - S_{NH,inmean_2} \cdot 0.2857 - 75.7143 \tag{6.4}$$

where the constants values are found by three experimental cases.

6.2 $S_{NH,e}$ Violations Removal

With the goal of removing $S_{NH,e}$ violations, Q_a is manipulated based on $S_{NH,5}$ and $S_{NH,in}$. Therefore, the MPC of the lower level that controls $S_{O,5}$ and $S_{NO,2}$ by manipulating K_La_5 and Q_a is replaced by an MPC with one input ($S_{O,5}$) and one output (K_La_5) (see Fig. 6.4). Thus, the MPC controller will leave the manipulation of Q_a.

To facilitate the understanding of the proposed solution some considerations about the propagation of the peaks in the reactor are provided: When a peak of pollution enters in the reactors, it is propagated through them with a delay determined by the retention time. Thus, any change in Q_{in} or in the Q_a directly affects the propagation of the peaks of pollution inside the tanks. On the contrary, the peaks of flow rate are transmitted to all the plants immediately, because the system is always full and any variation in the influent causes an identical variation in the effluent and inside the system. Thus, according to the mass balance equation in the first reactor (2.1), when $S_{NH,in}$ increases, Q_a is incremented to reduce the rise of S_{NH} in the first tank ($S_{NH,1}$), and when the increase of S_{NH} arrives to the fifth tank, Q_a is reduced to increase the retention time and so to improve denitrification process.

Two controllers are proposed for this control strategy: first, a combination of a linear function and an exponential function, and next, an FC with two different tunings.

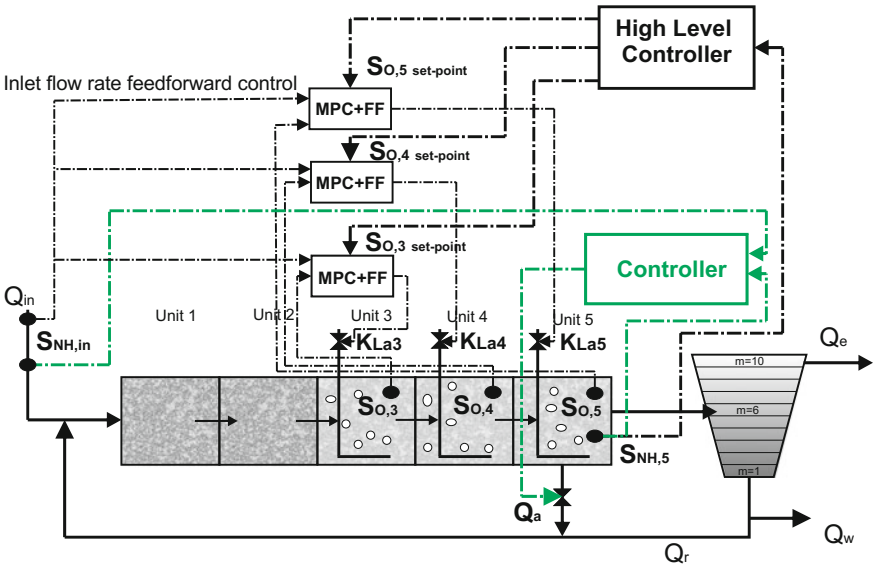

Fig. 6.4 BSM1 with a control strategy for $S_{NH,e}$ violations removal

6.2.1 Controllers Tuning

MPC+FF

As mentioned, to perform the control for removing violations of $S_{NH,e}$, the MIMO MPC+FF that controls $S_{O,5}$ and $S_{NO,2}$ by manipulating K_La_5 and Q_a, has been replaced by a SISO MPC+FF that controls $S_{O,5}$ by manipulating K_La_5, because Q_a will be the manipulated variable based on $S_{NH,5}$ and $S_{NH,in}$, to deal with the violations removal.

The model identification for the new MPC+FF was performed with the same methodology as with the previous MPC controller, but with one input and one output. However, in this case the model results in a second-order state-space model:

$$\begin{aligned} A &= \begin{bmatrix} 0.8349 & 0.2746 \\ 0.2512 & 0.2894 \end{bmatrix} \\ B &= \begin{bmatrix} 0.008745 & -2.729 \cdot 10^{-5} \\ -0.02118 & 1.307 \cdot 10^{-5} \end{bmatrix} \\ C &= \begin{bmatrix} 1.512 & -0.3525 \end{bmatrix} \\ D &= \begin{bmatrix} 0 & 0 \end{bmatrix} \end{aligned} \tag{6.5}$$

The selected values to tune the MPC are $m = 5$, $p = 20$, $\triangle t = 0.00025$ days (21.6 s), $\Gamma_y = 1$ and $\Gamma_{\triangle u} = 0.01$, and overall estimator gain = 0.8.

Functions

Here, the tunings of the controllers based on functions are described. First, the tuning of the higher level affine function, and next, the combination of the linear function and the exponential function for $S_{NH,e}$ violations removal.

For the higher level affine function (5.1), any parameter values within the tuning region given by the OCI and EQI trade-off representation (see Fig. 5.18) can be selected. In this case the chosen parameters are: $k = 0.1$ and S_O maximum $= 4.5$.

For the control of $S_{NH,e}$ violations removal, a combination of exponential function and linear function is proposed for this control strategy. When there are peaks of $S_{NH,in}$ multiplied by Q_{in} or $S_{NH,5}$ ($S_{NH,in} \cdot Q_{in} > 10^6$ or $S_{NH,5} > 3.75$), the following exponential function is applied:

$$Q_a = \frac{c}{e^{S_{NH,5} \cdot d}} \tag{6.6}$$

Otherwise the following linear function is applied:

$$Q_a = \frac{S_{NH,in}}{S_{NH,5}} \cdot e, \tag{6.7}$$

where c, d, and e are used as tuning parameters.

A trade-off analysis of OCI and percentage of operating time of $S_{N_{tot,e}}$ violation is made by varying the tuning parameters c and e of the exponential and linear functions, reflecting only the results that avoid the $S_{NH,e}$ violations. It is obtained an area where OCI and the operating time of $S_{N_{tot,e}}$ violation are decreased compared to default PI controllers (see Fig. 6.5). The value of d is fixed at 6, and c and e values are chosen according to the Nash solution (see Appendix A): $c = 2.5 \cdot 10^{14}$ and $e = 7 \cdot 10^{-4}$.

Fuzzy Controllers

Now, the tuning parameters of the higher level FC and the FC for $S_{NH,e}$ violations removal are defined.

The *MaxIn* and *MaxOut* values of the higher level FC have been also selected by a trade-off analysis of OCI and percentage of operating time of $S_{NH,e}$ violation (see Fig. 6.6), choosing the lowest percentage of $S_{NH,e}$ violation in order to facilitate its posterior total elimination, but considering the increased costs that will be generated by the new control strategy. In this case the chosen parameters are: $MaxIn = 3$ and $MaxOut = 5.5$.

In the case of the FC for the $S_{NH,e}$ violations removal, two tunings are determined, one when there are peaks of $S_{NH,in}$ or $S_{NH,5}$, and the other the rest of the time. For both cases, three triangular membership functions for input and output are used (*low*, *medium*, and *high*). The rules implemented are

if ($S_{NH,5}$ is *low*) **then** (Q_a is *high*)
if ($S_{NH,5}$ is *medium*) **then** (Q_a is *medium*)
if ($S_{NH,5}$ is *high*) **then** (Q_a is *low*)

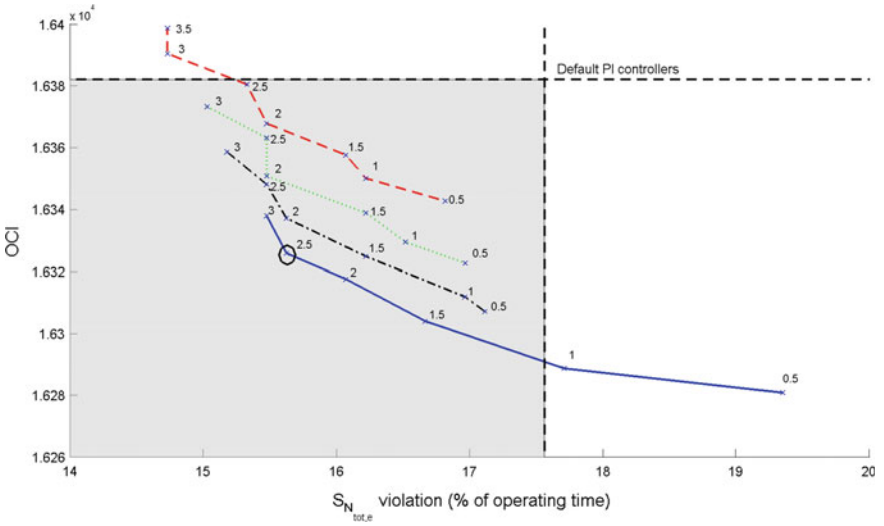

Fig. 6.5 Trade-off representation of OCI and the percentage of operating time of $S_{N_{tot,e}}$ violations for a range of c values from 0.5 to 4 with increments of 0.5 (points marked with *crosses*) and e values = 7 (*solid line*), 6 (*dash-dotted line*), 5.5 (*dotted line*), 5 (*dashed line*)

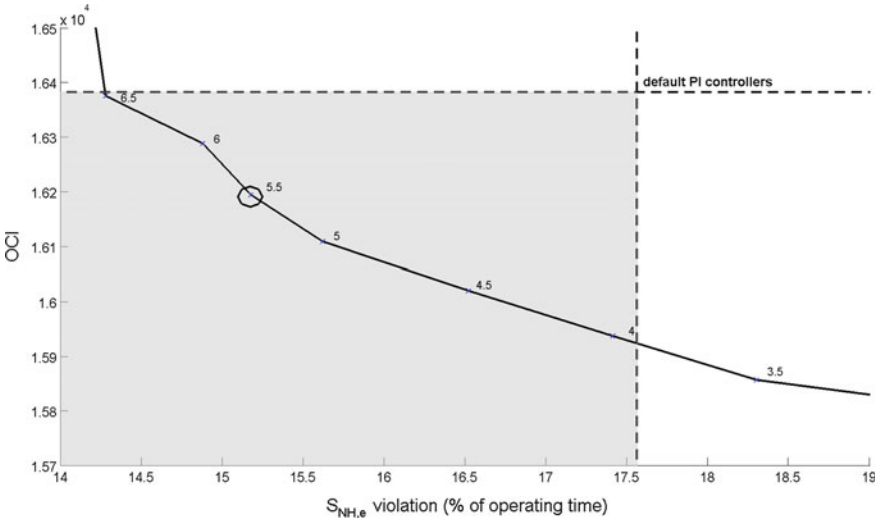

Fig. 6.6 Trade-off representation of OCI and the percentage of operating time of $S_{NH,e}$ violations for $MaxIn = 3$ and a range of $MaxOut$ from 3 to 7 with increments of 0.5 (points marked with *crosses*)

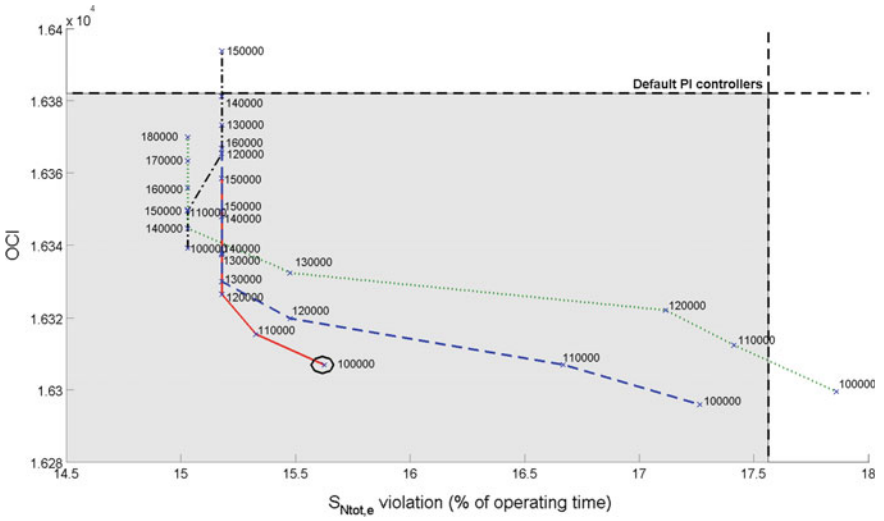

Fig. 6.7 Trade-off representation of OCI and the percentage of operating time of $S_{N_{tot,e}}$ violations for a range of *MaxOut* from 90,000 to 180,000 with increments of 10,000 (points marked with *crosses*) and *MaxIn* = 2 (*dotted line*), 2.2 (*dashed line*), 2.4 (*solid line*), 2.6 (*dash-dotted line*)

When there are peaks of $S_{NH,in}$ or $S_{NH,5}$, the tuning parameters are set looking for a great variation in Q_a when $S_{NH,e}$ is increasing. Therefore, *MinIn*, *MaxIn*, *MinOut*, and *MaxOut* are 3.5, 4.1, $-2 \cdot 10^4$, and $14 \cdot 10^4$, respectively. For the rest of the time, *MinOut* and *MaxOut* are set by a trade-off analysis of OCI and percentage of operating time of $S_{N_{tot,e}}$ violation, reflecting only the results that avoid the $S_{NH,e}$ violations. An area is obtained where OCI and the operating time of $S_{N_{tot,e}}$ violation are decreased compared to default PI controllers (see Fig. 6.7). Each one of the lines corresponds to the results obtained with *MaxIn* = 2, 2.2, 2.4, and 2.6 and each one of the points marked with crosses is the result of a different *MaxOut* that varies from 90,000 to 180,000 with increments of 10,000. The results obtained with default PI controllers alone are also shown. The parameters have been selected according to the Nash Solution [2]: *MaxIn* = 2.4 and *MaxOut* = 100,000.

6.2.2 *Considerations for Rain and Storm Influents*

For rain and storm events the reduction of $S_{NH,e}$ using the presented control strategy is not enough to eliminate violations. This is due to that, during rain and storm periods, the $Q_{in} \cdot S_{NH,in}$ relationship is similar to that of dry weather, but Q_{in} increases and $S_{NH,in}$ decreases. This $S_{NH,in}$ reduction decreases the growth of $X_{B,A}$ and therefore the nitrification process (2.7) is worsened. For this reason, during a rain or storm event, when there is a peak of $S_{NH,in} \cdot Q_{in}$ and until $S_{NH,5}$ is decreased, a dosage of

$5\,m^3/d$ of q_{EC} in the fourth and fifth tanks ($q_{EC_{4-5}}$) is added, which is the maximum limit value. Normally, $q_{EC_{4-5}}$ is added to reduce S_{NO}, nevertheless in r_{NH} Eq. (2.3) it is observed that although the elimination of S_{NH} largely depends on nitrification (2.7), S_{NH} is also reduced with the growth of $X_{B,H}$ ((2.5) and (2.6)).

The days after the rain and storm events present also problems with $S_{NH,e}$ limits violations due to the fact that the $X_{B,A}$ population decreases during those periods and does not recover its normal level until some days later. During those days $q_{EC_{4-5}}$ is added. As $X_{B,A}$ reduction is due to a $S_{NH,in}$ decrease, the addition of $q_{EC_{4-5}}$ is based on $S_{NH,inmean_2}$, using the following affine function:

$$q_{EC_{4-5}} = S_{NH,inmean_2}(-0.2667) + 7; \tag{6.8}$$

where the constants values are found by two experimental cases, which correspond to the extreme cases of highest and lowest dosage of $q_{EC_{4-5}}$ that is needed to eliminate violations of $S_{NH,e}$.

6.3 Simulation Results

The above control strategies with the proposed tuning parameters for $S_{N_{tot,e}}$ and $S_{NH,e}$ violations removal are tested in this section for dry, rain, and storm influents.

6.3.1 $S_{N_{tot,e}}$ Violations Removal

Figure 6.8 corresponds to the evolution of $q_{EC,1}$, $S_{N_{tot,e}}$, and $S_{NH,e}$ from day 7 to 14, with the default PI controllers, applying control strategies for $S_{N_{tot,e}}$ violations removal with functions and applying control strategies for $S_{N_{tot,e}}$ violations removal with FCs. It is observed that, for both alternatives (functions and FCs), $S_{N_{tot,e}}$ violations are removed and the behavior of the variables are very similar. As it is shown, $q_{EC,1}$ dosage varies every day, while $S_{N_{tot,e}}$ peaks are very similar. It proves that the minimum necessary $q_{EC,1}$ is added, increasing the lowest possible costs. For this reason, and with the correct selection of the tuning parameters of the higher level explained in previous sections, the removal of $S_{N_{tot,e}}$ violations without increasing OCI, in comparison with default control strategy is possible. The choice of the right tuning parameters of the higher level affine function also makes possible to reduce the time of $S_{NH,e}$ violation.

Table 6.1 presents the results for EQI and OCI as well as the percentage of operating time out of the limits of $S_{N_{tot,e}}$ and $S_{NH,e}$ obtained with the control strategies for $S_{N_{tot,e}}$ violations removal and compared to the default control strategy of BSM1. It is shown that by adding $q_{EC,1}$ and applying a hierarchical control of S_O in the three aerated tanks, the violations of $S_{N_{tot,e}}$ can be avoided. Moreover, the results of EQI and OCI as well as the operating time percentage of $S_{NH,e}$ violations are also

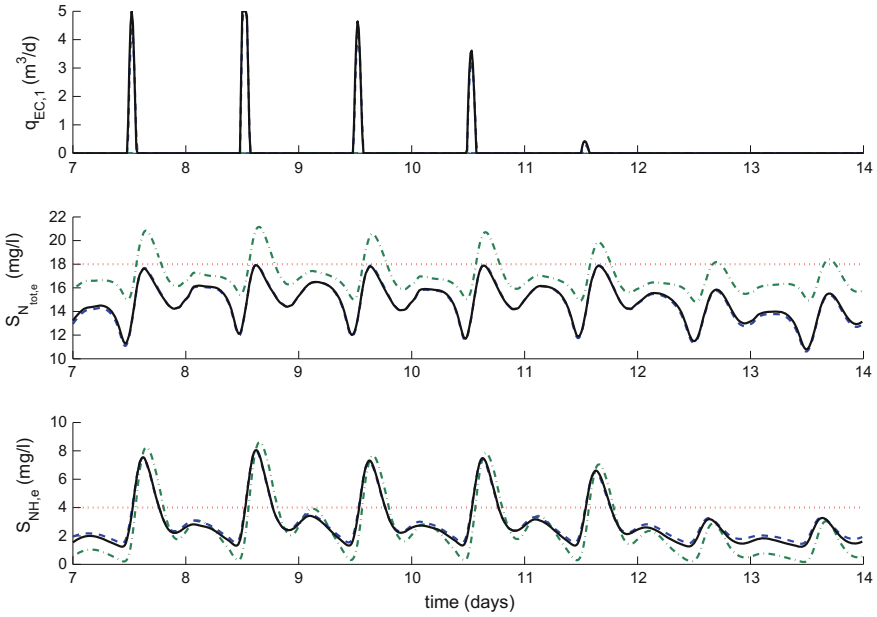

Fig. 6.8 $q_{EC,1}$, $S_{NH,e}$, and $S_{N_{tot,e}}$ evolution from day 7 to 14 with default PI controllers (*dash-dotted line*), applying control strategies for $S_{N_{tot,e}}$ violations removal with functions (*dashed line*) and applying control strategies for $S_{N_{tot,e}}$ violations removal with FCs (*solid line*)

improved in comparison with the default PI controllers. This is achieved for the three influents provided by the BSM1 scenario.

Figures 6.9 and 6.10 show the time evolution of the most important variables for the cases of simulating with rain and storm influents. Due to the great similarity of the results between functions and FCs, only the simulated variables using functions are shown. During a rain or storm event, the nitrification process (2.7) is worsened as explained in Sect. 6.2.2. Due to this reason, there is an increase of S_{NH} without incrementing the generation of S_{NO} ((2.4) and (2.7)). Therefore, the resulting $S_{N_{tot,e}}$ is lower than for dry weather and less $q_{EC,1}$ is needed for removing $S_{N_{tot,e}}$ violations. In the periods after the rain or storm events, $q_{EC,1}$ needs to be added until $X_{B,H}$ and $X_{B,A}$ recover their normal levels. Even so, this $q_{EC,1}$ addition is small, and OCI is reduced for the three influents with the proposed control strategy in comparison with the default control strategy. Nonetheless, it has to be said that the reduction of costs would be greater if the savings costs obtained by avoiding the fines due to the effluent violations were considered.

Table 6.1 Results with default PI controllers and with control for $S_{N_{tot,e}}$ violations removal for dry, rain, and storm influents

	Default PI controllers	Control for $S_{N_{tot,e}}$ violations removal with functions	% of reduction (%)	Control for $S_{N_{tot,e}}$ violations removal with FCs	% of reduction (%)
Dry influent					
EQI	6115.63	5910.83	3.3	5862.03	4.1
OCI	16381.93	16242.97	0.8	16336.36	0.3
$S_{N_{tot,e}}$ violations (% of operating time)	17.56	0	100	0	100
$S_{NH,e}$ violations (% of operating time)	17.26	16.81	2.6	16.66	3.4
Rain influent					
EQI	8174.98	8072.5	1.2	8021.54	1.88
OCI	15984.85	15780.83	1.3	15770.78	1.34
$S_{N_{tot,e}}$ violations (% of operating time)	10.86	0	100	0	100
$S_{NH,e}$ violations (% of operating time)	27.08	26.04	3.8	25.3	6.57
Storm influent					
EQI	7211.48	7022.25	2.6	6979.22	3.22
OCI	17253.75	17243.73	0.06	17229.49	0.14
$S_{N_{tot,e}}$ violations (% of operating time)	15.03	0	100	0	100
$S_{NH,e}$ violations (% of operating time)	26.79	25	6.6	25	6.6

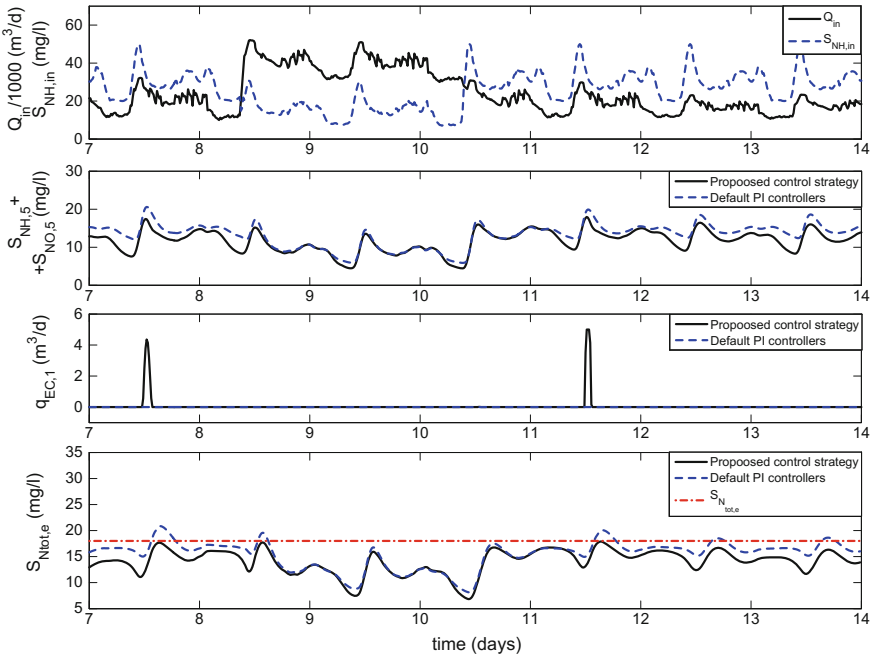

Fig. 6.9 Rain influent: time evolution of the most important variables applying the proposed control strategy for $S_{N_{tot,e}}$ violations removal with functions and applying the default control strategy of BSM1

6.3.2 $S_{NH,e}$ Violations Removal

Figure 6.11 shows the evolutions of Q_a, $S_{N_{tot,e}}$, and $S_{NH,e}$ from day 7 to 14 with default PI controllers, applying control strategies for $S_{NH,e}$ violations removal with functions and applying control strategies for $S_{NH,e}$ violations removal with FCs. It can be observed that, with this control strategy, $S_{NH,e}$ peaks are reduced under the limits established. This fact is due to the increment of S_O by the hierarchical control (explained in the previous section) and mainly to the Q_a manipulation. As shown in Fig. 6.11, Q_a evolution by applying control strategies for $S_{N_{tot,e}}$ violations removal is very different from the one obtained with the default control strategy. When a $S_{NH,in}$ peak is detected, Q_a is increased to its maximum allowed value (92,280 m^3/d) in order to dilute S_{NH}, and when this increase of S_{NH} arrives to the fifth tank, the exponential function rapidly reduces Q_a in order to decrease also the hydraulic retention time and so to improve the nitrification process. As a result, a large decrease of $S_{NH,e}$ peaks is achieved and limits violations are avoided. The correct choice of the tuning parameters of the higher level controller results also in obtaining a decrease in OCI and time of $S_{N_{tot,e}}$ violation.

Table 6.2 shows the results of EQI, OCI, and percentage of time over the limits of $S_{NH,e}$ and $S_{N_{tot,e}}$ for the three weather conditions. It can be seen that with the reg-

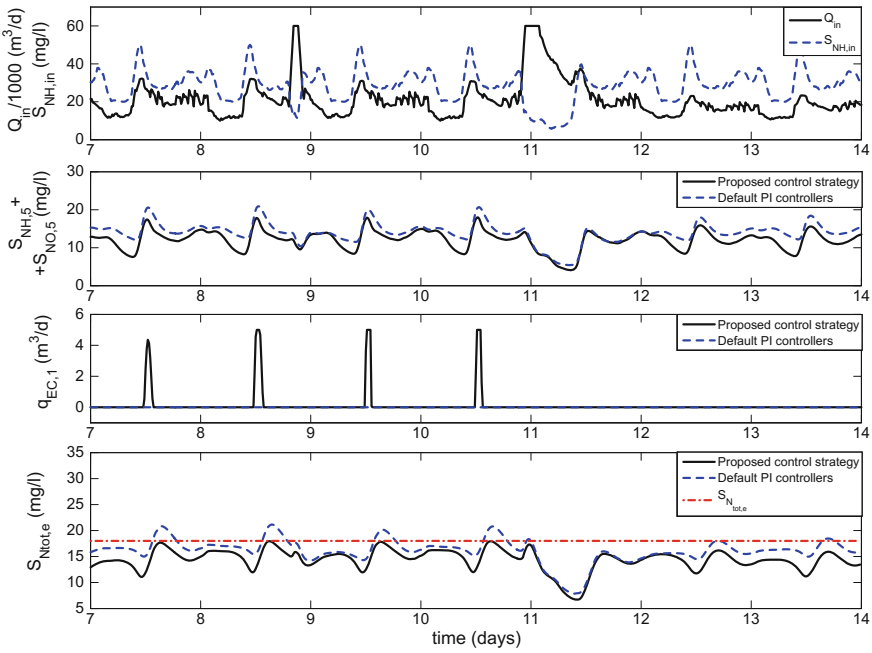

Fig. 6.10 Storm influent: time evolution of the most important variables applying the proposed control strategy for $S_{N_{tot,e}}$ violations removal with functions and applying the default control strategy of BSM1

ulation of Q_a based on $S_{NH,5}$ and $S_{NH,in}$, and also with the hierarchical control of S_O in the three aerated tanks, it is possible to avoid $S_{NH,e}$ violations. In addition, an improvement of 5.8 or 4.26 % of EQI and 0.4 or 0.45 % of OCI in comparison with the default control strategy of BSM1 is achieved for dry influent. It is important to highlight this performance indicator improvement, because all the operations objectives are harder to accomplish. Here the EQI is improved by decreasing costs at the same time that the pollutant in the effluent accomplish with the legal requirements.

For rain and storm events, the elimination of $S_{NH,e}$ violations is completely achieved with the proposed control strategy and, in addition, a reduction of EQI and the percentage of time of $S_{N_{tot,e}}$ violation is achieved. However, an increase of costs is required, due to the fact that, during rain and storm periods, the nitrification process (2.7) is worsened as explained in Sect. 6.2.2. For this reason, extra addition of q_{EC} is needed when there is a rain or storm event, generating an increase of costs (see Figs. 6.12 and 6.13). It should be noted that costs saved due to avoid violations are not reflected in the OCI equation and therefore the cost comparison is not completely fair.

OCI and percentage of operating time of $S_{N_{tot,e}}$ violation are influenced by $q_{EC_{4-5}}$ value and therefore by the intensity and the duration of the rainfall. When there is rain or storm event, greater nitrification is performed by Q_a manipulation and therefore

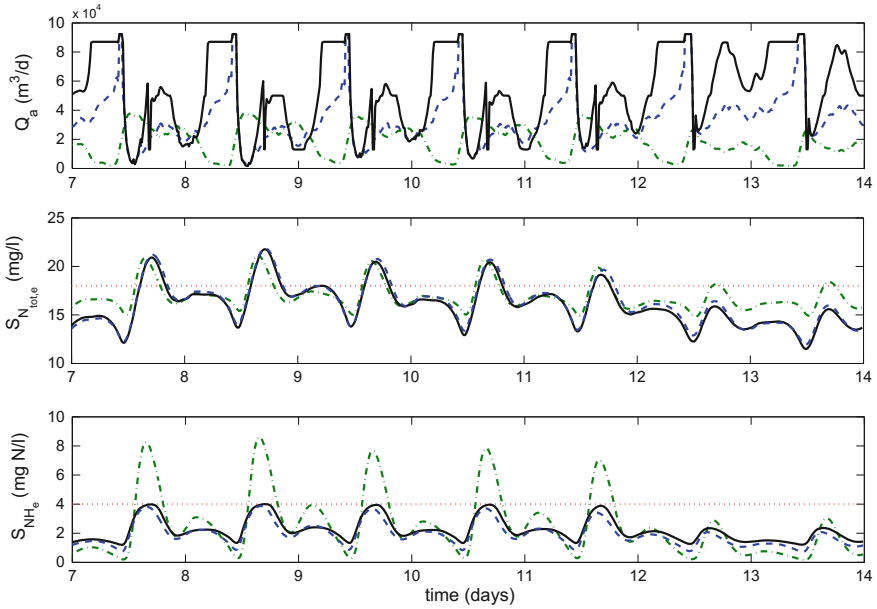

Fig. 6.11 Q_a, $S_{NH,e}$, and $S_{N_{tot,e}}$ evolution from day 7 to 14 with default PI controllers (*dash-dotted line*), applying control strategies for S_{NH_e} violations removal with functions (*dashed line*) and applying control strategies for S_{NH_e} violations removal with FCs (*solid line*)

S_{NO} and also $S_{N_{tot,e}}$ increase. However, adding $q_{EC_{4-5}}$ also decreases the value of S_{NO} and thus $S_{N_{tot,e}}$. With storm influent, the percentage of the cost increase is lower than in the case of rain influent because less $q_{EC_{4-5}}$ is needed for the $S_{NH,e}$ removal. On the other hand, as in the case of rain influent the dosage of $q_{EC_{4-5}}$ is greater, there is a reduction in the percentage of operating time of $S_{N_{tot,e}}$ violation in comparison with the storm influent.

6.3.3 $S_{N_{tot,e}}$ and $S_{NH,e}$ Violations Removal

Up to now, $S_{N_{tot,e}}$ and $S_{NH,e}$ limits violations have been considered separately. Now, both control strategies for $S_{N_{tot,e}}$ and $S_{NH,e}$ violations removal have been tested together. As $S_{NH,e}$ violations present more difficulties to be removed than the ones of $S_{N_{tot,e}}$, especially during rain and storm events, the tuning for the higher level determined to avoid $S_{NH,e}$ violations is also applied in this case.

Table 6.3 shows the results obtained by applying the control strategies to eliminate both $S_{N_{tot,e}}$ and S_{NH} violations for the three weather conditions. As it can be observed, the simultaneous $S_{N_{tot,e}}$ and S_{NH} violations removal is possible for dry, rain, and storm weather conditions. However, removing the two pollutants simultaneously gives rise

Table 6.2 Results with default PI controllers and with control for $S_{NH,e}$ violations removal for dry, rain, and storm influents

	Default PI controllers	Control for $S_{NH,e}$ violations removal with functions	% of reduction (%)	Control for $S_{NH,e}$ violations removal with FCs	% of reduction (%)
Dry influent					
EQI	6115.63	5760.95	5.8	5854.06	4.26
OCI	16381.93	16323.48	0.4	16307.26	0.45
$S_{N_{tot},e}$ violations (% of operating time)	17.56	15.62	11.04	15.62	11.04
$S_{NH,e}$ violations (% of operating time)	17.26	0	100	0	100
Rain influent					
EQI	8174.98	7814.98	4.4	7829.12	4.23
OCI	15984.85	17463.78	−9.2	17675.26	−10.57
$S_{N_{tot},e}$ violations (% of operating time)	10.86	13.84	−27.4	8.93	17.77
$S_{NH,e}$ violations (% of operating time)	27.08	0	100	0	100
Storm influent					
EQI	7211.48	6903.02	4.3	6925.24	3.97
OCI	17253.75	17582.3	−1.9	17633.58	−2.2
$S_{N_{tot},e}$ violations (% of operating time)	15.03	22.32	−48.5	20.24	−34.66
$S_{NH,e}$ violations (% of operating time)	26.79	0	100	0	100

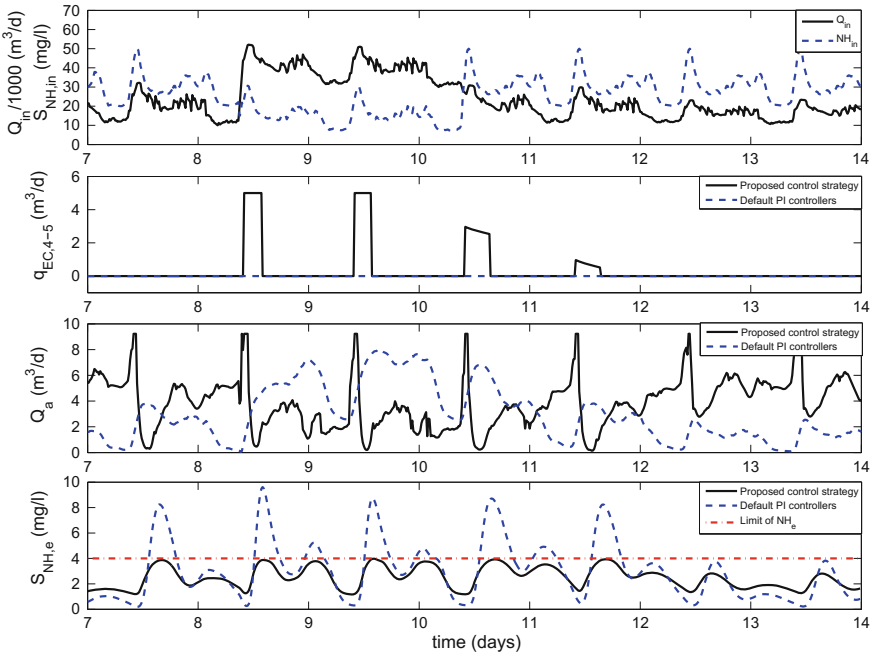

Fig. 6.12 Rain influent: time evolution of the most important variables applying the proposed control strategy for $S_{NH,e}$ violations removal with functions and applying the default control strategy of BSM1

to an increase of OCI. It is due to the fact that the reduction of S_{NH} peaks is based on an improvement in the nitrification process, what causes a great generation of S_{NO} ((2.4) and (2.7)) and also a $S_{N_{tot,e}}$ increase. To counteract it, the dosage of q_{EC} is increased, and q_{EC} in the second tank ($q_{EC,2}$) is also added, as shown in Fig. 6.14 in the case of applying functions, and in Fig. 6.15 for the application of FCs. Therefore, when a peak of $S_{NH,in} \cdot Q_{in}$, and there is not a rainfall or storm event, $q_{EC,1}$ is added at its maximum value (5 m^3/d) and $q_{EC,2}$ is calculated with the affine function or the FC implemented for the control strategy for $S_{N_{tot,e}}$ violations removal. This q_{EC} increase results in the total elimination of $S_{N_{tot,e}}$ and $S_{NH,e}$ violations and an EQI reduction, but the counterpart is an OCI increase. However, as explained in the previous section, the OCI equation does not take into account the reduction of costs of avoiding violations and thus, the cost comparison is not completely fair. The OCI increase is higher using FCs because the addition of $q_{EC,2}$ is based on NH5 plus NO5. In the case of using functions, the addition of $q_{EC,2}$ is only based on the maximum value of the previous week. This alternative lets to add $q_{EC,2}$ in advance and therefore reduces their doses and consequently reduces costs. However, this option would not be entirely satisfactory in the case of having a more variable dry influent.

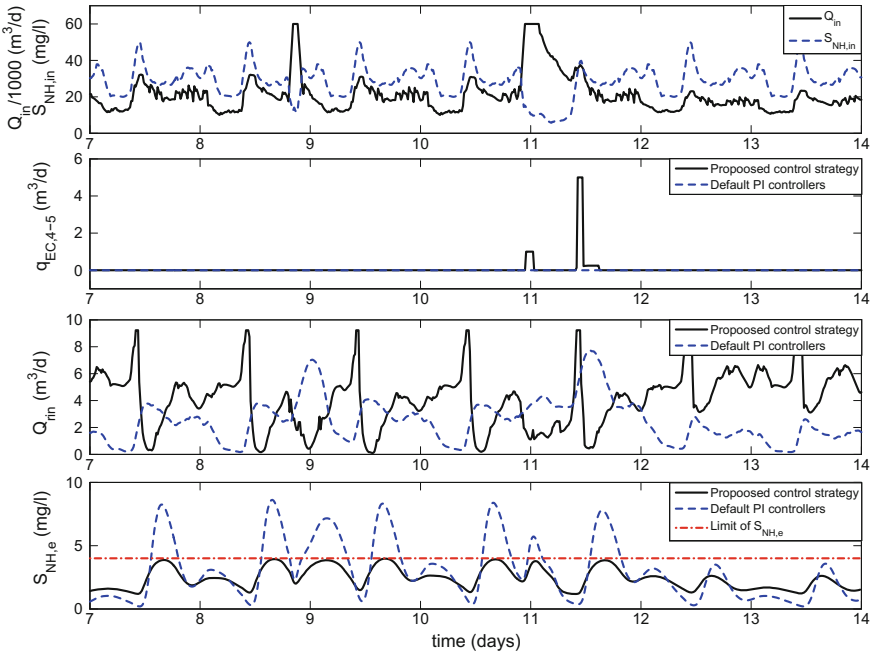

Fig. 6.13 Storm influent: time evolution of the most important variables applying the proposed control strategy for $S_{NH,e}$ violations removal with functions and applying the default control strategy of BSM1

6.4 Summary

This chapter has been focused on the objective of effluent violations removal using BSM1 as testing plant. With this aim, two control loops have been added to the hierarchical structure explained in previous chapters. These control loops consist in the manipulation of $q_{EC,1}$ based on $S_{NH,5}$ plus $S_{NO,5}$ and the manipulation of Q_a based on $S_{NH,5}$, $S_{NH,in}$, and Q_{in}. Functions and FCs have been proposed for these control strategies basing their control on the biological processes.

The improvement of the denitrification process, by adding $q_{EC,1}$, achieves the complete elimination of $S_{N_{tot},e}$ violations. This control strategy has been tested with an affine function with a sliding window and with an FC. Both have been implemented to dosage the minimum $q_{EC,1}$ necessary for this aim. The improvement of the nitrification process by manipulating Q_a makes possible the $S_{NH,e}$ violations removal. It has been tested first, with the combination of a linear function and an exponential function, and next, with an FC which uses different tuning parameters depending on if there are peaks of pollution in the tanks or not.

Simulation results show that $S_{N_{tot},e}$ and $S_{NH,e}$ violations have been removed for dry, rain, and storm influents. In the cases of $S_{N_{tot},e}$ violations removal for the three weather conditions and $S_{NH,e}$ violations removal for dry weather, a simultaneous reduction of

Table 6.3 Results with default PI controllers and with control strategies for the simultaneous $S_{N_{tot,e}}$ and $S_{NH,e}$ violations removal with functions and with FCs for dry, rain, and storm influents

	Default PI controllers	Control for $S_{N_{tot,e}}$ and $S_{NH,e}$ violations removal with functions	% of reduction (%)	Control for $S_{N_{tot,e}}$ and $S_{NH,e}$ with FCs	% of reduction (%)
Dry influent					
EQI	6115.63	5624.41	8.03	5598.4	8.46
OCI	16381.93	17494.44	−6.8	17747.85	−8.34
$_{N_{tot,e}}$ violations (% of operating time)	17.56	0	100	0	100
$S_{NH,e}$ violations (% of operating time)	17.26	0	100	0	100
Rain influent					
EQI	8174.98	7695.03	5.9	7658.32	6.32
OCI	15984.85	18524.71	−15.9	18735.84	−17.21
$S_{N_{tot,e}}$ violations (% of operating time)	10.86	0	100	0	100
$S_{NH,e}$ violations (% of operating time)	27.08	0	100	0	100
Storm influent					
EQI	7211.48	6685.15	7.3	66615.09	7.75
OCI	17253.75	19524.67	−13.2	19672.72	−14.02
$S_{N_{tot,e}}$ violations (% of operating time)	15.03	0	100	0	100
$S_{NH,e}$ violations (% of operating time)	26.79	0	100	0	100

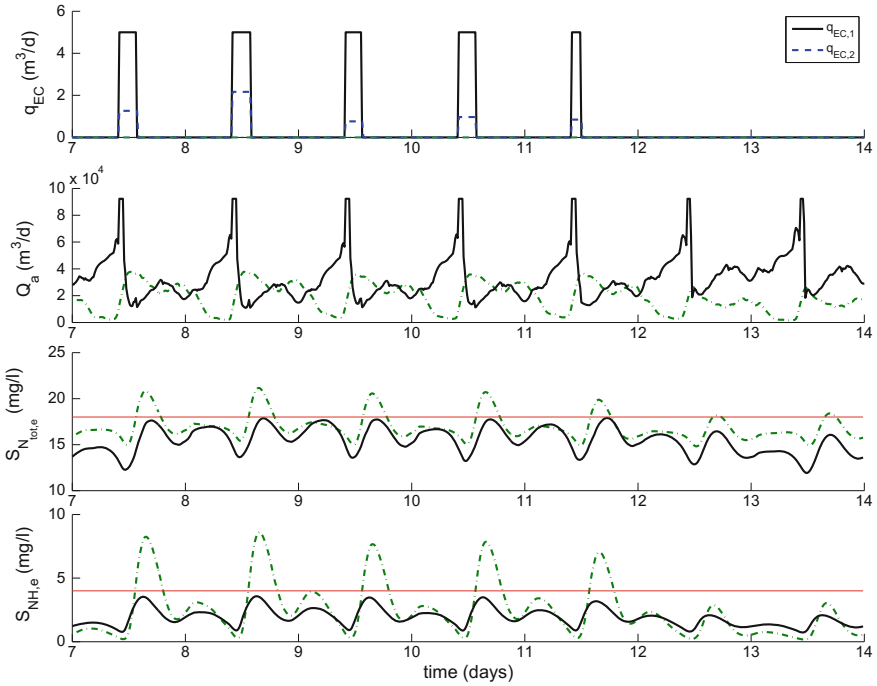

Fig. 6.14 q_{EC}, Q_a, $S_{NH,e}$, and $S_{N_{tot,e}}$ evolution from day 7 to 14 with default PI controllers (*dash-dotted line*) and with the control strategies for $S_{NH,e}$ and $S_{N_{tot,e}}$ violations removal using functions (*solid line*)

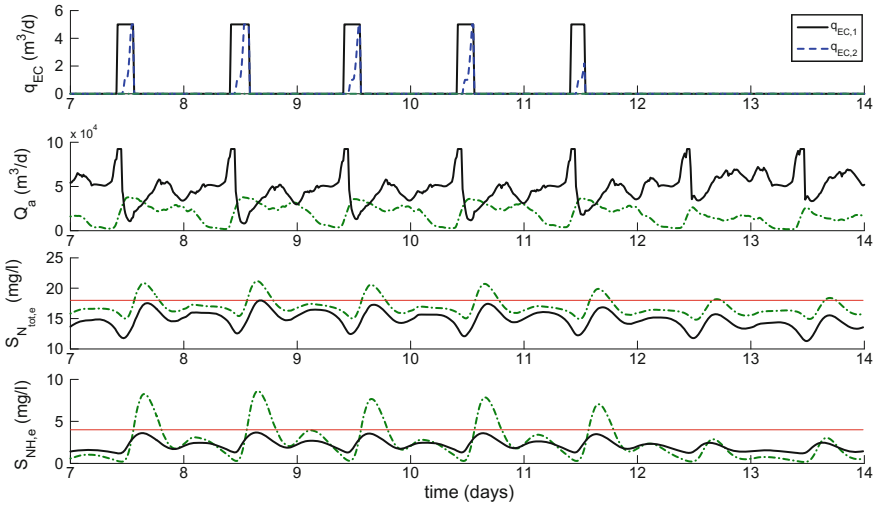

Fig. 6.15 q_{EC}, Q_a, $S_{NH,e}$, and $S_{N_{tot,e}}$ evolution from day 7 to 14 with default PI controllers (*dash-dotted line*) and with the control strategies for $S_{NH,e}$ and $S_{N_{tot,e}}$ violations removal using FCs (*solid line*)

EQI and OCI is achieved in comparison with the default control strategy. The $S_{NH,e}$ violations removal for rain and storm influents and the simultaneous elimination of $S_{N_{tot},e}$ and $S_{NH,e}$ make inevitable an increase of OCI. In any case, it has to be said that, with the removal of effluent violations, a reduction of costs has been obtained for not paying fines, which is not considered in OCI.

Chapter 7
Effluent Predictions for Violations Risk Detection

This chapter deals with the elimination of $S_{N_{tot,e}}$ and $S_{NH,e}$ using BSM2, which provides a more elaborated and variable influent with an assessment of one year. Applying control strategies to avoid effluent violations, only when an increase of contaminants is already detected in the reactors, is not enough in BSM2. Due to this fact, an effluent prediction of the pollutants based on some variables in the influent is required. ANNs are implemented with this aim.

7.1 Implementation of Artificial Neural Networks

For an efficient elimination of effluent violations, risk detection in advance is essential to react as soon as possible and to apply immediately the necessary preventive actions to the plant; otherwise most violations cannot be avoided. This violations risk detection is carried out by ANNs that estimate the future effluent values, based on information at the entry point of the biological treatment.

ANN models have been tested in previous works for prediction of real WWTP performance, due to their ability for learning its large nonlinearities. For instance, in [26] to predict BOD and TSS of a WWTP in Cairo, Egypt; in [25] to predict COD and TSS of a WWTP in Ankara, Turkey; in [45] to predict COD, BOD, and TSS in a WWTP in Alexandria, Egypt and in [64] to predict COD in a WWTP in India.

Two ANNs are proposed in this chapter with the mentioned objectives. One ANN predicts the $S_{NH,e}$ value ($S_{NH,ep}$) and the other ANN predicts the $S_{N_{tot,e}}$ value ($S_{N_{tot,ep}}$). When the ANNs detect a risk of $S_{N_{tot,e}}$ or $S_{NH,e}$ violation, special control strategies using FCs (explained in the next subsection) are applied to avoid them. When a risk of $S_{NH,e}$ violation is detected, Q_a is manipulated based on $S_{NH,5}$ to reduce $S_{NH,e}$ peak. The rest of the time Q_a is manipulated in order to control $S_{NO,2}$ at the set-point of 1 mg/l. Regarding $S_{N_{tot,e}}$, when a risk of violation is detected (the value of $S_{N_{tot,ep}}$

I. Santín et al., *Control and Decision Strategies in Wastewater Treatment Plants for Operation Improvement*, Intelligent Systems, Control and Automation: Science and Engineering 86, DOI 10.1007/978-3-319-46367-4_7

exceeds the limit), q_{EC} is manipulated based on $S_{N_{tot,ep}}$, instead of being kept at a fixed value as usual.

An accurate violations risk detection of $S_{NH,e}$ and $S_{N_{tot,e}}$ is not possible due to the fact that ANNs use only influent variables as inputs, while the effluent concentrations also depend on other variables of the process, as S_O and q_{EC} which have a significant impact on $S_{NH,e}$ and $S_{N_{tot,e}}$. Those variables cannot be taken into account because it is necessary to detect the risk of effluent violations in advance. Moreover, all data used to detect the risk has to be easily measurable. However, with an adequate choice of the input variables of ANNs, it is possible to achieve an adequate approximation in order to detect a risk of violation for applying the suitable control strategy.

Therefore, the inputs of ANNs have been determined according to the mass balance equations (2.19) and (2.20) explained in Sect. 2. The variables used to perform the violations risk detection for both ANNs are Q_{po}, Z_{po} and T_{as}. The variable Q_a has also been used as an input for the ANN to detect the risk of $S_{N_{tot,e}}$ violation, but it is not used to detect the risk of $S_{NH,e}$ violation because it is a manipulated variable in the control strategy applied to remove $S_{NH,e}$ violations and it would cause dependency values problems. Specifically, S_{NH} from the primary clarifier overflow ($S_{NH,po}$) is the pollutant concentration chosen as an input for both ANNs. On one hand, S_{NH} and S_{NO} are the pollutants with higher influence on $S_{N_{tot,e}}$, but S_{NO} from the primary clarifier overflow ($S_{NO,po}$) is very low and it is not taken into account. On the other hand, $S_{NH,po}$ not only affects largely $S_{NH,e}$, but also affects the nitrification process, the consequent S_{NO} production and therefore the resulting $S_{N_{tot,e}}$.

T_{as} is also added as an input variable for both ANNs due to its influence in the nitrification and denitrification processes ((2.25) and (2.26)). The $S_{NH,e}$ and $S_{N_{tot,e}}$ values are inversely proportional to the T_{as} values. Due to the fact that the T_{as} variations during the day are not too large, the average value of each day has been selected. However, it should be noted that variations in T_{as} throughout the year have a significant effect on $S_{NH,e}$ and $S_{N_{tot,e}}$ making its selection as ANN input necessary for an accurate violations risk detection.

Finally, due to the mentioned reasons, the inputs for the ANNs are

- Inputs of ANN for $S_{NH,e}$ model prediction: Q_{po}, $S_{NH,po}$, $Q_{po} \cdot S_{NH,po}$, T_{as}.
- Inputs of ANN for $S_{N_{tot,e}}$ model prediction: Q_{po}, $S_{NH,po}$, $Q_{po} \cdot S_{NH,po}$, T_{as}, Q_a.

It should be taken into account that in a real plant application, sensor failures are quite common, particularly if they are located in the influent. For this reason, controllers applied to a real plant should use some sensor failure detection algorithm. On the other hand, in spite of that the S_{NH} sensor needs an extra maintenance cost, it is essential for the risk detection of violations and thus to achieve the effluent violations removal.

To train and validate ANNs, a collection of input and output data is necessary. The variations in the inputs affect the outputs with a variable delay that depends on the hydraulic retention time. Due to this fact, and in order to simplify the data collection process, for the ANNs inputs and outputs only the maximum and minimum values of each day have been selected. Except for T_{as}, where the daily average value has been considered. As a large number of data is necessary to generate a satisfactory model

Fig. 7.1 Structures of the proposed ANNs

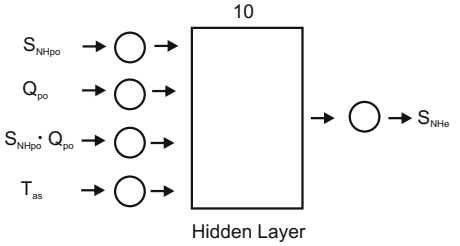

(a) ANN for $S_{NH,e}$ violations risk detection

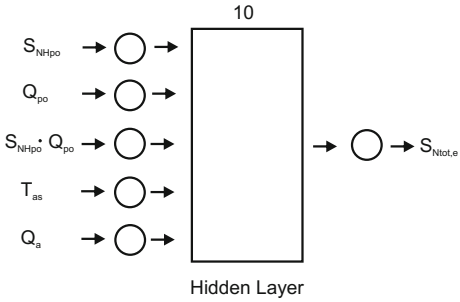

(b) ANN for $S_{N_{tot,e}}$ violations risk detection

for an ANN, the data is obtained during a one year simulation period with the plant working without the control strategies for avoiding $S_{N_{tot,e}}$ and $S_{NH,e}$ violations. In a real plant, the stored historical data could be used for this purpose. Each ANN has one hidden layer with 10 neurons. ANNs have been trained with the aim of obtaining a reasonable fitting rate of 0.93 or above. The structures are shown in Fig. 7.1.

For the training of the ANN the MATLAB® NNToolbox has been used. As already mentioned, recorded data corresponding to one year of running the plant with the hierarchical control in place has been used. The data is partitioned in different sets that are used for training (70 % of data), another one to validate the network is generalizing and to stop training before overfitting (15 % of data). The rest of the data (the remaining 15 %) is used as a completely independent test of network generalization. The training results are evaluated by means of error histogram. Figure 7.2 shows the error histograms corresponding to both ANN. The blue bars represent training data, the green bars represent validation data, and the red bars represent testing data. As it can be seen, the ANN for $S_{N_{tot,e}}$ prediction is more difficult to train. Even this, there are practically no significant outliers and, if any, their magnitude is really small. It remains a subject of further exploration about the suitability of more complex network structures if precise effluent following is needed.

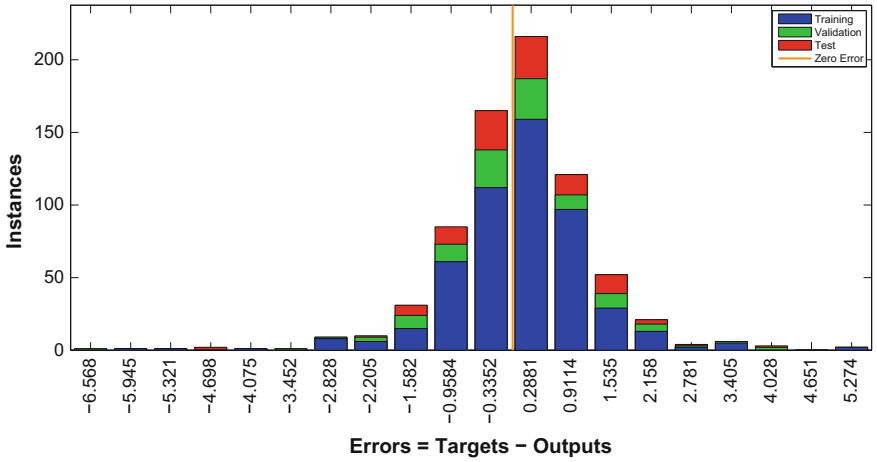

(a) Error histogram of ANN for $S_{N_{tot,e}}$ violations risk detection

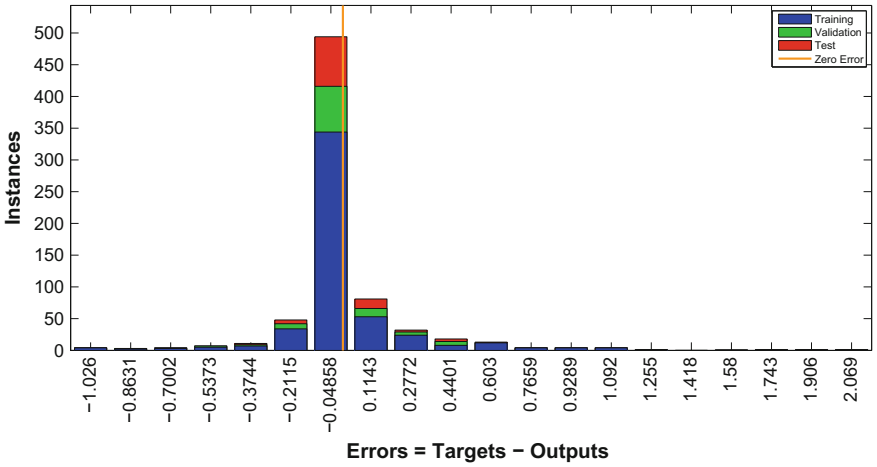

(b) Error histogram of ANN for $S_{NH,e}$ violations risk detection

Fig. 7.2 ANN training error histograms

7.2 Simulation Results

There are moments where the high disturbances coming from the influent make plant operation very difficult. Therefore, the ANN prediction will show the potential risk of effluent limit violations.

The BSM2 is now simulated by applying the hierarchical control scheme explained in next chapter. In parallel, the influent data feeds both ANN and output pollutant concentrations are predicted. As mentioned when describing the BSM2 scenario, the

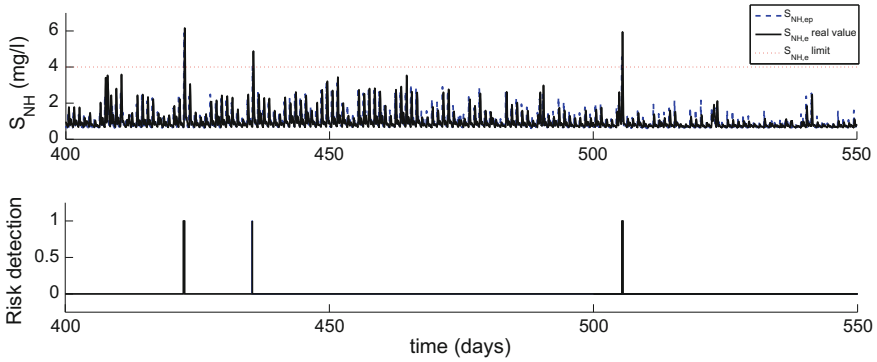

Fig. 7.3 $S_{NH,e}$ limit violation risk detection. Long time window

assessment period is extended to one year instead of one week. Figure 7.3 shows, as an example, the simulation results for $S_{NH,e}$ risk detection for a time window of 150 days. It can be seen that the hierarchical two-level control system operates the plant quite well, and only three risk situations are detected. It is in these cases when supplementary control actions will be needed.

In order to better show how the risk detection works, Figs. 7.4 and 7.5 show the risk detection for both output concentrations $S_{NH,e}$ and $S_{N_{tot,e}}$ in an enlarged time window. As it can be observed, the way of ANN have been trained allows for a real effluent pollutants prediction. This allows for an early detection of the possible limit violation. A flag signal is activated during 6 h. For future use, this boolean signal could be used to activate a decision system that signals for appropriate corrective actions regarding these violations.

On the other hand, in Fig. 7.5, it is shown that there is a mismatch between the number of real limit violations and the times that the risk signal is activated. This is because of the three maximums the effluent do has during the violation period. In any case, the fact that during one day the signal is activated three times, corresponds to a really dangerous situation.

In order to assess the violations risk detections made by the ANNs, they have been compared with the situations where there is, effectively, a limit violation (without applying the control strategies for removing limit violations of the pollutants). For $S_{NH,e}$, there are four limit violations and 100 % of the violations are detected and subsequently eliminated. Moreover, the ANN detects six risks of violations, therefore there are two situations that can be classified as "false alarm". Regarding $S_{N_{tot,e}}$, not all violations are detected. There are in fact 47 violations and 43 violation risk detections. From these 43 detections, 34 violations are correct. Therefore, a total of 72.34 % of violations are detected.

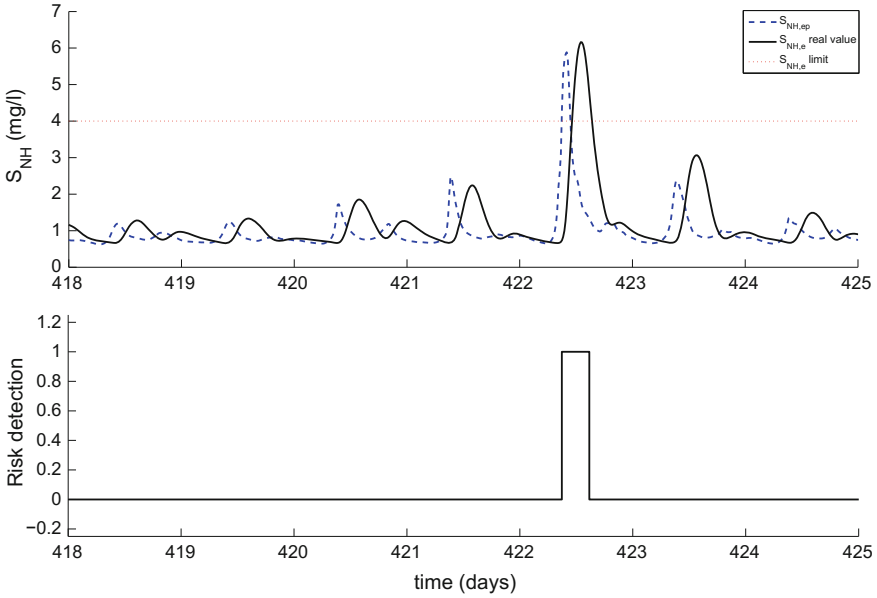

Fig. 7.4 $S_{NH,e}$ limit violation risk detection

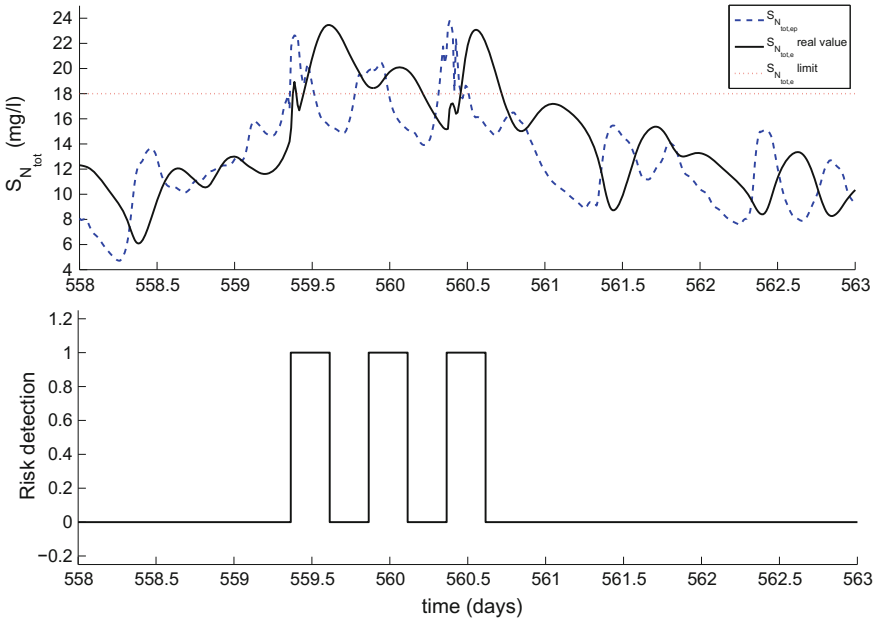

Fig. 7.5 $S_{N_{tot},e}$ limit violation risk detection

7.3 Summary

For effluent violations removal in BSM2, effluent predictions are necessary in order to select the suitable control strategy to be applied. In this chapter, the implementation of the ANNs for these effluent predictions has been described. Specifically two ANNs have been applied, one for $S_{N_{tot,e}}$ prediction and the other for $S_{NH,e}$ prediction. For the case of $S_{N_{tot,e}}$ prediction, the input variables have been Q_{po}, $S_{NH,po}$, $Q_{po} \cdot S_{NH,po}$ and T_{as}. And for $S_{NH,e}$ prediction the input variables have been Q_{po}, $S_{NH,po}$, $Q_{po} \cdot S_{NH,po}$, T_{as} and Q_a.

Simulations have shown satisfactory predictions of $S_{N_{tot,e}}$ and $S_{NH,e}$, which are used for risk detection and thus for selecting the suitable control strategy. For $S_{NH,e}$ prediction, the threshold has been established at 4 mg/l, the same as the limit value. For the case of $S_{N_{tot,e}}$ prediction, the threshold has been reduced to 17 mg/l (1 mg/l less than the established limit) to ensure the avoidance of violation, but without reducing it too much for not increasing costs.

Chapter 8
Advanced Decision Control System

This chapter presents the control strategies applied in BSM2 for $S_{N_{tot,e}}$ or $S_{NH,e}$ violations removal. This chapter continues with special emphasis on dealing with the concentration limits of effluent pollutants, in order to accomplish the established legal requirements. In this case, the greater variability in the influent provided by BSM2 requires an advanced decision control system in order to select the control strategies to be applied based on the effluent predictions explained in the previous chapter.

8.1 $S_{O,4}$, $S_{O,5}$ and $S_{NO,2}$ Tracking

The simulations and evaluations of the control strategies presented in this chapter are carried out with BSM2. In the literature some works use BSM2 as testing plant. Some of them are focused on the implementation of control strategies in the biological treatment, as in the present chapter. Specifically, they propose a multi-objective control strategy based on S_O control by manipulating K_La of the aerated tanks, S_{NH} hierarchical control by manipulating the S_O set-points, $S_{NO,2}$ control by manipulating Q_a or TSS control by manipulating Q_w [7, 19, 20, 37]. These referred works have different goals, but all of them obtain an improvement in effluent quality and/or a reduction of costs. However, none of them aim to avoid the limits violations of the effluent pollutants.

The control configurations proposed in this chapter are based on MPC + FF and FCs. MPC + FF is used in order to keep the $S_{O,4}$, $S_{O,5}$ and $S_{NO,2}$ at the given set-point. FCs are applied, on one side, as higher level controller in a hierarchical structure to vary the S_O references to be tracked by the MPC controllers, and, on the other hand, to remove $S_{N_{tot,e}}$ and $S_{NH,e}$ violations by determining $q_{EC,1}$ and Q_a values. The application of FCs are based on the biological processes, but without the goal of keeping the controlled variable at a set-point. In this case, the control objectives are: the improvement of OCI and EQI, and the violations removal of $S_{N_{tot,e}}$ and $S_{NH,e}$. The

I. Santín et al., *Control and Decision Strategies in Wastewater Treatment Plants for Operation Improvement*, Intelligent Systems, Control and Automation: Science and Engineering 86, DOI 10.1007/978-3-319-46367-4_8

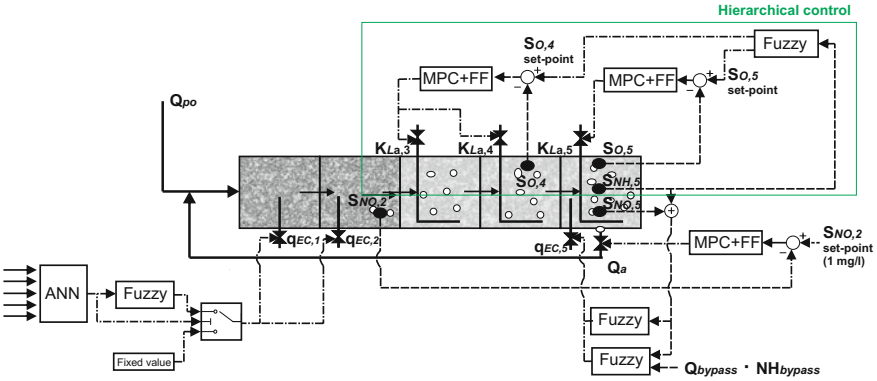

(a) Control strategy for $S_{N_{tot,e}}$ violations removal

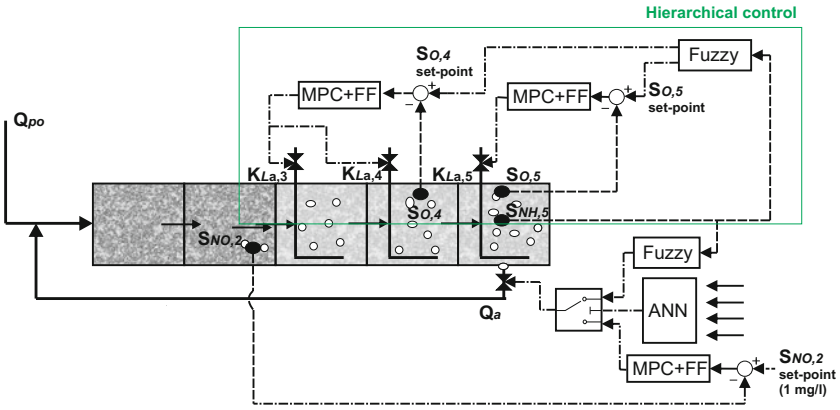

(b) Control strategy for $S_{NH,e}$ violations removal

Fig. 8.1 Proposed control strategies for $S_{N_{tot,e}}$ or $S_{NH,e}$ violations removal with a simultaneous EQI and OCI reduction

advanced decision control system to be presented in this chapter relies on the effluent predictions developed in the previous chapter (see Fig. 8.1) in order to appropriately select the control strategy that better fits the actual state of the plant.

Two MPC + FF controllers are proposed for the aerated zone, to control $S_{O,5}$ by manipulating $K_L a_5$ and to control $S_{O,4}$ by manipulating $K_L a_3$ and $K_L a_4$ based on [46]. The aim of these MPC + FF controllers is to improve the set-points tracking regarding the PI controllers of defCL. Also, an MPC + FF is applied to control $S_{NO,2}$ at a reference value of 1 mg/l by manipulating Q_a, based on the default strategy of BSM1. In the same way as in BSM1, in order to adjust the manipulated variables immediately

to compensate the disturbances, Q_{po} has been selected for the feedforward action of the MPC + FF controllers.

In this chapter, unlike the defCL, $S_{O,4}$ and $S_{O,5}$ references are not maintained at a fixed value. Instead of this, a FC varies the set-point, adapting it based on the conditions of the nitrification process. Due to this reason, it should be noted the importance of the MPC + FF controllers performance to ensure that the $S_{O,4}$ and $S_{O,5}$ values are as close as possible to the set-point given by the FC.

The variables of the state-space model (3.6) for the three MPC + FF controllers are described following:

In the MPC + FF for $S_{O,4}$ control the variable $u_1(k)$ is $K_L a_4$ and $K_L a_3$, $u_2(k)$ is Q_{po} and $y_1(k)$ is $S_{O,4}$; in the MPC + FF for $S_{O,5}$ control the variable $u_1(k)$ is $K_L a_5$, $u_2(k)$ is Q_{po} and $y_1(k)$ is $S_{O,5}$; finally, in the MPC + FF for $S_{NO,2}$ control the variable $u_1(k)$ is Q_a, $u_2(k)$ is Q_{po} and $y_1(k)$ is $S_{NO,2}$.

The identification of the linear predictive models of the MPC + FF controllers was performed using Matlab® System Identification toolbox. The data of the output variables ($S_{O,4}$, $S_{O,5}$ and $S_{NO,2}$) are obtained by making changes to the input variables ($K_L a_3$, $K_L a_4$, $K_L a_5$ and Q_a) with a maximum variation of 10 % regarding its operating point, which is the value of $K_L a$ necessary to obtain 2 mg/l of $S_{O,4}$, 1 mg/l of $S_{O,5}$ and the value of Q_a necessary to obtain 1 mg/l of $S_{NO,2}$. Specifically, the working points are 120 day^{-1}, 60 day^{-1} and 61944 m^3/day for $K_L a_3$/$K_L a_4$, $K_L a_5$ and Q_a respectively. PEM was selected to determine the model with the obtained data. Therefore the following second-order state-space models are obtained.

$S_{O,4}$ Control

$$\begin{aligned} A &= \begin{bmatrix} 0.9768 & 0.1215 \\ 0.09664 & 0.2635 \end{bmatrix} \\ B &= \begin{bmatrix} 0.002984 & -3.673 \cdot 10^{-6} \\ -0.01796 & 8.318 \cdot 10^{-6} \end{bmatrix} \\ C &= \begin{bmatrix} 3.682 & -0.4793 \end{bmatrix} \\ D &= \begin{bmatrix} 0 & 0 \end{bmatrix} \end{aligned} \tag{8.1}$$

$S_{O,5}$ Control

$$\begin{aligned} A &= \begin{bmatrix} 0.9794 & 0.1109 \\ 0.0976 & 0.3544 \end{bmatrix} \\ B &= \begin{bmatrix} 0.001836 & -1.259 \cdot 10^{-5} \\ -0.01153 & 7.04e-005 \end{bmatrix} \\ C &= \begin{bmatrix} 8.412 & -0.1429 \end{bmatrix} \\ D &= \begin{bmatrix} 0 & 0 \end{bmatrix} \end{aligned} \tag{8.2}$$

$S_{NO,2}$ Control

$$
\begin{aligned}
A &= \begin{bmatrix} 0.8301 & 0.2828 \\ 0.0578 & 0.8674 \end{bmatrix} \\
B &= \begin{bmatrix} 3.264 \cdot 10^{-6} & -1.358 \cdot 10^{-5} \\ -1.767 \cdot 10^{-6} & -2.87 \cdot 10^{-6} \end{bmatrix} \\
C &= \begin{bmatrix} 5.035 & 0.2777 \end{bmatrix} \\
D &= \begin{bmatrix} 0 & 0 \end{bmatrix}
\end{aligned}
\tag{8.3}
$$

The selected values to tune the MPC + FF controllers are $m = 5$, $p = 20$, $\triangle t = 0.00025$ days (21.6 s), $\Gamma_y = 1$ and $\Gamma_{\triangle u} = 1 \cdot 10^{-5}$ and overall estimator gain =0.8 for $S_{O,4}$ control; $m = 5$, $p = 20$, $\triangle t = 0.00025$ days (21.6 s), $\Gamma_y = 1$ and $\Gamma_{\triangle u} = 5 \cdot 10^{-4}$ and overall estimator gain =0.8 for $S_{O,5}$ control; $m = 5$, $p = 50$, $\triangle t = 0.00025$ days (21.6 s), $\Gamma_y = 1$ and $\Gamma_{\triangle u} = 1 \cdot 10^{-5}$ and overall estimator gain = 0.9 for $S_{NO,2}$ control.

Data acquisition for the model identification is based on simulations. However, data can be acquired in a similar way in a real plant. In order to predict the possible application in a real plant, the data acquisition for the identification is performed while the plant is working around an operating point, whose values are considered suitable for the biological wastewater treatment of this plant. Therefore, identification can be performed adding some changes to those operating conditions. As mentioned before, these changes correspond to a maximum variation of 10 % of the manipulated variables. Therefore they will not disturb the actual plant operation. The generated outputs will reflect the effect of such variables manipulation. Data has been acquired by simulating one week. However, in the case of a real plant, the identification could be carried out in different periods and not necessarily in consecutive days. Plants operator knowledge can in addition be used to know the more appropriate days to perform the identification.

8.2 Manipulation of S_O Set-Points, q_{EC} and Q_a

Five FCs have been implemented in the proposed control strategies with three objectives: to reduce EQI and OCI, to remove $S_{N_{tot,e}}$ violations and to eliminate $S_{NH,e}$ violations. They are based on the biological processes given by ASM1.

For the five FCs applied, Mamdani [40] is the method selected to defuzzify. The design of the FCs was based on the observation of the simulations results obtained by operating the plant with the default control of BSM2. The corresponding designs are described in the following.

8.2.1 Fuzzy Controller for EQI and OCI Reduction

A FC is applied as higher level controller to manipulate $S_{O,4}$ and $S_{O,5}$ set-points based on the $S_{NH,5}$ with the aim to reduce EQI and OCI. Specifically, it is based on the nitrification process, improving it or making it worse based on a trade-off between the values of S_{NH} and S_{NO}. The idea of this control is to improve the nitrification process by increasing $S_{O,4}$ and $S_{O,5}$ references (2.26) when there is an $S_{NH,5}$ increase caused by the influent, reducing thus $S_{NH,e}$ peaks. Conversely, to reduce the $X_{B,H}$ growth when the $S_{NH,5}$ level is low, in order to produce less S_{NO} (2.26) and (2.22) and at the same time to reduce operational costs (2.32).

For the higher level FC, three triangular membership functions for input and for output are used (low, $medium$ and $high$). The implemented $if - then$ rules are

if ($S_{NH,5}$ is low) **then** ($S_{O,4}$ set is low)
if ($S_{NH,5}$ is $medium$) **then** ($S_{O,4}$ is $medium$)
if ($S_{NH,5}$ is $high$) **then** ($S_{O,4}$ is $high$)

The range of the input values is from 0.2 to 4, and the range for the output values is from -0.75 to 4.5. $S_{O,5}$ set-point is equal to the half value of $S_{O,4}$.

8.2.2 Fuzzy Controllers for $S_{N_{tot},e}$ Violations Removal

The idea of this control strategy is to add q_{EC} in order to deal with $S_{N_{tot},e}$ peaks and remove the corresponding limit violations, but doing this only when there is a risk of violation in order to reduce operational costs. Instead of this, the default control strategy keeps $q_{EC,1}$ fixed at 2 m^3/d continuously. Three FCs are proposed. One FC is used as predictive control, adding q_{EC} in the first and second reactors ($q_{EC,1-2}$) when a violation is predicted, based on $S_{N_{tot,ep}}$ value given by the ANN (explained above). This control strategy is necessary, because acting only when a high $S_{N_{tot}}$ value in the reactors is detected could not be enough if $S_{N_{tot}}$ is quite high. The second FC adds q_{EC} in the fifth tank ($q_{EC,5}$) based on $S_{NH,5}$ plus $S_{NO,5}$, which are the contaminants with more influence on $S_{N_{tot}}$. This control acts when, in spite of the predictive control, $S_{NH,5} + S_{NO,5}$ increases excessively. As the biological process is designed to treat a maximum flow rate of 60,420 m^3/d, when the flow rate coming from the primary treatment surpasses this value, the excess is bypassed directly to the effluent without being treated. In the case of the bypass is active, the third fuzzy control manipulates $q_{EC,5}$ based on the bypass flow rate (Q_{bypass}) multiplied by S_{NH} in the bypass ($S_{NH,bypass}$), in order to compensate the increase of $S_{NH,e}$ due to the flow rate that cannot be treated.

The first FC, which is based on the $S_{N_{tot,ep}}$, has one input and one output, with three membership functions for each (*low*, *medium* and *high*). The implemented $if - then$ rules are

if ($S_{N_{tot,ep}}$ is *low*) **then** ($q_{EC,1-2}$ is *low*)
if ($S_{N_{tot,ep}}$ is *medium*) **then** ($q_{EC,1-2}$ is *medium*)
if ($S_{N_{tot,ep}}$ is *high*) **then** ($q_{EC,1-2}$ is *high*)

If $q_{EC,1-2}$ value is less than the maximum value of q_{EC} set in each reactor (5 m^3/d), it is only added to the first reactor. If q_{EC} is greater than 5 m^3/d, $q_{EC,1}$ is equal to 5 m^3/d and $q_{EC,2}$ is equal to the value of $q_{EC,1-2}$ minus 5. The range of the input values of the fuzzifier is from 17 to 19.5, and the range for the output values is from 4 to 15. Therefore, $q_{EC,1-2}$ is added when $S_{N_{tot,ep}}$ is over 17 mg/l instead of 18 mg/l which is the limit value, thus a margin of error of 5.5 % in the prediction is established.

When a situation of risk is detected ($S_{N_{tot,ep}} > 17$ mg/l), $q_{EC,1-2}$ is manipulated until the three following conditions are met to ensure that the risk has disappeared: $S_{N_{tot,ep}}$ is lower than 16 mg/l, $S_{NH,5}$ plus $S_{NO,5}$ is lower than 13.5 mg/l and the controller has been operating for at least 6 h. The controller calculates a $q_{EC,1-2}$ value at each sample time, but the true value applied to the plant is the maximum of all the previous samples, in order to ensure that the effluent violation is avoided.

The second FC, which manipulates $q_{EC,5}$ based on $S_{NH,5} + S_{NO,5}$, has one input and one output, with three membership functions for each input and output (*low*, *medium* and *high*). The range of the input values is from 15.3 to 15.9, and the range of the output values is from -1 to 6. The implemented $if - then$ rules are

if ($S_{NH,5} + S_{NO,5}$ is *low*) **then** ($q_{EC,5}$ is *low*)
if ($S_{NH,5} + S_{NO,5}$ is *medium*) **then** ($q_{EC,5}$ is *medium*)
if ($S_{NH,5} + S_{NO,5}$ is *high*) **then** ($q_{EC,5}$ is *high*)

The third FC, which manipulates $q_{EC,5}$ based on $S_{NH,5} + S_{NO,5}$ and $Q_{bypass} \cdot S_{NH,bypass}$, has two inputs and one output, with three membership functions for each input and output (*low*, *medium* and *high*). The range of the $S_{NH,5} + S_{NO,5}$ input values is from 12 to 12.5, the range of the $Q_{bypass} \cdot S_{NH,bypass}$ input values is from 0 to $1.4 \cdot 10^5$ and the range for the output values is from $-1 \cdot 10^4$ to $6 \cdot 10^5$. The implemented $if - then$ rules are:

if ($S_{NH,5} + S_{NO,5}$ is *low* and $Q_{bypass} \cdot S_{NH,bypass}$ is *low*) **then** ($q_{EC,5}$ is *low*)
if ($S_{NH,5} + S_{NO,5}$ is *medium* and $Q_{bypass} \cdot S_{NH,bypass}$ is *medium*) **then** ($q_{EC,5}$ is *medium*)
if ($S_{NH,5} + S_{NO,5}$ is *high* and $Q_{bypass} \cdot S_{NH,bypass}$ is *high*) **then** ($q_{EC,5}$ is *high*)

This controller works while bypass is active. As in the first FC, the $q_{EC,5}$ value applied to the plant by the second and third FCs is the maximum of all the previous calculated values during the situation of risk.

8.2.3 *Fuzzy Controller for S_{NH_e} Violations Removal*

A FC is proposed to eliminate $S_{NH,e}$ violations by manipulating Q_a based on $S_{NH,5}$. This control strategy is applied only when a $S_{NH,e}$ violation is predicted by the ANN, explained in the previous chapter. The rest of the time Q_a is manipulated to control $S_{NO,2}$.

When a risk of violation is detected ($S_{NH,ep} > 4$ mg/l), the proposed FC is applied, first to dilute $S_{NH,po}$ and subsequently to reduce the hydraulic retention time when the increase of S_{NH} reaches the reactors. Thus, according to the mass balance equation in the first reactor (2.19), when $S_{NH,po}$ increases, Q_a is incremented to reduce the rise of $S_{NH,1}$, and when the increase of S_{NH} arrives to the fifth tank, Q_a is reduced to increase the retention time and so to improve de nitrification process. When, in spite of this control, $S_{NH,5}$ reaches the value of 3.5 mg/l, a complementary action is applied and the $S_{O,4}$ ans $S_{O,5}$ set-points are increased by multiplying its value by 1.5.

The FC has one input and one output, with three membership functions for each (low, $medium$ and $high$). The implemented $if - then$ rules are

if ($S_{NH,5}$ is low) **then** (Q_a is $high$)
if ($S_{NH,5}$ is $medium$) **then** (Q_a is $medium$)
if ($S_{NH,5}$ is $high$) **then** (Q_a is low)

The tuning parameters are set looking for a great variation in Q_a. Thus, the range of the input values is from 3 to 4.1 mg/l, and the range for the output values is from $-3 \cdot 10^4$ to $2{\cdot}10^5$ m^3/d. A short range of input values is set in order to achieve a fast Q_a variation to reduce S_{NH} peaks. For a satisfactory plant performance, this control strategy is only active when there is a risk of $S_{NH,e}$ violation. Therefore, this FC is only applied to specific $S_{NH,5}$ values.

This control is interrupted when the risk of violation disappears ($S_{NH,ep} < 4$ mg/l and $S_{NH,5} < 3.5$ mg/l). When it happens, the MPC + FF controller needs time to recover a successfully $S_{NO,2}$ control. In order to avoid abrupt changes in the manipulated variable, variations of Q_a are limited during one day after of the control strategy application.

8.3 Simulation Results

In this section, the control configurations proposed in the above section are tested and compared. Ideal sensors have been considered. The simulation protocol is established in [33]: First, a steady state simulation of 200 days, and next a dynamic simulations of 609 days. Nevertheless, only the data generated during the final 364 days of the dynamic simulation are used for plant performance evaluation.

In Table 8.1 the results obtained with the proposed control strategies are shown. The chosen indicators to show the results obtained are based on the proposed objectives: EQI to evaluate the quality of effluent, OCI to evaluate costs, and the percentages of time of $S_{NH,e}$ and $S_{N_{tot,e}}$ violations.

The results have been compared with the default control strategy for BSM2 provided in [33], and with the two control strategies presented in the finalization of the plant layout in [46]. In addition, the results of [19, 37] are also shown for illustrative purposes. However, it should be noted that the comparison in these cases is not completely fair. In the case of [19], the EQI equation includes the different oxidized nitrogen forms, what makes worse the EQI result, and the simulation in [37] is carried out using only 275 days of influent data, what results in lower EQI and OCI. On the other hand, the comparison with the referenced works [7, 20, 21] is not possible. The reason is that [7, 20] use an earlier version of BSM2 (instead of the modified version in [46]), and [21] presents EQI and OCI graphs, but they do not provide numeric values.

As shown in Table 8.1, the results of the proposed strategies are obtained for various fixed $q_{EC,1}$ values. Obviously, when the control strategy for $S_{N_{tot,e}}$ violations removal is applied, the $q_{EC,1}$ value is modified. Logically, as $q_{EC,1}$ is increased, EQI is reduced but OCI is increased. In comparison with defCL, [37] and [19], applying $q_{EC,1} = 0.5$, both OCI and EQI are reduced, while the percentage of time of $S_{N_{tot,e}}$ and $S_{NH,e}$ violations is lower and sometimes zero. EQI and OCI reduction is mainly achieved with the hierarchical control structure. Important aspects to be considered in this hierarchical control are: first to get a good tracking through the lower level MPC + FF controllers and, on the other hand, to give a suitable S_O set-points by the higher level FC.

Regarding the tracking of the lower level control, Fig. 8.2 shows one week evolution of $S_{O,4}$ control, where the improvement of MPC + FF controller compared to the PI controllers of defCL can be observed. Table 8.2 shows the numerical results of the performance of both controllers, including the percentage of improvement of MPC + FF for the $S_{O,4}$ control. The results of $S_{O,5}$ and $S_{NO,2}$ control obtained in this work are also shown.

One reason of the EQI and OCI reduction obtained with the proposed control strategies, in comparison with the referred works of Table 8.1, is the way how the controllers of the higher level work. The referred papers try always to control S_{NH} at a fixed reference, but always with a very large error. This is not the case of the FC of the present work, which modifies the S_O set-points based on the biological processes, but without trying to maintain $S_{NH,5}$ at a fixed reference. It is also important to note that the referred works only vary the S_O set-point of one aerobic reactor, whereas in the present work $S_{O,4}$ and $S_{O,5}$ set-points are modified. Figure 8.3 shows one week evolution of the most important variables when there are $S_{NH,5}$ peaks. It shows the comparison between hierarchical control and the control strategy with fixed S_O set-points. In the case of hierarchical control, when $S_{NH,5}$ increases, $S_{O,4}$ and $S_{O,5}$ set-points are also increased and $S_{NH,e}$ peaks are reduced, and when $S_{NH,5}$ decreases, $S_{O,4}$ and $S_{O,5}$ are also decremented generating less S_{NO} and reducing operational costs.

Table 8.1 Comparative results of control strategy for S_{NH_e} violations removal and control strategy for $S_{N_{tot,e}}$ violations removal

		EQI	OCI	$S_{N_{tot,e}}$ violation (% of time)	$S_{NH,e}$ violation (% of time)
[33]	defCL	5577.97	9447.24	1.18	0.41
[46]	CL1	5447	9348	N/A	0.29
	%	2.35	1.05	N/A	29.27
	CL2	5274	8052	N/A	0.23
	%	5.45	14.77	N/A	43.9
[37] (different simulation time)	S1	5249	7154	N/A	N/A
	%	5.9	24.27	N/A	N/A
	S2	5927	8773	N/A	N/A
	%	−62.6	7.14	N/A	N/A
	S3	5530	8072	N/A	N/A
	%	0.86	14.56	N/A	N/A
	S4	5593	7442	N/A	N/A
	%	0.27	21.22	N/A	N/A
[19] (different EQI equation)	A1	6239	13324	2.17	19.44
	%	−11.85	−41.04	−83.9	−4641.46
	A2	6172	13323	1.09	20.83
	%	−10.65	−41.02	7.63	−4980.49
	A3	5995	13580	1.35	5.4
	%	−7.48	−43.74	−14.4	−1217.07
Control strategy for $S_{N_{tot,e}}$ violations removal	$q_{EC,1} = 0$	5318.95	6289.59	0.046	0.15
	%	4.64	33.42	96.1	63.41
	$q_{EC,1} = 0.5$	5197.49	6873.65	0.037	0.14
	%	6.82	27.24	96.86	65.85
	$q_{EC,1} = 1$	5069.51	7573.34	0.037	0.14
	%	9.11	19.83	96.86	65.85
	$q_{EC,1} = 2$	4852.49	9196.59	0.028	0.13
	%	13	2.65	97.63	68.29
Control strategy for $S_{NH,e}$ violations removal	$q_{EC,1} = 0$	5387.81	5942.77	2.39	0
	%	3.41	37.09	−102.54	100
	$q_{EC,1} = 0.5$	5217.9	6680.66	1.027	0
	%	6.45	29.28	12.97	100
	$q_{EC,1} = 1$	5112.01	7399.13	0.69	0
	%	8.17	21.68	41.52	100
	$q_{EC,1} = 2$	4875.14	9066.01	0.25	0
	%	12.6	4.03	78.81	100

Regarding the effluent violations, Table 8.1 shows that all $S_{NH,e}$ violations are removed, while the vast majority of $S_{N_{tot,e}}$ violations are also eliminated. There are a few special cases where the $S_{N_{tot,e}}$ violation is not possible to be avoided. Specifically, it happens three times in the simulation year in the cases when $q_{EC,1}$ is equal to 0, 0.5

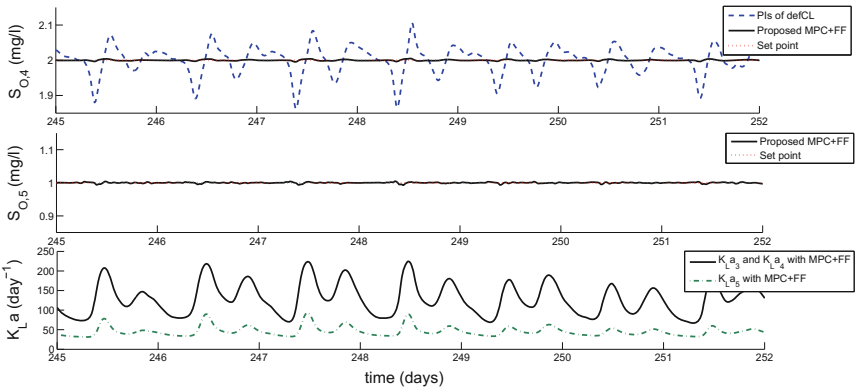

(a) Control performance with fixed S_O set-points and fixed Q_a

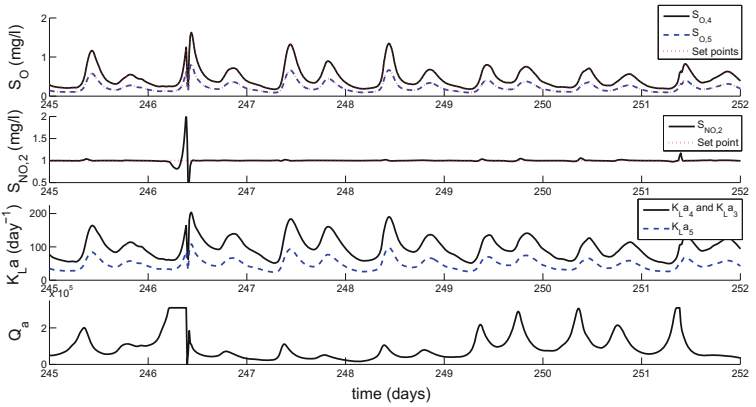

(b) Control performance with $S_{NO,2}$ control and varying S_O set-points with hierarchical control

Fig. 8.2 Simulation of the first evaluated week of the control performance of the MPC + FF controllers with fixed $S_{O,4}$ and $S_{O,5}$ set-points (2 and 1 mg/l respectively) and fixed Q_a (61944 m^3/d) (**a**); and with $S_{NO,2}$ control at a set-point of 1 mg/l and varying $S_{O,4}$ and $S_{O,5}$ set-points with hierarchical control (**b**)

Table 8.2 Control performance results with fixed $S_{O,4}$ and $S_{O,5}$ set-points (2 and 1 mg/l respectively) and fixed Q_a (61944 m^3/d) and with $S_{NO,2}$ control at a set-point of 1 mg/l and varying $S_{O,4}$ and $S_{O,5}$ set-points with hierarchical control

	Fixed S_O set-points and fixed Q_a				Hierarchical control and $S_{NO,2}$ control		
	$S_{O,4}$ control			$S_{O,5}$ control	$S_{O,4}$ control	$S_{O,5}$ control	$S_{NO,2}$ control
	PI of defCL	MPC + FF	%	MPC + FF	MPC+FF	MPC + FF	MPC + FF
IAE	9.079	0.33	96.36	0.44	0.44	0.37	3.91
ISE	0.4	0.0005	99.87	0.001	0.0049	0.0011	2.76

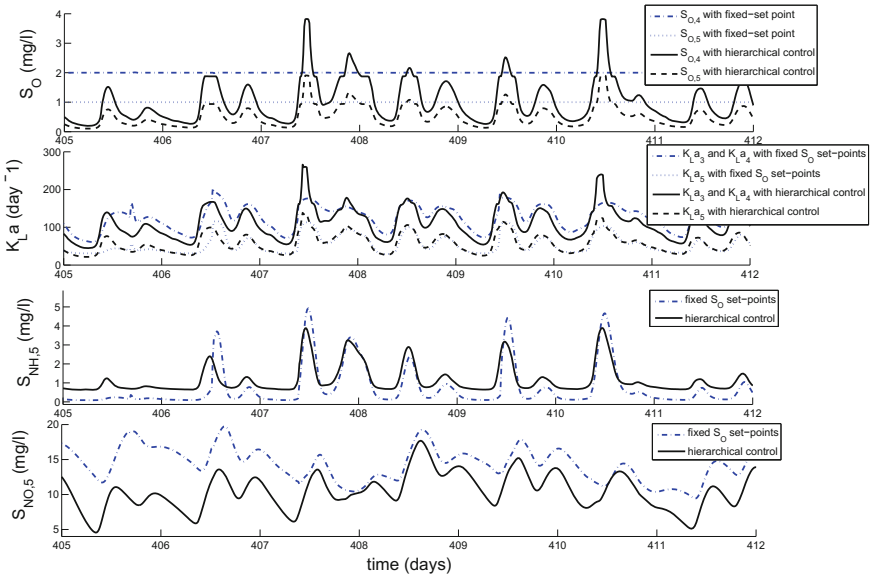

Fig. 8.3 One week simulation comparison between control strategy with fixed S_O set-points and varying S_O set-points with hierarchical control

and 1; and one time in the simulation year in the case when $q_{EC,1}$ is equal to 2. These violations are due to an increased flow rate just when peaks of pollutants are in the last reactors, possibly due to a heavy rain. Furthermore, in two of these three times, the influent flow rate exceeds the capacity of the plant and is partially led directly to the effluent through the bypass, without being treated. Therefore, although the FC acts adding $q_{EC,5}$, there is not enough time in advance to avoid the violation. Figures 8.4 and 8.5 show some cases where $S_{N_{tot},e}$ and $S_{NH,e}$ violations are eliminated, unlike what happens with only hierarchical control. Figure 8.5c shows one case where $S_{N_{tot},e}$ violation removal is not possible.

As it can be seen in Figs. 8.4 and 8.5, the violations risk detections made by the ANNs, explained in the previous chapters, allows to apply the appropriate control strategy enough in advance to prevent violations. In case that a risk of $S_{NH,e}$ violation is predicted, Q_a is increased by a FC to dilute S_{NH}, and when the increasing of S_{NH} reaches the fifth reactor, Q_a is decreased to reduce the hydraulic retention time and thus to improve the nitrification process. In the case that a risk of $S_{N_{tot},e}$ violation is predicted, $q_{EC,1-2}$ is added according to the value calculated by a FC.

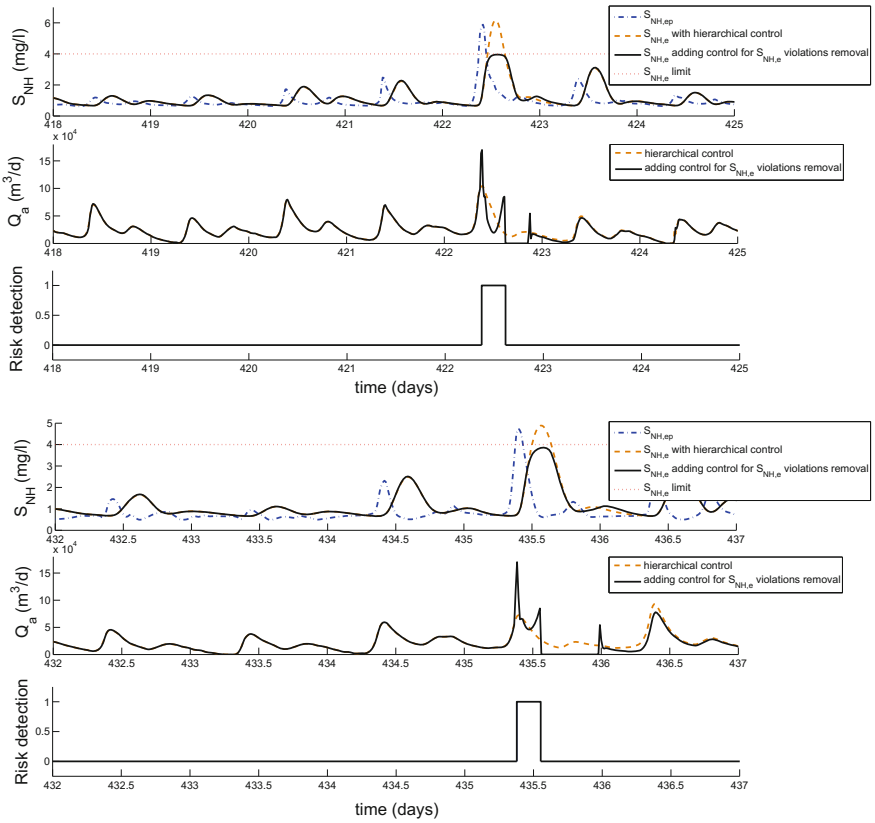

Fig. 8.4 Simulation of two cases of the control strategy for $S_{NH,e}$ violations removal application and its comparison with hierarchical control alone

8.4 Summary

In this chapter, control strategies for effluent violations removal have been tested in BSM2. The main novelty is that, due to the variability of the influent, an intelligent control system selects the control strategies to be applied based on the effluent predictions.

For the lower level of the hierarchical control structure, a satisfactory $S_{O,4}$, $S_{O,5}$ and $S_{NO,2}$ control performance, by applying MPC + FF controllers, have been also achieved. Due to the similar results obtained with functions and FCs in BSM1, in this case only FCs have been proposed for the higher level and also to manipulate q_{EC} and Q_a when a risk of $S_{N_{tot,e}}$ or $S_{NH,e}$ violation is detected.

Simulation results have shown the complete elimination of $S_{NH,e}$ violations. Regarding $S_{N_{tot,e}}$ violations, they have been avoided except one time in a simulation year, in which a large increase of flow rate coincides with a peak of pollutants in

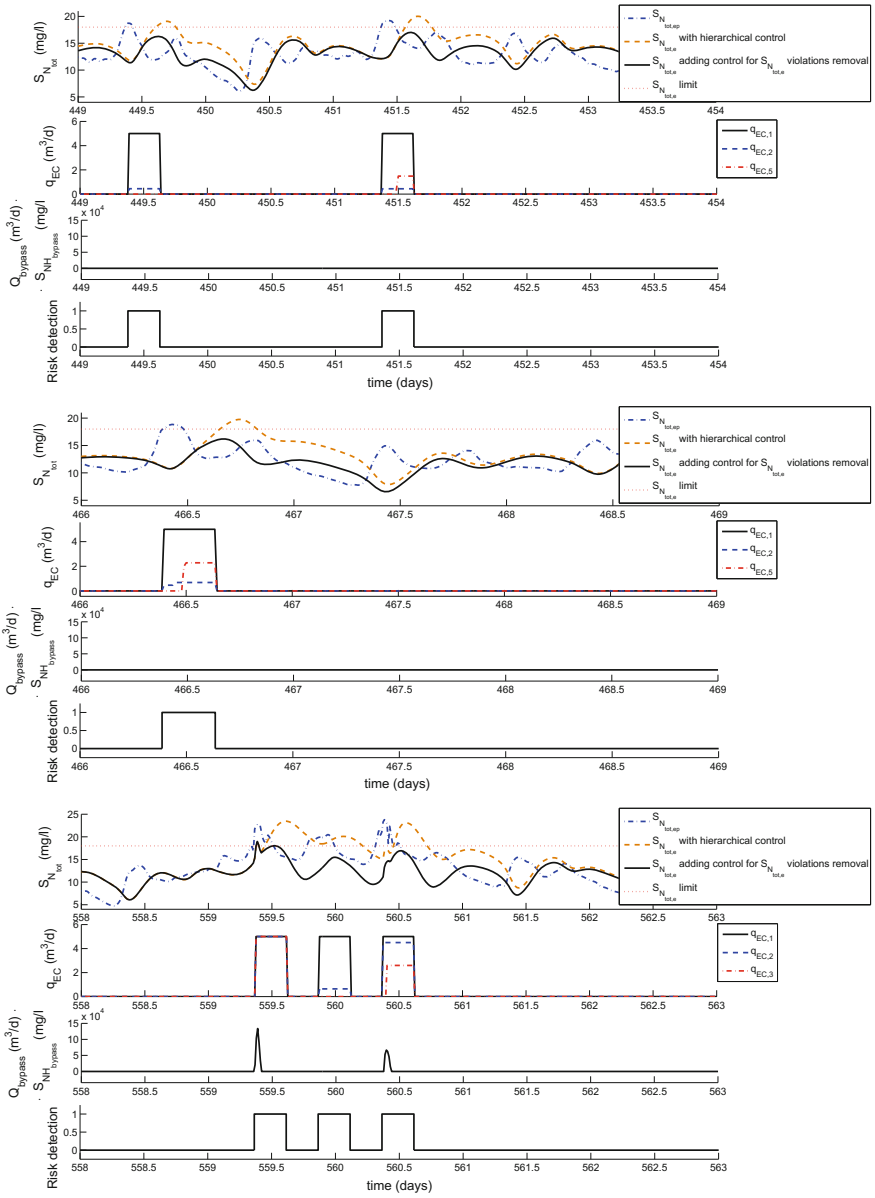

Fig. 8.5 Simulation of some cases of the control strategy for $S_{N_{tot,e}}$ violations removal application and its comparison with hierarchical control alone

the last reactor and with a situation of bypass. In addition, an EQI and OCI reduction has been achieved in comparison with defCL, CL1, CL2 and the referred works. The percentage of reduction is compared to defCL, obtaining a maximum EQI reduction of 13 % and a maximum OCI reduction of 37 %.

Chapter 9
Concluding Remarks

Concluding Remarks

In this book new control strategies have been applied in WWTPs. Being main objectives the improvement of effluent quality, the reduction of operational costs (evaluated by EQI and OCI indices respectively) and avoiding to exceed the established limits of effluent pollutants concentrations.

The evaluation and comparison of different control strategies have been based on two benchmarks, developed by IWA: BSM1 and BSM2. First, BSM1 has been used as a testing plant because it requires a smaller simulation time and therefore different control strategies can be tested more quickly. Subsequently, the operation of these control strategies, adding some modifications, has been tested in BSM2. This is an updated version of BSM1, closer to a real plant, extending to one year of simulation, with a much more complex plant model, including also a pretreatment process and a sludge treatment processes. In this case, a prediction of the effluent has been required for the selection of the control strategy to be applied. In any case, control strategies have been applied in the zone of the activated sludge reactors.

The book has been divided into nine chapters. The proposed control strategies have been based on MPC, FC, functions that relate the input with the manipulated variable and ANN. MPC controllers have been applied in order to improve the tracking. The control of the FCs and the functions was based on the biological processes that take place in the reactors. ANNs have been proposed in BSM2 to detect risks of violation by effluent predictions, in order to apply the appropriate control strategy. Both benchmarks and these control approaches have been explained in Chaps. 2 and 3 respectively.

Next, a hierarchical control has been applied in order to improve effluent quality and to reduce operational costs. In Chap. 4 the lower level has been implemented, where the MPC+FF controllers track the S_O in the aerated tanks and $S_{NO,2}$, improving the control performance with an ISE reduction of more than 90 % compared to

I. Santín et al., *Control and Decision Strategies in Wastewater Treatment Plants for Operation Improvement*, Intelligent Systems, Control and Automation: Science and Engineering 86, DOI 10.1007/978-3-319-46367-4_9

the default PI controllers. The control performance of the MPC+FF controllers has been also compared to the referenced works, showing the improvement of the proposed method and thus the successful tracking. In Chap. 5, the higher level has been performed, which regulates the S_O set-points of the aerated tanks based on $S_{NH,5}$. First, for the selection of the higher level controller, three different alternatives were proposed manipulating only $S_{O,5}$ set-point: a MPC, an affine function and a FC. They were tested and compared in the three weather conditions: dry, rain, and storm. As a result, EQI and OCI were reduced significantly. The results of OCI and EQI with higher level affine function and higher level FC were similar and better than those obtained with higher level MPC. This is due to the fact that the higher level MPC tries to keep the value of $S_{NH,5}$ at a reference level, but this is not possible. For that reason, the alternatives of affine function and FC for the higher level were tested with the idea of varying $S_{O,5}$ based on the $S_{NH,5}$ measured, taking into account the variables behavior in the biological processes, but without trying to keep $S_{NH,5}$ at a fixed reference. Thus, improving the nitrification process when $S_{NH,5}$ increases, to oxidize more S_{NH} and worsening the nitrification process when $S_{NH,5}$ decreases to generate less S_{NO} and to reduce costs. To ensure the right tuning of the controllers and therefore the correct relationship between the applied control and the results, a trade-off analysis between OCI and EQI has been performed by varying two tuning parameters for each controller. Next, the higher level control has been extended, manipulating the three aerobic tanks, achieving a greater reduction in EQI and OCI. Simulation results show that manipulating the S_O set-points of the three aerobic tanks, an EQI reduction of 5 % and an OCI reduction of 3.9 % is achieved for dry weather compared to the default control strategy. For the rain and storm influent cases, also a satisfactory reduction of EQI and OCI is obtained, higher than 3 %.

After this point, control strategies have been added with the objective of effluent violations removal. In Chap. 6, BSM1 has been used as testing plant. Functions and FCs are proposed for these control strategies basing their control on the biological processes. The improvement of the denitrification process, by adding $q_{EC,1}$, achieves the complete elimination of $S_{N_{tot,e}}$ violations. This control strategy has been tested with an affine function with a sliding window and with an FC. Both are implemented to dosage the minimum $q_{EC,1}$ necessary for this aim. The improvement of the nitrification process by manipulating Q_a makes possible the $S_{NH,e}$ violations removal. It has been tested first, with the combination of a linear function and an exponential function, and next, with an FC which uses different tuning parameters depending on if there are peaks of pollution in the tanks or not. Simulation results show that $S_{N_{tot,e}}$ and $S_{NH,e}$ violations are removed for dry, rain, and storm influents. In the cases of $S_{N_{tot,e}}$ violations removal for the three weather conditions and $S_{NH,e}$ violations removal for dry weather, a simultaneous reduction of EQI and OCI is achieved in comparison with the default control strategy. The $S_{NH,e}$ violations removal for rain and storm influents and the simultaneous elimination of $S_{N_{tot,e}}$ and $S_{NH,e}$ makes inevitable an increase of OCI. In any case, it has to be said that, with the removal of effluent violations, a reduction of costs is obtained for not paying fines, which is not considered in OCI.

In Chaps. 7 and 8, BSM2 is used as working scenario. For the application of the control strategies for effluent violations removal in BSM2, effluent predictions are necessary in order to detect risks of violation and thus selecting the suitable control strategy to be applied. In Chap. 7, the implementation of the ANNs for these effluent predictions is described. Simulations have shown a satisfactory predictions of $S_{N_{tot,e}}$ and $S_{NH,e}$, which are used for detection of risk violations and thus for selecting the suitable control strategy. In Chap. 8, the control strategies selected by an advanced decision control system have been implemented. For the lower level of the hierarchical structure, a satisfactory $S_{O,4}$, $S_{O,5}$ and $S_{NO,2}$ control performance, by applying MPC+FF controllers, have been also achieved. Due to the similar results obtained with functions and FCs in BSM1, in this case only FCs have been proposed for the higher level. Also, FCs are implemented to manipulate q_{EC} and Q_a when a risk of $S_{N_{tot,e}}$ or $S_{NH,e}$ violation is detected. The simulation results have been presented for different fixed values of $q_{EC,1}$. They have shown the complete elimination of $S_{NH,e}$ violations. Regarding $S_{N_{tot,e}}$ violations, they have been avoided except one time in a simulation year, in which a large increase of flow rate coincides with a peak of pollutants in the last reactor and with a situation of bypass. In addition, an EQI and OCI reduction has been achieved in comparison with defCL, CL1, CL2 and the referred articles. The percentage of reduction is compared to defCL, obtaining a maximum EQI reduction of 13 % and a maximum OCI reduction of 37 %.

Appendix A
Pareto Optimality

Satisfying a set of specifications and constraints required by real-control engineering problems is often a challenge. Problems in which the designer must deal with the fulfillment of multiple objectives are known as multiobjective problems (MOPs). It is common to define an optimization statement to deal with MOPs to calculate a solution with the desired balance among (usually conflictive) objectives.

While dealing with an MOP, we usually seek a Pareto optimal solution [43] in which the objectives have been improved as much as possible without giving anything in exchange. Different optimization procedures and search techniques [41] have been employed for the purpose of approximating the so-called Pareto set, where all solutions are Pareto optimal. However, for a successful implementation of the solution to the MOP, a Multi-Criteria Decision- Making (MCDM) step needs to be carried out to select the most preferable solution from the approximated set. Hereafter, this procedure (MOP definition, Pareto ser approximation and MCDM step) will be known as the Multi-Objective Optimization Design (MOOD) procedure. Since the MOOD procedure provides the opportunity to obtain a set of solutions to describe the objective trade off for a given MOP, its use is worthwhile for controller tuning. Due to the fact that several specifications need to be fulfilled by the control engineer, a procedure to appreciate the trade off exchange for complex processes could be useful. Nevertheless, the different MOOD steps are usually handled separately.

There are two different approaches to solve an optimization statement for an MOP. According to [42]; first, the Aggregate Objective Function (AOF) where the designer needs to describe all the trade-off at once and from the beginning of the optimization process, for example, the designer can use a weighting vector to indicate relative importance among the objective. Second, the Generate-First Choose-Later (GFCL) approach in which the target is to generate a set of Pareto optimal solutions and then the designer will select, a posteriori, the most preferable solution according to his/her preferences [41]. This is the option used in this book.

I. Santín et al., *Control and Decision Strategies in Wastewater Treatment Plants for Operation Improvement*, Intelligent Systems, Control and Automation: Science and Engineering 86, DOI 10.1007/978-3-319-46367-4

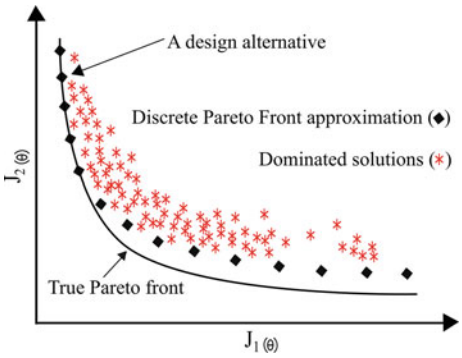

Fig. A.1 Pareto front concept for two objectives

A.1 Pareto Optimal Solutions

In order to generate such set of desirable solutions in the GFCL approach, the Multi-Objective Optimization (MOO) techniques might be used. Such techniques generate what is called the Pareto front approximation, where all the solutions are Pareto optimal. This means that there is no solution that is better in all objectives, but a set of solutions with different trade-offs among the conflicting objective.

Therefore, a set of optimal solutions is defined as the Pareto set Θ_P and each solution within this set defines an objective vector. The projection into the objective space is known as Pareto front J_P. All the solutions in the Pareto front are said to be nondominated and Pareto optimal solutions. This means in the Pareto front, there is not a solution that is better than another one for all the competitive objectives. To improve one objective will imply to introduce a loss regarding the other ones. It is important to mention that the true Pareto front is unknown, for this reason MOO techniques search for a discrete description of the Pareto set Θ_P^* capable of generating a good approximation of the Pareto front J_P^*, see Fig. A.1. In this way, the decision-maker can analyze the set and select the most preferable solution. This set of solutions implies that there is flexibility at the decision-making stage. The role of the designer is to select the most preferable solution for a particular situation.

A.2 Multicriteria Decision

All points within the Pareto front are equally acceptable solutions. Once the Pareto front approximation is provided, the designer needs to choose one of those points as the final solution to the MOP for the implementation phase. Several tools and methodologies are available, in order to facilitate the decision-making stage [8, 10, 22, 32, 61], a review with different techniques for decision-making analysis can be consulted in [18] and a taxonomy to identify the visualizations is presented in [52].

Somehow, the decision-making can be undertaken using two different approaches: (i) by including additional criteria such that at the end only one point from the Pareto front satisfies all of them, and (ii) by considering one point that represents a fair compromise between all used criteria. In other words, as the MOP establishes the search among the Pareto front for a compromise among a set of performance indices, and additional performance (probably of secondary importance) can be introduced. In this way, a new optimization problem will start with the search domain located in the Pareto set in order to find the best solution. The second option does not introduce more information for the decision-making and a *fair* point should be selected in order to represent an appropriate trade-off among the different considered cost functions.

Obviously, the ideal setup would be to reach the utopia point. However, the utopia point is normally unattainable and does not belong to the Pareto front approximation. This is because it is not possible to optimize all individual objective functions independently and simultaneously. Thus, it is only possible to find a solution that is as close as possible to the utopia point. Such solution is called the *compromise solution* (CS) and is Pareto optimal. This approach, however, starts from a neither attainable nor feasible solution. Therefore, it is not very practical as it does not take into account what can be achieved for each one of the individual objectives functions. Another procedure to select a fair point is to use bargaining games [3]. This solution leads us to a practical procedure for choosing a unique point from the Pareto front, as it will be seen in the next section.

A.3 Bargaining and *Trade-Off* Solutions Selection

In a transaction, when the seller and the buyer value a product differently, a surplus is created. A bargaining solution is then a way in which buyers and sellers agree to divide the surplus. There is an analogous situation regarding a controller design method that is facing two different cost functions for a system. When the controller locates the solution on the disagreement point (D), as shown in Fig. A.2, there is a way for the improvement of both cost functions. We can move within the feasible region towards the Pareto front in order to get lower values for both cost functions. Let θ_1^* and θ_2^* denote the values for the free parameter vector θ that achieve the optimal values for each one of the cost functions f_1 and f_2, respectively. Let these optimal values be $f_1^* = f_1(\theta_1^*)$ and $f_2^* = f_2(\theta_2^*)$. On that basis, the utopia point will have coordinates f_1^* and f_2^* whereas the disagreement point will be located at $(f_1(\theta_2^*), f_2(\theta_1^*))$. As the utopia (U) point is not attainable, we need to analyze the Pareto front in order to obtain a solution. A fair point that represents an appropriate trade off among the cost functions f_1 and f_2 is defined by the coordinates $(f_1^{Pf}, f_2^{Pf}) = (f_1(\theta_1^{Pf}), f_2(\theta_2^{Pf}))$, where the superindex *Pf* means Pareto front. On the basis of this formalism, we can identify, in economic terms the benefit of each one of the cost functions (buyer and seller) as the differences $f_1(\theta_2^*) - f_1^{Pf}$ and $f_2(\theta_1^*) - f_2^{Pf}$. The bargaining solution will provide a choice for (f_1^{Pf}, f_2^{Pf}) therefore a benefit for both f_1 and f_2 with respect

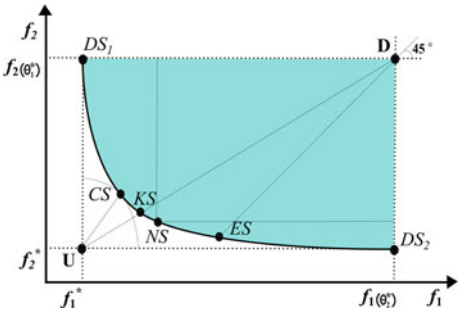

Fig. A.2 Location of the bargaining solutions into the Pareto front

to the disagreement. It is important to notice that the problem setup is completely opposite to the one that generates the compromise solution (CS) as the closest one to the utopia point.

Formally, a bargaining problem is denoted by a pair $< S; d >$ where $S \in \mathbb{R}^2, d \in S$ represents the disagreement point and there exists $s = (s_1, s_2) \in S$ such that $s_i < d_i$. In our case, S is the shaded area shown in Fig. A.2 delimited by the Pareto front and its intersection with the axis corresponding to the coordinates of the disagreement point. In Fig. A.2, different solutions for selecting a point from the Pareto front can bee seen:

1. The disagreement solution (D): it is the solution associated to the disagreement point. Even, if it is not the preferred solution for none of the players, it is a well-defined solution.
2. The dictatorial solution for player 1 (DS1): it is the point that minimizes the cost function for player 1. The same concept can be applied to player 2, yielding the dictatorial solution for player 2 (DS2).
3. The egalitarian solution (ES): it is the greatest feasible point (f_1^{Pf}, f_2^{Pf}) that satisfies $f_1(\theta_2^*) - f_1^{Pf} = f_2(\theta_1^*) - f_2^{Pf}$. This point coincides with the intersection of the 45° diagonal line that passes through the disagreement point with the Pareto front.
4. The Kalai–Smorodinsky solution (KS): it is the point (f_1^{Pf}, f_2^{Pf}) corresponding to the intersection of the Pareto front with the straight line that connects the utopia and the disagreement point.
5. The Nash Solution (NS): it selects the unique solution to the following maximization problem:

$$\begin{aligned} \max_{(f_1^{Pf}, f_2^{Pf})} \quad & (f_1(\theta_2^*) - f_1^{Pf})(f_2(\theta_1^*) - f_2^{Pf}) \\ s.t. \quad & f_1^{Pf} \leq f_1(\theta_2^*) \\ & f_2^{Pf} \leq f_2(\theta_1^*) \end{aligned}$$

A.4 The Nash Selection

In his pioneering work on bargaining games, Nash in [34] established a basic two-person bargaining framework between two rational players, and proposed an axiomatic solution concept which is characterized by a set of predefined axioms and does not rely on the detailed bargaining process of players. Nash proposed four axioms that should be satisfied by a reasonable bargaining solution:

- Pareto efficiency: none of the players can be made better off without making at least one player worse off.
- Symmetry: if the players are indistinguishable, the solution should not discriminate between them. The solution should be the same if the cost function axis are swapped.
- Independence of affine transformations: an affine transformation of the cost functions and of the disagreement point should not alter the outcome of the bargaining process.
- Independence of irrelevant alternatives: if the solution (f_1^{Pf}, f_2^{Pf}) chosen from a feasible set A is an element of a subset $B \in A$, then (f_1^{Pf}, f_2^{Pf}) must be chosen from B.

Nash proved that, under mild technical conditions, there is a unique bargaining solution called *Nash bargaining solution* satisfying the four previous axioms. Indeed, by considering the different options for selecting a point from the Pareto front, the NS is the only solution that satisfies these four axioms [34]. In fact, the Nash solution is simultaneously utilitarian (Pareto efficient) and egalitarian (fair). Also from a MOO point of view, by maximizing the product $(f_1(\theta_2^*) - f_1^{Pf})(f_2(\theta_1^*) - f_2^{Pf})$, we are maximizing the area of the rectangle that represents the set of solutions dominated by the NS. Actually, the NS provides the Pareto front solution that dominates the larger number of solutions, therefore being absolutely better (that is, with respect to both cost functions at the same time) than any one of the solutions of such rectangle. These are the reasons why the NS represents an appropriate choice for the (semi)-automatic selection of the fair point from the Pareto front.

References

1. Alex, J., Benedetti, L., Copp, J., Gernaey, K.V., Jeppsson, U., Nopens, I., Pons, N., Rieger, L., Rosen, C., Steyer, J.P., Vanrolleghem, P., Winkler, S.: Benchmark Simulation Model no. 1 (BSM1). Technical report, Department of Industrial Electrical Engineering and Automation, Lund University, Sweden (2008)
2. Aumann, R., Hart, S.: Handbook of Game Theory with Economic Applications, vol. 3, pp. 1521–2351. Elsevier, Amsterdam (2002)
3. Aumann, R.J., Hart, S.: Handbook of Game Theory with Economic Applications, vol. 2. Elsevier, Amsterdam (1994)
4. Bai, Y., Zhuang, H., Wang, D.: Advanced Fuzzy Logic Technologies in Industrial Applications (Advances in Industrial Control). Springer, London (2006)
5. Batstone, D.J., Keller, J., Angelidaki, I., Kalyuzhnyi, S., Pavlostathis, S., Rozzi, A., Sanders, W., Siegrist, H., Vavilin, V.: The iwa anaerobic digestion model no 1 (adm1). Water Sci. Technol. **45**(10), 65–73 (2002)
6. Belchior, C.A.C., Araujo, R.A.M., Landeckb, J.A.C.: Dissolved oxygen control of the activated sludge wastewater treatment process using stable adaptive fuzzy control. Comput. Chem. Eng. **37**, 152–162 (2011)
7. Benedetti, L., Baets, B.D., Nopens, I., Vanrolleghem, P.: Multi-criteria analysis of wastewater treatment plant design and control scenarios under uncertainty. Environ. Model. Softw. **25**(5), 616–621 (2009)
8. Blasco, X., Herrero, J., Sanchis, J., Martínez, M.: A new graphical visualization of n-dimensional pareto front for decision-making in multiobjective optimization. Inf. Sci. **178**(20), 3908–3924 (2008)
9. Camacho, E.F., Bordons, C.: Model Predictive Control, 2nd edn. Springer, London (2007)
10. Cela, R., Bollaín, M.: New cluster mapping tools for the graphical assessment of non-dominated solutions in multi-objective optimization. Chemom. Intell. Lab. Syst. **114**, 72–86 (2012)
11. Chen, G., Pham, T.T.: Introduction to Fuzzy Sets, Fuzzy Logic, and Fuzzy Control Systems. CRC Press, Boca Raton (2000)
12. Clarke, D.W., Mohtadi, C., Tuffs, P.S.: Generalized predictive control-part i. The basic algorithm. Automatica **23**(2), 137–148 (1987)
13. Copp, J.B.: Development of standardised influent files for the evaluation of actived sludge control strategies. IAWQ scientific and technical report, IAWQ (1999)
14. Corriou, J.P., Pons, M.N.: Model predictive control of wastewater treatment plants: application to the BSM1 benchmark. Comput. Chem. Eng. **32**, 625–630 (2004)

I. Santín et al., *Control and Decision Strategies in Wastewater Treatment Plants for Operation Improvement*, Intelligent Systems, Control and Automation: Science and Engineering 86, DOI 10.1007/978-3-319-46367-4

15. Cristea, V., Pop, C., Serban, P.: Model predictive control of the wastewater treatment plant based on the benchmark simulation model 1 - BSM1. In: Proceedings of the 18th European Symposium on Computer Aided Process Engineering- ESCAPE. Lyon, France (2008)
16. Cutler, C.R., Remaker, B.L.: Dinamic matrix control- a computer control algorithm. In: AICHE national meeting. Houston, TX (1979)
17. Ekman, M., Bjorlenius, B., Andersson, M.: Control of the aeration volume in an activated sludge process using supervisory control strategies. Water Res. **40**(8), 1668–1676 (2006)
18. Figueira, J., Greco, S., Ehrgott, M.: Multiple Criteria Decision Analysis: State of the Art Surveys, vol. 78. Springer Science & Business Media, Heidelberg (2005)
19. Flores-Alsina, X., Corominas, L., Snip, L., Vanrolleghem, P.A.: Including greenhouse gas emissions during benchmarking of wastewater treatment plant control strategies. Water Res. **45**(16), 4700–4710 (2011)
20. Flores-Alsina, X., Gallego, A., Feijoo, G., Rodriguez-Roda, I.: Multiple-objective evaluation of wastewater treatment plant control alternatives. J. Environ. Manag. **91**(5), 1193–1201 (2010)
21. Flores-Alsina, X., Saagi, R., Lindblom, E., Thirsing, C., Thornberg, D., Gernaey, K.V., Jeppsson, U.: Calibration and validation of a phenomenological influent pollutant disturbance scenario generator using full-scale data. Water Res. **51**, 172–185 (2013)
22. de Freitas, A., Fleming, P., Guimarães, F.: Aggregation trees for visualization and dimension reduction in many-objective optimization. Inf. Sci. **298**, 288–314 (2015)
23. Garcia, C.E., Morshedi, A.: Quadratic programming solution of dynamic matrix control (QDMC). Chem. Eng. Commun. **46**(1–3), 73–87 (1986)
24. Gernaey, K., Jeppsson, U., Vanrolleghem, P., Copp, J.: Benchmarking of control strategies for wastewater treatment plants. Scientific and Technical Report No.23. IWA Publishing, London, UK (2014)
25. Güçlü, D., Dursun, S.: Artificial neural network modelling of a large-scale wastewater treatment plant operation. Bioprocess Biosyst. Eng. **33**(9), 1051–1058 (2010)
26. Hamed, M.M., Khalafallah, M.G., Hassanien, E.A.: Prediction of wastewater treatment plant performance using artificial neural networks. Environ. Model. Softw. **19**(10), 919–928 (2003)
27. Han, H.G., Qian, H.H., Qiao, J.F.: Nonlinear multiobjective model-predictive control scheme for wastewater treatment process. J. Process Control **24**, 47–59 (2014)
28. Hassoun, M.H.: Fundamentals of Artificial Neural Networks. MIT Press, Massachusetts (1995)
29. Haykin, S.S.: Neural Networks and Learning Machines. Prentice-Hall, New York (2009)
30. Henze, M., Grady, C., Gujer, W., Marais, G., Matsuo, T.: Activated sludge model 1. Scientific and Technical Report No.1. IAWQ, London, UK (1987)
31. Holenda, B., Domokos, E., Redey, A., Fazakas, J.: Dissolved oxygen control of the activated sludge wastewater treatment process using model predictive control. Comput. Chem. Eng. **32**(6), 1270–1278 (2008)
32. Inselberg, A.: The plane with parallel coordinates. Vis. Comput. **1**(2), 69–91 (1985)
33. Jeppsson, U., Pons, M.N., Nopens, I., Alex, J., Copp, J., Gernaey, K., Rosen, C., Steyer, J.P., Vanrolleghem, P.: Benchmark simulation model no 2: general protocol and exploratory case studies. Water Sci. Technol. **56**(8), 67–78 (2007)
34. Nash, J.F. Jr.: The bargaining problem. Econometrica: J. Econom. Soc. 155–162 (1950)
35. Kailath, T.: Linear Systems. Prentice-Hall, New York (1980)
36. Karunanithi, N., Grenney, W.J., Whitley, D., Bovee, K.: Neural networks for river flow prediction. J. Comput. Civil Eng. **8**(2), 201–220 (1994)
37. Kim, M., Yoo, C.: Multi-objective controller for enhancing nutrient removal and biogas production in wastewater treatment plants. J. Taiwan Inst. Chem. Eng. **45**(5), 2537–2548 (2014)
38. Ljung, L.: System Identification - Theory For the User. PTR Prentice Hall, New York (1987)
39. Maciejowski, J.: Predictive Control with Constraints, 1st edn. Pearson Education, Harlow (2002)
40. Mamdani, E.: Application of fuzzy algorithms for control of simple dynamic plant. Proc. Inst. Electr. Eng. **121**(12), 1585–1588 (1976)
41. Marler, R.T., Arora, J.S.: Survey of multi-objective optimization methods for engineering. Struct. Multidiscip. Optim. **26**(6), 369–395 (2004)

42. Mattson, C.A., Messac, A.: Pareto frontier based concept selection under uncertainty, with visualization. Optim. Eng. **6**(1), 85–115 (2005)
43. Miettinen, K.M.: Nonlinear Multiobjective Optimization. Kluwer Academic Publishers, Boston (1998)
44. Muske, K.R., Rawlings, J.B.: Model predictive control with linear models. AICHE J. **39**(2), 262–287 (1993)
45. Nasr, M.S., Moustafa, M.A., Seif, H.A., Kobrosy, G.E.: Application of Artificial Neural Network (ANN) for the prediction of EL-AGAMY wastewater treatment plant performance-EGYPT. Alex. Eng. J. **51**(1), 37–43 (2012)
46. Nopens, I., Benedetti, L., Jeppsson, U., Pons, M.N., Alex, J., Copp, J.B., Gernaey, K.V., Rosen, C., Steyer, J.P., Vanrolleghem, P.A.: Benchmark simulation model no 2: finalisation of plant layout and default control strategy. Water Sci. Technol. **62**(9), 1967–1974 (2010)
47. Ostace, G.S., Cristea, V.M., Agachi, P.S.: Investigation of different control strategies for the bsm1 waste water treatment plant with reactive secondary settler model. In: 20th European Symposium on Computer Aided Process Engineering. 6–9 June, Ischia, Naples, Italy (2010)
48. Ostace, G.S., Gal, A., Cristea, V.M., Agachi, P.S.: Operational costs reduction for the wwtp by means of substrate to dissolved oxygen correlation - a simulation study. In: Proceedings of the World Congress on Engineering and Computer Science. 19–21 October, San Francisco, USA (2011)
49. Overschee, P.V., Moor, B.D.: N4SID: Subspace algorithms for the identification of combined deterministic-stochastic systems. Automatica **30**, 75–93 (1994)
50. Przystalka, P., Moczulski, W.: Methodology of neural modelling in fault detection with the use of chaos engineering. Eng. Appl. Artif. Intell. **41**, 25–40 (2015)
51. Qin, S.J., Badgwell, T.A.: A survey of industrial model predictive control technology. Control Eng. Pract. **11**(7), 733–764 (2003)
52. Reynoso-Meza, G., Blasco, X., Sanchis, J., Herrero, J.: Comparison of design concepts in multi-criteria decision-making using level diagrams. Inf. Sci. **221**, 124–141 (2013)
53. Richalet, J., Rault, A., Testud, J.L., Papon, J.: Model predictive heuristic control: applications to industrial processes. Automatica **14**(5), 413–428 (1978)
54. Santín, I., Pedret, C., Vilanova, R.: Fuzzy control and model predictive control configurations for effluent violations removal in wastewater treatment plants. Ind. Eng. Chem. Res. **54**(10), 2763–2775 (2015)
55. Shaw, I.S.: Fuzzy Control of Industrial Systems: Theory and Applications. Kluwer Academic Publishers, Boston (1998) (ISBN 0792382498)
56. Shen, W., Chen, X., Corriou, J.P.: Application of model predictive control to the BSM1 benchmark of wastewater treatment process. Comput. Chem. Eng. **32**(12), 2849–2856 (2008)
57. Shen, W., Chen, X., Pons, M., Corriou, J.: Model predictive control for wastewater treatment process with feedforward compensation. Comput. Chem. Eng. **155**(1–2), 161–174 (2009)
58. Stare, A., Vrecko, D., Hvala, N., Strmcnick, S.: Comparison of control strategies for nitrogen removal in an activated sludge process in terms of operating costs: a simulation study. Water Res. **41**, 2004–2014 (2007)
59. Tackacs, I., Patry, G., Nolasco, D.: A dynamic model of the clarification-thickening process. Water Res. **25**, 1263–1271 (1991)
60. Takagi, T., Sugeno, M.: Fuzzy identification of system and its applications to modeling and control. IEEE Trans. Syst., Man, Cybern. **15**(1), 116–132 (1985)
61. Tusar, T., Filipic, B.: Visualization of pareto front approximations in evolutionary multiobjective optimization: a critical review and the prosection method. IEEE Trans. Evolution. Comput. **19**(2), 225–245 (2015)
62. Vilanova, R., Katebi, R., Wahab, N.: N-removal on wastewater treatment plants: a process control approach. J. Water Resour. Prot. **3**(1), 1–11 (2011)
63. Vrecko, D., Hvala, N., Stare, A., Burica, O., Strazar, M., Levstek, M., Cerar, P., Podbevsek, S.: Improvement of ammonia removal in activated sludge process with feedforward-feedback aeration controllers. Water Sci. Technol. **53**(4–5), 125–132 (2006)

64. Vyas, M., Modhera, B., Sharma, A.K.: Artificial neural network based model in effluent treatment process. Int. J. Adv. Eng. Technol. **2**(2), 271–275 (2011)
65. Wahab, N.A., Katebi, R., Balderud, J.: Multivariable PID control design for activated sludge process with nitrication and denitrication. Biochem. Eng. J. **45**(3), 239–248 (2009)
66. Wang, N., Adeli, H.: Self-constructing wavelet neural network algorithm for nonlinear control of large structures. Eng. Appl. Artif. Intell. **41**, 249–258 (2015)
67. Yegnanarayana, B.: Artificial Neural Networks. PHI Learning, New Delhi (2009)